Doctoral Dissertations   Dissertations and Theses

October 2019

Mechanisms that Limit Oxidative Phosphorylation during High-Intensity Muscle Contractions In Vivo

Miles F. Bartlett
University of Massachusetts Amherst

Follow this and additional works at: https://scholarworks.umass.edu/dissertations_2

Part of the Biochemistry Commons, Exercise Physiology Commons, and the Exercise Science Commons

MECHANISMS THAT LIMIT OXIDATIVE PHOSPHORYLATION DURING HIGH-

INTENSITY MUSCLE CONTRACTIONS IN VIVO

A Dissertation Presented

By

MILES F. BARTLETT

Submitted to the Graduate School of the
University of Massachusetts Amherst in partial fulfillment
of the requirements for the degree of

DOCTOR OF PHILOSOPHY

September 2019

Department of Kinesiology

MECHANISMS THAT LIMIT OXIDATIVE PHOSPHORYLATION DURING HIGH-

INTENSITY MUSCLE CONTRACTIONS IN VIVO

A Dissertation Presented

By

MILES F. BARTLETT

Approved as to style and content by:

_____

Jane A. Kent, Chair

_____

Mark S. Miller, Member

_____

Edward P. Debold, Member

_____

Alexander R. Gerson, Outside Member

_____

Jane A. Kent, Department Chair
Department of Kinesiology

DEDICATION

Dedicated to no one; as all science should be.

ACKNOWLEDGEMENTS

ABSTRACT

MECHANISMS THAT LIMIT OXIDATIVE PHOSPHORYLATION DURING HIGH-INTENSITY MUSCLE CONTRACTIONS IN VIVO

SEPTEMBER 2019

MILES F. BARTLETT, B.S. UNIVERSITY OF MAINE ORONO

M.A., THE UNIVERSITY OF NORTH CAROLINA AT CHAPEL HILL

PH.D, UNIVERSITY OF MASSACHUSETTS AMHERST

Directed by: Professor Jane A. Kent

Skeletal muscle oxidative capacity plays a critical role in human health and disease. Although current models of oxidative phosphorylation sufficiently describe skeletal muscle energetics during moderate-intensity contractions, much is still unknown about the mechanisms that control and limit oxidative phosphorylation during high-intensity contractions. In particular, the oxygen cost of force generation is augmented during exercise at workloads above the lactate threshold. Presently, it is unclear whether this augmentation in muscle oxygen consumption is driven by increased rates of oxidative ATP synthesis (ATP_{OX}) or by decreases in the efficiency of ATP_{OX} due to mitochondrial uncoupling. To address this gap, ^{31}P-MRS was used in two separate studies to measure rates of ATP_{OX} at the end of: 1) repeated bouts of supramaximal knee extensions, and 2) each stage of an isotonic stepwise knee extension protocol. In both studies, high-intensity contractions impaired the maximal capacity for ATP_{OX} and reduced the sensitivity of ATP_{OX} to changes in ADP and cytosolic phosphorylation potential. However, high-intensity contractions did not cause rates of ATP_{OX} to increase relative to workload, suggesting that the increased oxygen cost of exercise above the lactate threshold is due to changes in mitochondrial coupling control (i.e., P/O ratio).

TABLE OF CONTENTS

LIST OF TABLES

LIST OF FIGURES

CHAPTER 1

INTRODUCTION

Apart from a few recently-discovered marine species (51), oxidative phosphorylation is essential to multicellular life. Complete oxidation of foodstuffs not only results in greater molar ATP yields than anaerobic metabolism, it also produces gaseous waste products, which in contrast to the non-gaseous waste products of most anaerobic energy producing pathways, can be excreted from multicellular organisms in copious quantities via simple pulmonary ventilation. This is particularly important to our understanding of skeletal muscle fatigue, where rates of ATP demand can increase more than 100-fold over resting values in the transition from rest to maximal exercise (182). Specifically, when the rate of skeletal muscle ATP demand exceeds the rate at which ATP can be synthesized by oxidative phosphorylation, glycolytic ATP synthesis increases dramatically, which leads to the accumulation of fatigue inducing metabolites, such as protons (H^+) and inorganic phosphate (Pi) (52, 53, 100, 157), that cannot be excreted as quickly as they are being produced.

During moderate-intensity contractions ATP demand is met entirely by oxidative ATP synthesis and steady-state muscle metabolism is linearly related to power output (58, 219). However, during high-intensity contractions above the lactate threshold, muscle oxygen consumption increases more than would be predicted by the linear relationship observed for power outputs below the lactate threshold (58, 109) (Figure 1.1). This 'excess' oxygen consumption is also accompanied by augmentations in phosphocreatine (PCr) breakdown, lactate accumulation, and acidosis (10, 44, 83, 85, 104, 170, 174, 191). The attainment of metabolic steady-state is also delayed, or in some

cases, unachievable (58, 212, 213, 219). These metabolic changes indicate that high-intensity contractions impair either the mechanical efficiency of skeletal muscle force production or the efficiency of ATP synthesis via oxidative phosphorylation.
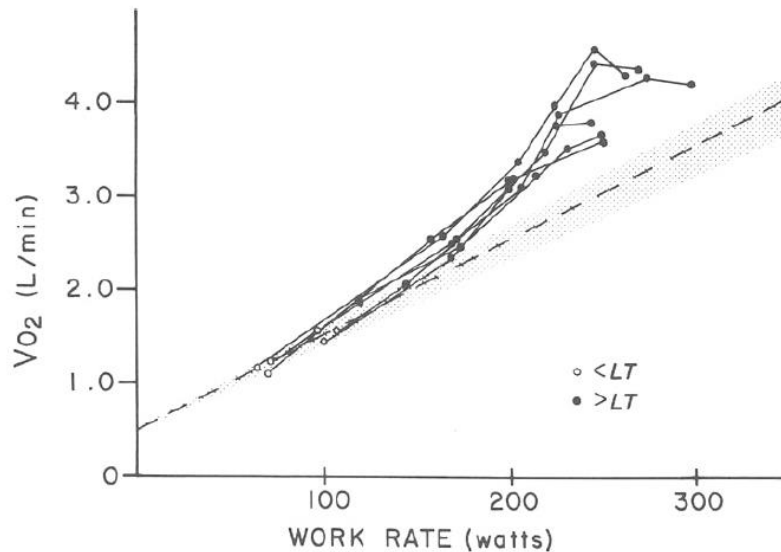
Figure 1.1: Augmentation of pulmonary VO₂ during cycling exercise at power outputs below the lactate threshold. Oxygen uptake increases linearly at a rate of about 10ml/Kg/Watt (11, 175). However, for power outputs above the lactate threshold (filled circles), the increment in oxygen uptake per Watt of power output increases. This 'excess' increase in the oxygen cost of high-intensity exercise denotes a reduction in either the mechanical efficiency of skeletal muscle force production or the efficiency of ATP synthesis via oxidative phosphorylation. *Figure from Roston et al.* (175).

Collectively, these augmentations in skeletal muscle metabolism have become known as the slow component of oxygen uptake kinetics (VO₂SC). The VO₂SC has primarily been studied from changes in pulmonary oxygen uptake and blood lactate accumulation during cycling exercise (58, 109). Although these variables reflect whole body responses to exercise, multiple investigations have demonstrated that approximately 85% of the VO₂SC originates within the contracting muscle mass (107, 167, 174), particularly within fatiguing muscle fibers (29, 221). However, the biochemical and molecular mechanisms underlying the VO₂SC are not fully understood.

2

At present, the leading hypothesis predicts that the VO_{2SC} reflects an increased ATP cost of force generation (35, 174), or a reduction in the mechanical efficiency of force generation or summation (166). Rossiter *et al.* first proposed this explanation after observing similar kinetic responses between pulmonary oxygen uptake and intramuscular PCr breakdown during single leg knee extensions (Figure 1.2) (174). Given the relationship between oxidative phosphorylation and creatine kinase shuttling (15, 149), this led the authors to predict that the ATP cost of force generation increases during high intensity contractions.
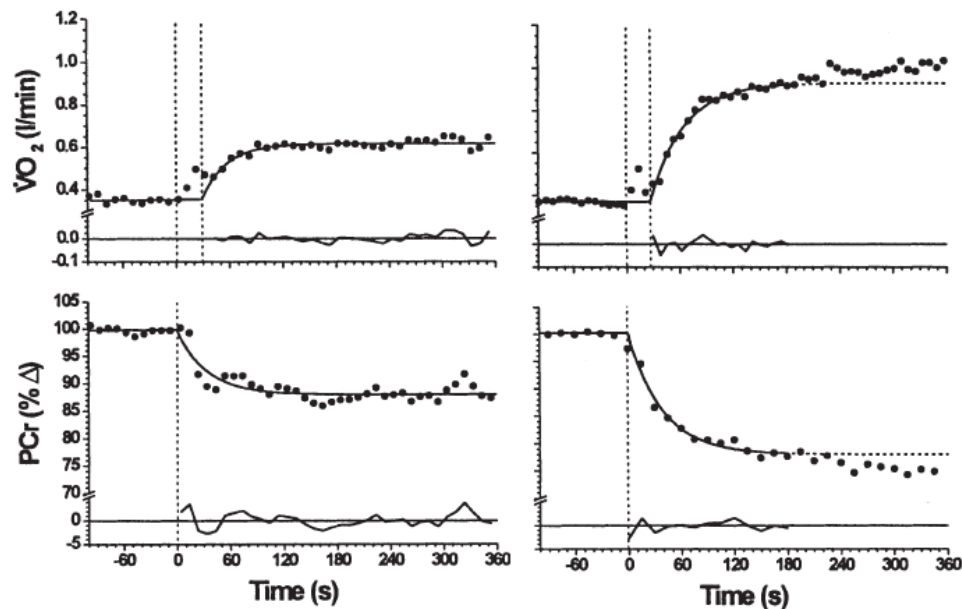
Figure 1.2: Changes in pulmonary VO$_2$ and intramuscular PCr during moderate and high-intensity dynamic contractions. Pulmonary oxygen uptake (upper left panel) and intramuscular PCr breakdown (lower left panel) plateau within 3 minutes. However, during high-intensity contractions, neither pulmonary VO$_2$ (upper right panel) nor intramuscular [PCr] (lower right panel) achieve a steady-state plateau. Given the relationship between creatine kinase shuttling and oxidative phosphorylation (15, 149), Rossiter *et al.* predicted the VO_{2SC} is caused by an increased ATP cost of muscle force generation (174). *Figure from Rossiter et al.* (174).

One mechanism that could increase the ATP cost of force generation during high-intensity contractions is Type-II muscle fiber recruitment. Type-II muscle fibers exhibit a significantly greater ATP cost of force generation than Type-I fibers (50, 69, 75) and are

selectively recruited at higher power outputs (60). Moreover, the magnitude of the VO_{2SC} (i.e., the volume of excess muscle oxygen consumption) correlates well with Type-II myosin heavy chain (MHC) content (142, 143, 220). Inversely, greater expression of Type-I MHC content is correlated higher mechanical efficiency during cycling (152), as well as higher critical power thresholds, a marker of endurance capacity and skeletal muscle fatigue resistance (200).

However, there are several biochemical aspects of the VO_{2SC} that are difficult to reconcile under the increased ATP cost of force generation hypothesis. For example, the magnitude of the VO_{2SC} is positively correlated with blood lactate accumulation (175), the paradox being that the acidosis accompanying lactate accumulation should actually *impair* muscle oxygen consumption due to its inhibitory effect on mitochondrial respiration (70, 93). The augmentation of muscle oxygen consumption also occurs despite a significant impairment to skeletal muscle oxidative capacity following high-intensity contractions (28, 193). That is, it is difficult to explain how muscle oxygen consumption can increase if the capacity for oxidative phosphorylation is decreased. That the non-linear increase in muscle oxygen consumption is predicted to originate within fast-twitch muscle fibers is also paradoxical given that they exhibit lower mitochondrial density and tend to produce lower rates of ADP-limited respiration than slow-twitch fibers (63, 86, 115), though this latter finding is not always consistent and can depend on the substrates being oxidized (116, 153).

The alternative hypothesis for the VO_{2SC} is that high-intensity contractions cause mitochondrial uncoupling, a process that impairs the coupling between mitochondrial oxygen consumption and oxidative ATP synthesis (i.e., P/O ratio; the ratio of ATP

synthesized by ATP synthase per O_2 molecule reduced by cytochrome c-oxidase) (35, 169, 214). Similar to reducing a car's gas mileage, mitochondrial uncoupling increases the volume of oxygen necessary to maintain a given rate of ATP synthesis. This directly explains the non-linear increase in muscle oxygen consumption and may also explain why the magnitude of the VO_{2SC} (i.e., the volume of excess muscle oxygen consumption) is so highly correlated with lactate accumulation (Figure 1.3) and augmentations in phosphocreatine hydrolysis (174, 175), as progressive declines in P/O would increasingly impair oxidative ATP synthesis, thereby necessitating greater recruitment of anaerobic energy pathways to meet cellular ATP demand.
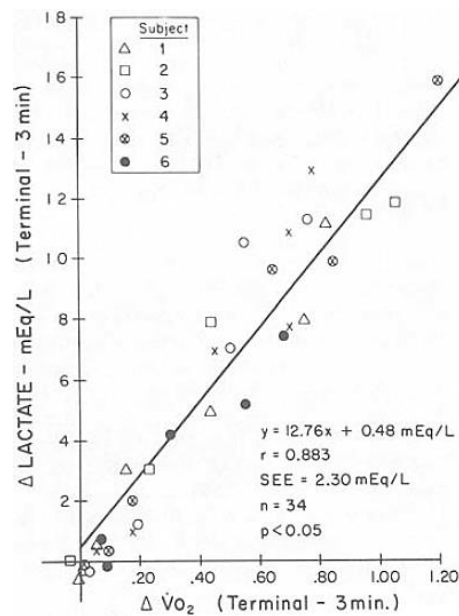
Figure 1.3: Correlation between the VO_{2SC} magnitude and blood lactate accumulation. During high-intensity cycling, the magnitude of the VO_{2SC}, calculated as the increase in oxygen uptake measured from minute 3 to the end of exercise, correlates well (r=0.883) with the increase in blood lactate accumulation measured over the same time period. *Figure from Roston et al.* (175).

Statement of the Problem

Myriad experimental limitations have hindered definitive demonstration of either hypotheses for the VO_{2SC}, with the primary limitation being that both hypotheses offer

logical and experimentally supported explanations for nearly every change in skeletal muscle bioenergetics observed during high intensity contractions. Put another way, there are very few changes in skeletal muscle bioenergetics during high-intensity contractions that are exclusively predicted by one hypothesis but not the other, which has made developing experiments that can separate the two hypotheses *in vivo* difficult. However, one predictive difference between the two hypotheses is the impact high-intensity contractions have on oxidative ATP synthesis. Whereas the increased ATP cost of force generation hypothesis predicts the augmentation in skeletal muscle oxygen uptake is a direct reflection of increased oxidative ATP synthesis, the mitochondrial uncoupling hypothesis predicts oxidative ATP synthesis is reduced due to an impairment of the mitochondrial P/O ratio. This predictive difference offers an opportunity to study and compare the competing hypotheses for explaining the VO_{2SC}.

Yet, where one opportunity presents itself, another challenge arises. Several methods exist for using ^{31}phosphorous magnetic resonance spectroscopy (^{31}P-MRS) to study changes in oxidative ATP synthesis within contracting skeletal muscles, but most of these methods are inherently based on assumptions that either the ATP cost of contraction does not change (99) or that mitochondrial uncoupling does not occur (29, 119, 206), and therefore cannot be used to study the VO_{2SC} because of an inherent bias against one hypothesis or the other. A third method for using ^{31}P-MRS to study changes in ATP_{OX} is to measure the initial rate of post-exercise phosphocreatine resynthesis (V_{iPCr}) (19, 35). Although this method only yields one measure of ATP_{OX} per bout of contractions, it does not make any assumptions about the ATP cost of force generation or mitochondrial uncoupling, and therefore offers an opportunity to study the VO_{2SC} by

6

having participants perform multiple durations of high-intensity contractions. Cannon *et al*. recently used this approach and reported that although the ATP cost of force generation did appear to increase during 8 minutes of high-intensity knee extensions, the magnitude of the increase was insufficient to fully account for the VO_{2SC}, suggesting mitochondrial uncoupling may have played a role (35).

Another major experimental limitation is that there are only a few techniques available for measuring mitochondrial uncoupling and P/O *in vivo*. Some groups have tried to bridge this gap by combining pulmonary oxygen uptake with ^{31}P-MRS (38, 128). Although the VO_{2SC} does primarily originate within the working muscle mass (167, 174), the fact that pulmonary oxygen uptake is not just a measure of oxygen consumption by the working muscle mass, but also includes oxygen uptake from other tissues, erodes enthusiasm for using this technique to calculate skeletal muscle P/O ratio. Marcinek *et al*. have combined optical and magnetic resonance spectroscopies to directly measure mitochondrial uncoupling *in vivo* within <u>resting</u> muscle (1, 49, 146), but to the best of my knowledge, this approach has not been applied following a period of contractions.

<u>Study 1: Oxidative ATP Synthesis during High-Intensity Contractions</u>

The primary aim of this study is to demonstrate that the rate of oxidative ATP synthesis becomes impaired during high-intensity contractions. As discussed above, the increased ATP cost of force generation hypothesis predicts that the augmentation in skeletal muscle oxygen uptake during high-intensity contractions is directly caused by increases in oxidative ATP synthesis. Consequently, this hypothesis can be eliminated if it is demonstrated that rates of oxidative ATP synthesis decline during high-intensity

contractions, leaving mitochondrial uncoupling as the primary hypothesis remaining for the VO_{2SC}. The secondary aim of Study 1 is to demonstrate that the accuracy of traditional ATP_{OX} calculations can be improved for bouts of high-intensity contractions by making adjustments for changes in oxidative capacity (i.e., k_{PCr}), thereby allowing ATP_{OX} to be calculated over time without needing to assume constant ATP cost of contraction or maintained mitochondrial coupling (29, 99, 119, 206).

Nine healthy young men and women (ages 25-40) will complete multiple trials of a high-intensity isokinetic ($120°·s^{-1}$) knee extension protocol during a single visit to the Human Magnetic Resonance Center (*h*MRC). One maximal voluntary dynamic contraction (MVDC) will be performed every two seconds for 4 trials lasting 24, 60, 120, and 240 seconds. Continuous measures of ^{31}P-MRS will be collected before, during, and after each of these trials, thereby allowing us to measure k_{PCr} and V_{iPCr} at 4 separate time points. The primary outcome variables for this study will be k_{PCr} ($·s^{-1}$), V_{max} (mM/s), K_m (i.e., the substrate concentration at $½V_{max}$), the Hill coefficient (n^H), and V_{iPCr} (mM/s) following each of the 4 isokinetic MVDC protocols (all shown in Figure 1.4), as well as the rates of ATP_{OX} (mM/s), ATP_{tot} (mM/s), and ATP_{cost} (Watts/ATP_{tot}) calculated using the traditional and modified methods at 24, 60, 120, and 240 s of the 4th (240 s) experimental trial. Secondary outcome measures will include muscle fatigue (% peak power), total work (Joules), and changes in intramuscular metabolite concentrations such as PCr, Pi, and H^+. These variables will be compared across all 4 isokinetic MVDC trials to ensure muscle performance and energetics are consistent across trials, thereby allowing us to assume that the V_{iPCr} measured after the 24, 60, and 120 trials is representative of the true ATP_{OX} rate observed during the 240 s trial.
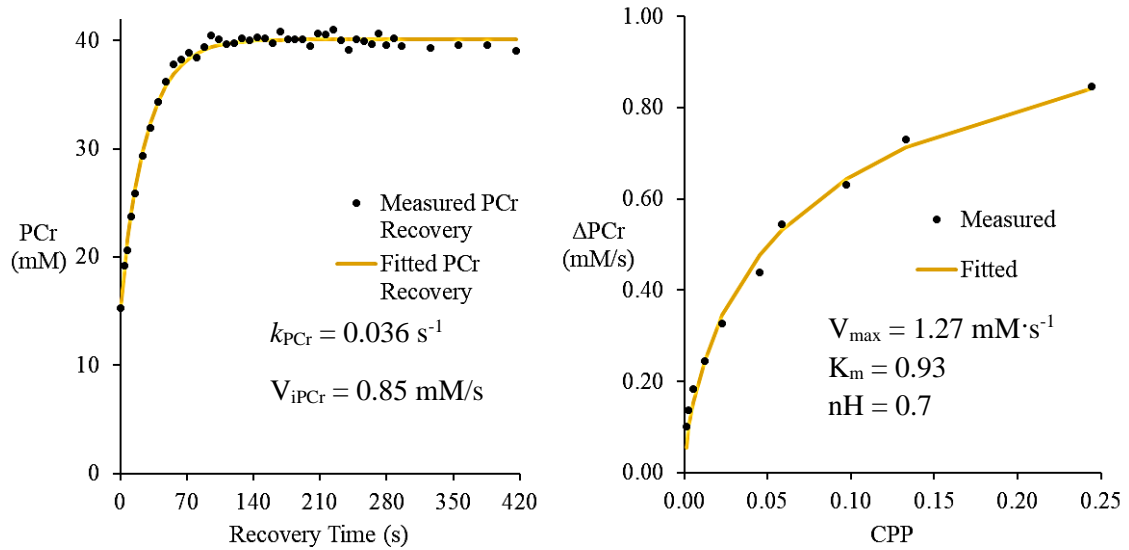
Figure 1.4: Skeletal muscle oxidative capacity and multiparametric analysis of V_{max} and K_m for ATP_{OX}. Skeletal muscle oxidative capacity will be measured as the rate constant (k_{PCr}) of the PCr recovery response following each bout of contractions (left). The fitted PCr recovery curve will then be used to calculate rates of ATP_{OX} ($\Delta PCr/\Delta time$), which will then be fitted against either the measured [ADP] or cytosolic phosphorylation potential (CPP; shown in the right hand figure) to determine V_{max}, K_m, and n^H, according to the equation: $PCr(t)=V_{max}/(1+((K_m/CPP)^{\wedge nH}))$

Aim 1: Demonstrate that oxidative ATP synthesis is impaired during high-intensity contractions.

Hypothesis 1a: Skeletal muscle oxidative capacity (k_{PCr}) will steadily decline as the duration of the fatigue trials get longer such that $k_{PCr24} > k_{PCr60} > k_{PCr120} > k_{PCr240}$.

Hypothesis 1b: Oxidative ATP synthesis, measured as the V_{iPCr}, will steadily decline beyond the first minute of the fatigue trials such that $V_{iPCr60} > V_{iPCr120} > V_{iPCr240}$.

Aim 2: Demonstrate that the accuracy of predicting V_{iPCr} during high-intensity contractions is improved by adjusting traditional ATP_{OX} calculation methods (29, 119, 206) for measured changes in V_{max}.

Although V_{iPCr} does not make assumptions about the ATP cost of force generation or mitochondrial coupling, it only yields one measure of ATP_{OX} per bout of contractions

9

and therefore cannot be used to study changes in ATP_{OX} over time unless participants perform multiple bouts of performance-matched contractions. This appears feasible in healthy young adults (35), but is not a long term solution to studying ATP_{OX} in clinical populations where muscle fatigue would make it difficult to repeat multiple bouts of contractions. Consequently, a continuous method for calculating ATP_{OX} that is not based on assumptions about the ATP cost of force generation or mitochondrial coupling is needed.

Hypothesis 2a: Calculations of ATP_{OX} will be significantly greater than V_{iPCr} following the 120 and 240 second trials when using traditional ATP_{OX} calculations, but not when the traditional ATP_{OX} calculations are adjusted to account for changes in V_{max}.

Exploratory Aim 1: Compare methods of estimating V_{max} for ATP_{OX} calculations

Two methods exist for using oxidative capacity measurements to estimate V_{max} for ATP_{OX} calculations. One method assumes creatine acts as a capacitor for distributing oxidatively generated ATP and calculates V_{max} as the product of $k_{PCr-baseline} \cdot [PCr]_{rest}$, with $k_{PCr-baseline}$ being the oxidative capacity of the muscle and $[PCr]_{rest}$ indicating maximal capacitance capacity (149). The alternative approach is to calculate V_{max} by fitting the instantaneous rates of PCr recovery and ADP or cytosolic phosphorylation potential (CPP) to a sigmoidal function using a multi-point analysis (90, 133). Recent work from Layec *et al*. suggests accurate prediction of V_{max} *in vivo* is only accomplished using the multipoint analysis method, as $k_{PCr-baseline} \cdot [PCr]_{rest}$ appears to grossly overestimate the State 3 *in vitro* measure of V_{max} (131). Consequently, the purpose of this

exploratory aim is to compare methods for calculating V_{max} and investigate their ability to predict V_{iPCr} throughout a 4-minute bout of high-intensity muscle contractions.

Hypothesis E1a: V_{max} estimations will be significantly higher when estimated by multiplying $k_{PCr\text{-}baseline} \cdot$ [PCr]$_{baseline}$ compared to the ADP and CPP multi-point analyses.

Hypothesis E1b: ATP$_{OX}$ calculations during the 4-minute fatigue protocol will be significantly greater when V_{max} is estimated by multiplying $k_{PCr} \cdot$ [PCr]$_{baseline}$, but not when using the ADP or CPP multi-point analysis methods.

Study 2: Mitochondrial Uncoupling and Oxidative ATP Synthesis during an Incremental Knee Extension Protocol

My working hypothesis is that mitochondrial uncoupling (i.e., reduced P/O ratio) impairs ATP$_{OX}$ during high-intensity contractions (12). This mitochondrial uncoupling not only coincides with the lactate threshold but is directly responsible for it and causes numerous other bioenergetic changes associated with high-intensity contractions and muscle fatigue such as intramuscular acidosis and augmentations in PCr depletion, Pi/PCr ratio, ADP accumulation, and changes in CPP.

To the best of my knowledge, methodological limitations have hindered the measurement of skeletal muscle P/O *in vivo* following a period of high-intensity contractions. To overcome this limitation, I adapted techniques used by Marcinek *et al*. (1, 49, 146) and Ryan *et al*. (177) to replicate *in vitro* mitochondrial respirometry under *in vivo* conditions using interleaved ^{1}H- and ^{31}P-MRS. Briefly, because PCr resynthesis is an oxidative process (71, 168), the rate of PCr recovery following a period of contractions can be used to estimate the rate of oxidative ATP synthesis. Similarly, the

rate of muscle oxygen consumption can be estimated by using ^{1}H-MRS to measure deoxymyoglobin appearance, an intramuscular protein that binds molecular O_2 and becomes visible in the ^{1}H-MRS spectrum as intramuscular pO_2 declines. Thus, P/O ratio within skeletal muscle can be estimated by measuring rates of PCr resynthesis and deoxymyoglobin appearance during brief bouts of ischemia; the ischemia being necessary to ensure that changes in deoxymyoglobin appearance are a direct reflection of the rate of muscle oxygen consumption and not affected by oxygen delivery from the cardiovascular system. Although muscle biopsy studies suggest PCr resynthesis does not occur in ischemia (71, 168), pilot testing in our lab has shown small changes (1-2 mM) can be observed early-on in the recovery period using ^{31}P-MRS, which is likely due to the faster temporal resolution of ^{31}P-MRS compared to biopsy studies.

Consequently, mitochondrial P/O ratio will be measured in eight healthy young men and women (21-40 years) after each stage of an incremental knee extension protocol. A total of 6 stages will be complete, each lasting 3 minutes with one isotonic knee extension being performed every 2 seconds. The starting workload will be equal to 10% of maximal voluntary isometric (MVIC) torque and increase by a load equal to 8% MVIC each stage thereafter. At the end of each stage, pressurized cuffs wrapped around the upper thigh and calf muscles will be inflated to induce ischemia in the quadriceps. During ischemia, the rates of PCr resynthesis and deoxymyoglobin appearance will be measured using interleaved ^{31}P- and ^{1}H-MRS, which will allow us to investigate the impact contraction intensity has on mitochondrial P/O ratio within skeletal muscle.

Aim 1: Directly demonstrate that P/O declines during high-intensity contractions.

Hypothesis 1a: During incremental contractions of the knee extensors, skeletal muscle P/O will remain constant for moderate-intensity contractions (i.e., power outputs below the lactate threshold) but will decrease during high-intensity contractions (i.e., power outputs above the lactate threshold).

Successful completion of the proposed work will provide critical insight into the mechanisms that limit oxidative phosphorylation *in vivo*. Study one will attempt to demonstrate that, in contrast to the progressive increases observed for muscle oxygen uptake, the rate of skeletal muscle oxidative ATP synthesis decreases throughout a bout of high-intensity contractions. This would eliminate the possibility that increases in muscle oxygen uptake are driven by increases in oxidative ATP synthesis (i.e., the increased ATP cost of force generation hypothesis), leaving mitochondrial uncoupling as the only remaining hypothesis to explain the VO_{2SC}. Study two will attempt to demonstrate that the onset of mitochondrial uncoupling within skeletal muscle coincides with the onset of the lactate threshold, which occurs well before skeletal muscles reach their capacity for maximal oxygen uptake. Together, these observations would all but eliminate the possibility that oxidative phosphorylation can be limited by factors such as oxygen availability or electron transport chain capacity and suggest instead that factors related to mitochondrial phosphorylation capacity set the upper limit to oxidative ATP synthesis. Subsequently, this would shift focus on the molecular limitations of oxidative phosphorylation to transport proteins and enzymes such as ATP synthase or adenine nucleotide translocase.

CHAPTER 2
LITERATURE REVIEW

Current models of oxidative phosphorylation are sufficient to describe skeletal muscle energetics during moderate-intensity contractions because ATP demand is met mainly by oxidative ATP synthesis and steady-state muscle metabolism is linearly related to power output. These metabolic conditions allow researchers to use 31-phosphorous magnetic resonance spectroscopy (^{31}P MRS) and basic principles of chemical thermodynamics to calculate rates of oxidative ATP synthesis (ATP$_{OX}$) from known relationships with cytosolic free creatine, [ADP], or phosphorylation potential (CPP) (119, 120, 129, 149, 215).

However, the mechanisms that limit and control oxidative phosphorylation *in vivo* during high-intensity contractions (i.e., above the lactate threshold) are not fully understood. Not only is steady-state metabolism delayed (58, 212, 213, 219), or unachievable, but the linearity between skeletal muscle metabolism and power output is distorted (58, 109). Specifically, the oxygen cost of high-intensity contractions is significantly greater than would be predicted by the linear relationship observed during moderate-intensity contractions, and is accompanied by non-linear augmentations in phosphocreatine (PCr) hydrolysis, acidosis, [ADP], and the free energy of ATP hydrolysis (10, 44, 83, 85, 104, 170, 174, 191). These non-linear changes in skeletal muscle oxygen consumption only occur during high-intensity contractions at power outputs above an individual's lactate threshold, and cumulatively describe the phenomenon known as the slow component of oxygen uptake kinetics (VO$_{2SC}$).

At present, the biochemical and molecular mechanisms underlying the VO$_{2SC}$ remain unclear (58, 109). The leading hypothesis for this response is that high-intensity

contractions increase the ATP cost of force generation, which was first proposed by

Rossiter *et al*. after observing similar kinetic responses between pulmonary oxygen

uptake and intramuscular PCr breakdown (174). However, there are several biochemical

aspects of the VO_{2SC} that increased ATP cost cannot reconcile. For example, the

magnitude of the VO_{2SC} is positively correlated with lactate accumulation (175), the

paradox being that the acidosis accompanying lactate accumulation should actually

impair muscle oxygen consumption due to its inhibitory effect on mitochondrial

respiration (70, 93). The augmentation of muscle oxygen consumption also occurs

despite the significant impairment to skeletal muscle oxidative capacity following high-

intensity contractions (28, 193). Thus, it is difficult to explain how muscle oxygen

consumption can increase if the capacity for oxidative phosphorylation is decreased. That

the non-linear increase in muscle oxygen consumption is predicted to originate within

Type-II muscle fibers is also paradoxical given that these fibers exhibit lower

mitochondrial density and tend to produce lower rates of ADP-limited respiration than

Type-I fibers (63, 86, 115), though this latter finding is not always consistent and can

depend on the substrates being oxidized (116, 153).

An alternative hypothesis for the VO_{2SC} is that high-intensity contractions cause

mitochondrial uncoupling (169), a process that dissipates the thermodynamic constraints

of the proton motive force and allows the electron transport chain (ETC) to consume

oxygen without restriction from the ATP-synthesizing components of oxidative

phosphorylation. Not only does this hypothesis provide a direct explanation as to why

muscle oxygen consumption increases non-linearly, but it also explains why acidosis

does not inhibit mitochondrial respiration, as mitochondrial uncoupling permits passive

movement of H^+ across the inner mitochondrial membrane. Mitochondrial uncoupling

may also directly explain why the VO_{2SC} coincides with both lactate accumulation and

increased PCr breakdown, as the mitochondrial malate-aspartate NADH shuttle and

adenine nucleotide translocator (ANT) are both electrophoretic (105, 118, 188), meaning

they rely on the electrical potential energy of the proton motive force to shuttle cytosolic

reducing equivalents (i.e., NADH) or ADP/ATP across the inner mitochondrial

membrane against their concentration gradients. Specifically, as the magnitude of

mitochondrial uncoupling increases, so too does dissipation of the electrical potential

energy across the inner mitochondrial membrane. Progressive impairment of the malate-

aspartate NADH shuttle would therefore be expected to cause progressively lower rates

of mitochondrial lactate oxidation, thereby explaining why the magnitude of the VO_{2SC} is

so closely associated with lactate accumulation. Similarly, progressive impairment of

ANT would cause a net efflux of ADP from the mitochondrial matrix into the

intermembranous space and cytosol, which would cause a right-shift in the cytosolic

creatine kinase equilibrium, thereby explaining why the VO_{2SC} also tends to coincide

with augmentations in PCr breakdown.

Despite several potential explanations for why mitochondrial uncoupling may be

responsible for altering muscle metabolism during high-intensity exercise, demonstration

of the concept has been hindered by a lack of testable predictions that can distinguish the

increased in ATP_{COST} and mitochondrial uncoupling hypotheses *in vivo*. That is, many of

mitochondrial uncoupling's predicted biochemical consequences are synonymous with

those that would be predicted in response to an increased ATP cost of force generation.

One difference between the two hypotheses is their predicted effect on ATP_{OX}. The

ATP$_{COST}$ hypothesis predicts that ATP$_{OX}$ increases during high-intensity contractions, whereas the mitochondrial uncoupling hypothesis predicts that the relationship between ATP$_{OX}$ and muscle power output is preserved, albeit at a higher rate of oxygen consumption, or under severe circumstances, diminished.

Muscle ATP$_{OX}$ can be calculated during skeletal muscle contractions using ^{31}P MRS, but most of these calculation methods inherently assume that the ATP cost of force generation remains constant (99) or that mitochondrial uncoupling does not occur (29, 55, 119, 206). Methods for measuring mitochondrial uncoupling in skeletal muscle *in vivo* are also limited. Techniques have been developed for estimating mitochondrial P/O (i.e., the ratio of ATP synthesized to oxygen consumed) in resting skeletal muscle (1, 145, 146), but to the best of my knowledge, this has not been replicated in muscles following a period of contraction.

Identifying experimentally-testable differences between these hypotheses requires an approach that integrates a general understanding of how the VO$_{2SC}$ manifests at the whole muscle and cellular levels with basic principles of chemical thermodynamics and their application to oxidative phosphorylation. The remainder of this review will be divided into sections that address each of these components.

Physiology Underlying the Slow Component of Oxygen Uptake Kinetics

The VO$_{2SC}$ primarily describes two important characteristics of skeletal muscle metabolism during high-intensity exercise. First, in contrast to the pulmonary oxygen uptake kinetics observed during moderate-intensity exercise, which increase monoexponentially and achieve steady-state within 2-3 minutes (219), attainment of

17

oxygen uptake steady state is significantly delayed, or unattainable, during high-intensity

exercise above the lactate threshold (219). Thus, the phrase 'slow component' developed

quite literally as a consequence of the slow and gradual increase in pulmonary oxygen

uptake observed beyond the 3rd minute of constant load work.
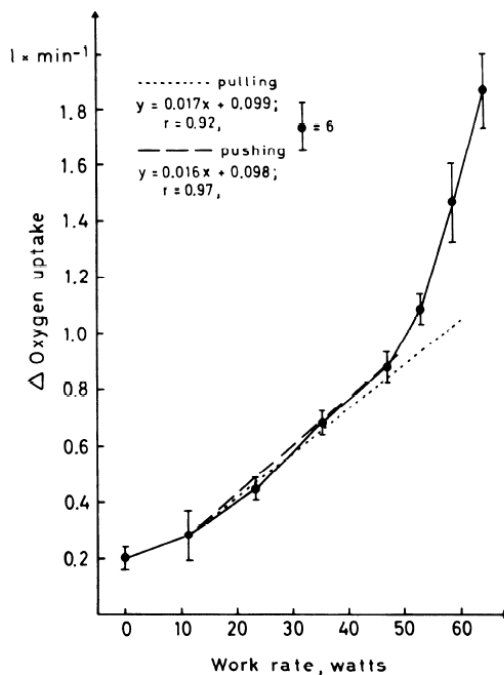
Figure 2.1: Augmentation of muscle oxygen consumption during incremental knee-extensions. Consistent with the whole-body response shown in Figure 1.1 (Chapter 1), the VO_{2SC} can also be observed in whole muscles using single-joint contraction modes. During high-intensity knee extensions at power outputs above the lactate threshold, the increment in oxygen uptake per Watt of power output is greater than would be predicted by the linear relationship established during moderate-intensity contractions (dashed line). *Figure from Andersen et al. (2).*

Second, the VO_{2SC} describes the augmentation in muscle oxygen uptake observed

for power outputs above the lactate threshold (Figure 2.1). Put another way, the oxygen

cost of high-intensity contractions is greater than would be predicted by the linear

relationship observed for power outputs below the lactate threshold (58). For example,

the oxygen cost of cycling equates to ~10 mL/W for power outputs below the lactate

threshold (11, 175) but increases by ~17 mL/W for power outputs approaching maximal

oxygen uptake (11). This increased oxygen cost of power production represents a

significant decline in the mechanical or metabolic efficiency of skeletal muscle and is

closely related to changes in muscle fatigue (29, 221).

18

Observations of the VO_{2SC} can be traced back to the early 1960s. In 1961, Astrand and Saltin demonstrated that pulmonary oxygen uptake does not plateau during bouts of exhaustive cycling lasting 2-8 minutes (4). Subsequent work by Whipp and Wasserman in the 1970s-80s demonstrated the VO_{2SC} only occurs above an individual's lactate threshold, regardless of fitness level (76, 208, 209, 212, 213). By the late 1980's researchers further understood that the magnitude of the VO_{2SC}, measured as the change in pulmonary oxygen uptake observed between the 3rd and 6th minute of exercise, is also highly correlated with blood lactate accumulation (175). However, because pulmonary oxygen uptake and blood lactate accumulation reflect whole body responses, it was unclear whether the VO_{2SC} originated within the contracting skeletal muscle or was caused by increases in heart rate or ventilatory activity by the diaphragm. Poole *et al*. resolved this question in 1991 by simultaneously measuring pulmonary and leg oxygen uptake in healthy young males during light and high-intensity cycling. Results showed that the exercising muscle mass accounts for approximately 85% of the pulmonary VO_{2SC} (167). Similar results have also been reported during knee-extension protocols (107, 111, 174). This was perhaps one of the most important findings in VO_{2SC} research because it established the contracting muscle mass as the primary origin of the VO_{2SC}, which stimulated new research investigations on the underlying whole muscle and cellular mechanisms.

Several studies have used surface electromyography (EMG) to investigate the relationship between the VO_{2SC} and increases in motor unit recruitment, with some reporting that increased EMG activity is associated with an increase in the VO_{2SC} (81, 113, 161, 179, 183) and others reporting that the VO_{2SC} can develop without changes in

EMG activity (37, 61, 186). The discrepancies between these results are not readily discernable but may be influenced by the methods used to calculate changes in VO_{2SC} magnitude or motor unit recruitment. Several studies have evaluated the VO_{2SC} during constant-load exercise by calculating changes in oxygen consumption or EMG activity after the 3rd minute (179, 181, 183). However, this calculation method assumes pulmonary or muscle oxygen consumption measured at 3-minutes reflects the response that would be predicted from the linear VO_2-power output relationship observed during moderate intensity contractions. Given that VO_2 on-kinetics can be influenced by factors such as training or starting intensity (217), this method may lead to inaccurate calculation of the VO_{2SC} magnitude or changes in other physiological variables such as EMG, to be calculated accurately.

The VO_{2SC} has traditionally been characterized as an increase in oxygen uptake during constant-load exercise (23, 173, 181). Recent investigations, however, have demonstrated that the increase in oxygen uptake relative to muscle power output can also be elicited by using 'all-out' exercise protocols in which oxygen uptake and muscle metabolism reach maximal levels despite a fall in power output or force generation (29, 221). Zoladz *et al*. demonstrated this concept by maximally recruiting dog gastrocnemius muscle for 4 minutes. Muscle oxygen consumption peaked within the first few minutes, but torque generation steadily declined, thereby causing the VO_2-torque time integral to increase. Because motor unit recruitment remained maximal due to the use of stimulated contractions, Zoladz *et al*. concluded that increased motor unit recruitment was not necessary to cause a increase in VO_2-power output or torque-time integral. Although this approach was criticized by Borrani *et al*. on the basis that the VO_{2SC} represents an

increase in VO_2 during constant load work (18), the data from all-out fatigue protocols indicate the VO_{2SC} manifests cellularly as a function of reduced metabolic or mechanical efficiency within fatiguing muscle fibers. Put another way, increases in motor unit recruitment or discharge rates are ultimately necessary to maintain muscle power output as higher-order motor units fatigue, and this may cause an increase in whole muscle oxygen consumption and the traditionally reported VO_{2SC} response (18). However, the VO_{2SC} can still manifest as an increase in the VO_2-power output relationship during all-out exercise, where increases in motor unit recruitment are not possible, suggesting that the mechanisms underlying the VO_{2SC} are closely linked to those underlying muscle fatigue.

Type-II muscle fibers have long been hypothesized to cause the VO_{2SC} at the cellular level due to the VO_{2SC}'s strong relationship with lactate accumulation and muscle fatigue (29, 175, 221). Consistent with this prediction, several studies have shown that the magnitude of the VO_{2SC} is positively correlated with MHC-II content (139, 141–143, 220), and Type-II fibers exhibit a greater ATP cost of force generation than Type-I fibers (50, 69). Moreover, Krustrup *et al*. have shown that neuromuscular blockade of Type-I fibers increases oxygen uptake during single-leg knee extension (112).

What remains unclear is *how* the VO_{2SC} may manifest within Type-II fibers at the biochemical and molecular levels. Once again, understanding that the onset of the VO_{2SC} coincides with the lactate threshold and progressively increases with increasing lactate accumulation is important (58, 175). Studies using ^{31}P-MRS to investigate other changes in skeletal muscle bioenergetics during incremental contraction protocols further suggest that the onset of the VO_{2SC} also coincides with non-linear increases in PCr breakdown,

acidosis, cytosolic ADP accumulation, and the cytosolic phosphorylation potential (10, 44, 83, 85, 104, 191). Although an increased ATP cost of force generation and mitochondrial uncoupling have been hypothesized as biochemical mechanisms for the VO_{2SC} (169, 174), there are presently no experimentally testable predictions that are unique to either hypothesis. Consequently, we must take a closer look at the thermodynamic mechanisms that regulate and control oxidative phosphorylation, as well as the integrative relationships between muscle fatigue and changes in energy demand by ion pumping and cross-bridge cycling ATPases.

Chemical Thermodynamics and the Mechanism of Oxidative Phosphorylation

The favorability and direction of a chemical reaction is determined by its Gibbs free energy (ΔG), which defines the energy required to do work. Negative ΔG values indicate that a reaction is exergonic, or favorable, and has the capacity to be used for work. In contrast, endergonic reactions exhibit a positive ΔG value, the magnitude of which indicates the minimum amount of energy required to catalyze the reaction. In biological systems, cellular work processes are accomplished by enzymes that physically couple endergonic reactions to exergonic reactions of greater (i.e., more negative) ΔG magnitude. That is, the free energy cost ($+\Delta G$) of endergonic reactions are overcome, or paid for, by enzymatic coupling with an exergonic reaction of greater free energy release ($-\Delta G$), such that the net ΔG of the combined reaction is negative and therefore overall thermodynamically favorable (189). The clearest examples of this are enzymes that have evolved to use the $-\Delta G$ of ATP hydrolysis to overcome the $+\Delta G$ cost of endergonic cellular work processes, such as ion pumping by the Na^+-K^+- and Ca^{2+}-ATPases or cross

bridge cycling by the myosin-ATPases. This means cellular work cannot occur unless the

ΔG release of ATP hydrolysis exceeds the ΔG cost of the work being done, which has

significant implications for muscle fatigue because the ΔG of ATP hydrolysis decreases

as contraction intensity increases (85).

The reactions of oxidative phosphorylation, including the reduction of O_2 to water

by cytochrome-c oxidase, also follow these simple principles of chemical

thermodynamics. At present, the currently accepted model of oxidative phosphorylation

is based upon the Chemiosmotic Theory detailed by Dr. Peter Mitchell in 1961 and

subsequent comprehensive works by others that elucidated the intracellular factors

responsible for regulating both the kinetics and stoichiometries of coupling mitochondrial

oxygen consumption to the phosphorylation of ADP within the mitochondrial matrix (15,

39, 88, 105, 151). Briefly, phosphorylation of matrical ADP by ATP synthase is driven

by the exploitation of an electrochemical potential energy (i.e., proton motive force),

generated by the unidirectional pumping of H^+s across the inner mitochondrial membrane
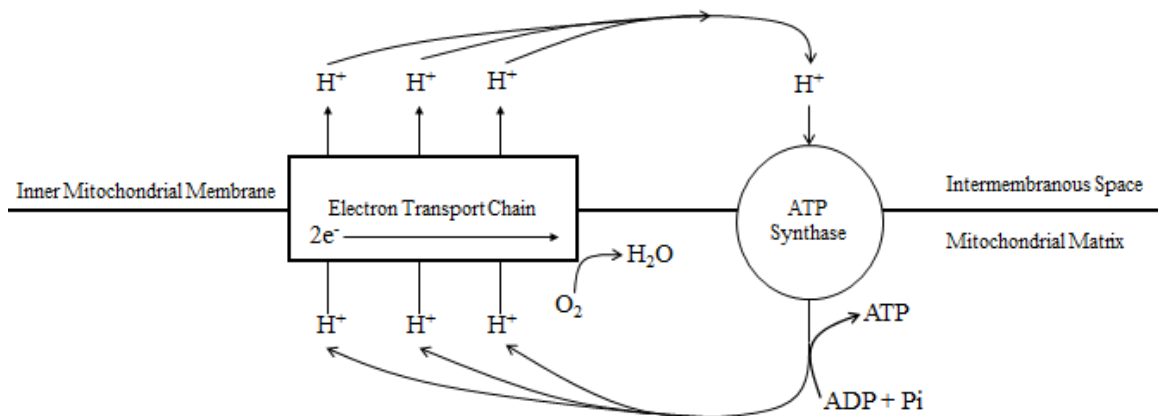
Figure 2.2: Basic schematic of Peter Mitchell's Chemiosmotic Theory of oxidative phosphorylation (151, 159).

(Figure 2.2). This H^+ pumping is accomplished by a series of enzymes forming an

electron transport chain that utilize the Gibbs free energy (ΔG) release of shuttling

electron pairs to overcome the ΔG cost of pumping H^+ against their concentration gradient. Electron shuttling by the ETC concludes with the reduction of molecular O_2 to H_2O by cytochrome-c oxidase, thereby releasing electron pairs from the ETC and yielding H_2O and CO_2 as "waste" products, the latter of which is produced during the oxidation of carbon-chain foodstuffs by enzymes of the citric acid cycle to generate the NADH and $FADH_2$ necessary to fuel the ETC with electron pairs.

The thermodynamics of ATP synthesis by ATP synthase are conceptually straightforward. The ATP synthase complex contains two protein structures, F_0 and F_1, that function cooperatively like a hydraulic turbine (136). Phosphorylation of ADP within the mitochondrial matrix is catalyzed by the F_0 subunits, which rotate mechanically when H^+s flow through the F_1 stalk structure. Consequently, the endergonic phosphorylation of ADP is thermodynamically favorable only when the electrochemical $-\Delta G$ of H^+ translocation through F_1 exceeds the $+\Delta G$ of ATP synthesis by F_0, the latter of which is controlled by the matrical phosphorylation potential (MPP).

The basic schematic in Figure 2.2 is expanded in Figure 2.3 (below) to incorporate the mechanisms that control MPP. Pioneering works by Chance and colleagues demonstrated that under state-3 conditions, in which thermodynamic equilibrium is attained between rates of ATP synthesis and hydrolysis, mitochondrial respiration *in vitro* is primarily controlled by changes in cytosolic [ADP] (39, 43), which is transported across the inner mitochondrial membrane in exchange for ATP by the adenine nucleotide translocator (ANT) (105, 188, 216). By the mid-1980s, advances in ^{31}P MRS technology significantly improved the study of skeletal muscle bioenergetics *in vivo*. Chance *et al*. leveraged these technological advances to show that changes in
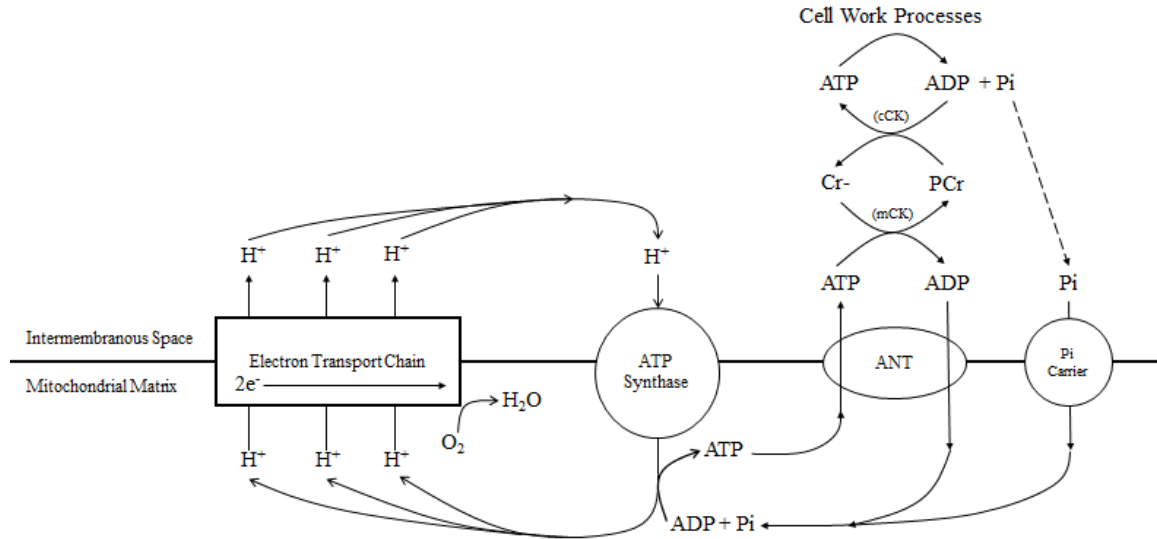
Figure 2.3: Expanded illustration of the control of oxidative phosphorylation.
Shuttling of ADP/ATP across the inner mitochondrial membrane (IMM) by adenine
nucleotide translocase (ANT) primarily controls the matrical phosphorylation potential
(MPP – ADP·Pi/ATP) and therefore the ΔG cost of ATP synthesis. Mitochondrial (mCK)
and cytosolic (cCK) creatine kinases act as chemical capacitors, which reduces ADP and
ATP diffusion distances and allows them to remain localized near sites of production
(ATP synthase) and consumption (cellular work processes). The outer mitochondrial
membrane has been omitted for visual clarity because it is permeable to most metabolites.

Pi/PCr, a proxy for cytosolic [ADP], are linearly related to increments in muscle work-

rate under steady-state conditions, suggesting the ADP-control of mitochondrial

metabolism observed *in vitro* is also observed *in vivo* when skeletal muscle metabolism

attains steady-state (40). Although others have shown that changes in [Pi] can also affect

the rate of oxygen consumption (84), recent work from Jeneson *et al.* has shown that

mitochondria are ultrasensitive to changes in cytosolic [ADP], which exhibits second-

order kinetic control over oxidative phosphorylation *in vivo* (90). Thus, while changes in

[Pi] can influence mitochondrial metabolism, the rate of oxidative phosphorylation is

overwhelmingly controlled by changes in cytosolic [ADP].

However, because cytosolic [ADP] is kept low, diffusion distances between sites

of production and phosphorylation may be limiting to oxidative phosphorylation. To

overcome this limitation, ANT is functionally coupled to the mitochondrial isoform of

creatine kinase (mCK), which catalyzes the conversion of free creatine (fCr^-) to PCr by hydrolyzing ATP in the intermembranous space. This process occurs in the immediate vicinity of ANT, allowing ADP to be quickly transported back into the mitochondrial matrix where it can be phosphorylated once again. Thus, the creatine kinase shuttle acts as a chemical capacitor that allows mitochondria to achieve rapid rates of oxidative phosphorylation at low concentrations of ADP (15, 149).

Similar to the thermodynamic control of ATP synthesis by ATP synthase, the thermodynamic control of oxygen consumption and ETC activity is relatively straightforward. Like ATP synthesis, proton pumping by the ETC is endergonic and therefore coupled to the exergonic electron shuttling reactions of complexes 1, 3, and 4. Consequently, proton pumping by the electron transport chain only occurs when the ΔG release of electron shuttling exceeds the ΔG cost of pumping H^+s against their concentration gradient. This relationship between proton pumping and electron shuttling highlights oxygen's importance to oxidative phosphorylation as an energetic system. Without oxygen, electron pairs cannot be released from the ETC, which decreases the thermodynamic favorability of electron shuttling and causes both electron shuttling and proton pumping by the ETC to slow or cease. In turn, this hinders generation of the proton motive force, thereby reducing the ΔG release of H^+ flow through the F_1 structure of ATP synthase and impairing its ability to synthesize ATP. Hence, inadequate oxygen supply, or hypoxia, hinders ATP synthesis by limiting the rate at which the proton motive force and be generated and then subsequently utilized.

However, oxidative phosphorylation is designed such that oxygen consumption and ETC activity are functionally controlled by the activity of ATP synthase. That is,

when cellular ATP demand is low there is no need to generate ATP and the ΔG cost of

ATP synthesis within the mitochondrial matrix exceeds the ΔG release of proton flow

through the F_1 structure. Because this inhibits proton flow through ATP synthase, the ΔG

cost of proton pumping exceeds the ΔG release of electron shuttling, causing both ETC

activity and oxygen consumption to slow or cease. Under these conditions, oxidative

phosphorylation and mitochondrial respiration are under state-3 control. Though this is

commonly described as 'ADP-limited respiration' due to the manner in which state-3

oxygen consumption rates are stimulated *in vitro* by boluses of ADP (39, 43, 78), I

believe the more appropriate conceptual description is MPP-limited, as the ΔG cost of

ATP synthesis within the mitochondrial matrix is not determined solely by ADP, but

rather the ΔG cost of the entire ATP synthesis reaction (i.e., ADP + Pi → ATP).

What is absolutely critical to understand, however, is that in contrast to the

obligatory coupling observed between H^+ flow and ATP synthesis by ATP synthase, or

H^+ pumping and electron shuttling by the ETC, mitochondrial oxygen consumption and

ETC activity are only *functionally* coupled to ATP synthesis by ATP synthase (159). That

is, the only thermodynamic limitation to ETC chain activity and oxygen consumption is

the ΔG cost of pumping protons against the electrochemical potential energy of the

proton motive force. Under state-3 conditions, ATP synthase is the only major conduit

for H^+ reentry into the mitochondrial matrix. However, if H^+s can reenter the

mitochondrial matrix through channels other than ATP synthase, such as uncoupling

proteins or chemical protonophores (187, 196), then the magnitude of the proton motive

force is dissipated, which causes the ΔG release of electron shuttling to once again

exceed the ΔG cost of proton pumping. This process, known as mitochondrial

uncoupling, is illustrated in Figure 2.4, which depicts the increased rate of oxygen

consumption and diminished capacity for ATP synthesis by ATP synthase due to passive

proton flow through an uncoupling protein (UCP). Thus, whereas oxygen consumption,

electron shuttling, and proton pumping are all obligatory for oxidative ATP synthesis

(Figures 2.2 and 2.3), oxidative ATP synthesis is not obligatory for proton pumping,

electron shuttling, and mitochondrial oxygen consumption.
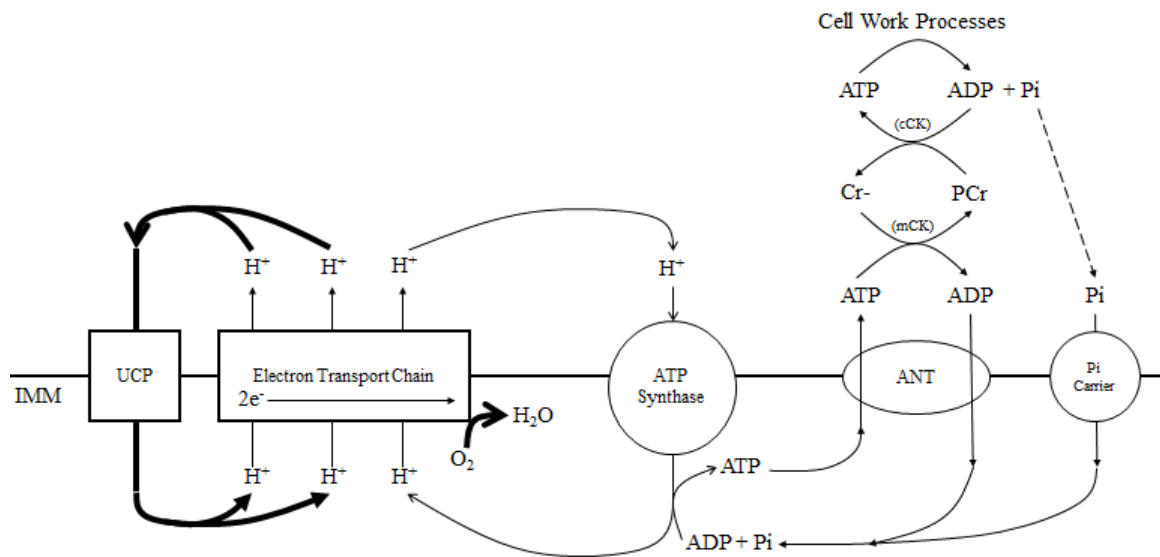
Figure 2.4: Dissipation of the proton motive force by mitochondrial uncoupling. H^+
flow through channels other than ATP synthase, such as an uncoupling protein (UCP),
diminishes the capacity for oxidative ATP synthesis while increasing ETC activity and
oxygen consumption. The bold lines indicate the relative activity level of each reaction.

This thermodynamic relationship between mitochondrial ATP synthesis and

oxygen consumption gives us an opportunity to investigate the biochemical mechanisms

underlying VO_{2SC} by using ^{31}P-MRS to examine the effect high-intensity contractions

have on oxidative ATP synthesis and PCr resynthesis. Before examining this relationship,

however, we need to review exactly how the increased ATP cost of force generation and

mitochondrial uncoupling hypotheses explain the VO_{2SC} and other non-linear changes in

skeletal muscle bioenergetics during high-intensity contractions.

Biochemical Mechanisms of the Slow Component of Oxygen Uptake Kinetics

The key predictions of the increased ATP cost (ATP_{COST}) of force generation hypothesis are that augmentations in muscle oxygen consumption reflect increased rates of oxidative ATP synthesis, and that the increase in PCr breakdown is a function of greater creatine kinase shuttling activity, due to its role as a chemical capacitor to the oxidative phosphorylation system (15, 149). Changes in lactate accumulation and acidosis are also predicted to coincide with the augmentation of muscle oxygen consumption as a result of oxidative ATP synthesis being unable to match cellular ATP demand. Physiologically, the ATP_{COST} hypothesis is predicted to reflect Type IIb muscle fiber recruitment, which is reasonable considering that these fibers exhibit lower mitochondrial content than Type I fibers but a greater ATP cost of force generation (50, 63, 69). However, this hypothesis does not readily explain why the magnitude of the VO_{2SC} would be so closely correlated to lactate accumulation. The difference between muscle ATP demand and oxidative ATP synthesis could progress linearly as power output above the lactate threshold increases, but to the best of my knowledge, this has not been investigated.

Alternatively, the mitochondrial uncoupling hypothesis predicts the increased rate of muscle oxygen consumption is a function of proton leak across the inner mitochondrial membrane (169), potentially due to the activation of mitochondrial uncoupling proteins (152, 176). This would also alter the function of electrophoretic transport proteins that rely on the proton motive force to shuttle metabolites across the inner mitochondrial membrane, such as the malate-aspartate NADH shuttle and ANT. Consequently, mitochondrial uncoupling could also explain why the VO_{2SC} coincides and correlates

29

with lactate accumulation and PCr breakdown, as increased uncoupling would progressively impair the electrophoretic behavior of the malate-aspartate NADH shuttle and ANT.

The only difference between the ATP_{COST} and mitochondrial uncoupling hypotheses are their predicted effects on oxidative ATP synthesis. The ATP_{COST} hypothesis predicts that increases in muscle oxygen consumption are a direct indication of increased oxidative ATP synthesis, whereas the mitochondrial uncoupling hypothesis predicts that oxidative ATP synthesis is impaired due to dissipation of the proton motive force through non-ATP synthase conduits. Several methods exist for using ^{31}P-MRS to measure the rate of oxidative ATP synthesis in contracting muscle, but only a few investigations have used ^{31}P MRS to study the VO_{2SC}. Broxterman *et al*. reported an increase in the ATP cost of force generation during 5-minutes of 'all-out' isometric knee extensions (29). However, a sigmoidal ADP model that excludes the possibility of mitochondrial uncoupling was used to calculate oxidative ATP synthesis. As discussed above, mitochondrial uncoupling impairs ANT function, which ultimately causes net ADP export from the mitochondrial matrix (105, 188). Thus, sustained increases in ADP may not necessarily reflect a concomitant increase in oxidative ATP synthesis, in which case the increased ATP cost of force generation reported by Broxterman *et al*. was a function of method bias (29).

Pilot work in our lab suggests that hyperbolic methods of calculating oxidative ATP synthesis overestimate the initial rate of phosphocreatine resynthesis (V_{iPCr}) during high-intensity contractions. V_{iPCr} is considered a gold standard for measuring oxidative ATP synthesis because it requires no assumptions about metabolic steady-state, changes

in the ATP cost of force generation, or mitochondrial coupling (Figure 2.5). However, a major weakness of using V_{iPCr} to calculate ATP_{OX} is that it only yields 1 measurement of oxidative ATP synthesis per bout of contractions, meaning multiple trials of varying duration must be performed to investigate changes in oxidative ATP synthesis over time. Cannon *et al*. recently used this method to study the VO_{2SC} during moderate- and high-intensity knee extensions and reported that, although the ATP cost of force generation tended to increase during the high-intensity trial, this increase was insufficient to fully account for the magnitude of the VO_{2SC} (35), suggesting mitochondrial uncoupling may have contributed to the augmentation of VO_2.

Figure 2.5: Hyperbolic ATP$_{OX}$ calculations vs. V_{iPCr}. Traditional methods for calculating oxidative ATP synthesis (black circles) overestimate the initial velocity of PCr resynthesis (red bar) following high intensity contractions. This suggests that previous reports of an increased ATP cost of force generation (13) may be due to calculation biases that fail to include the potential for mitochondrial uncoupling.

Notably, high inorganic phosphate concentration and acidosis have been shown to impair creatine-stimulated respiration *in vitro,* despite not affecting maximal ADP-stimulated respiration rates (205). This suggests V_{iPCr} may not necessarily indicate the true rate of oxidative ATP synthesis following high-intensity contractions, and may offer an explanation as to how the rate of oxidative ATP synthesis could increase despite the negative effects that high-intensity contractions have on oxidative capacity (28, 193), which is commonly measured as the rate constant of PCr resynthesis (k_{PCr}) (103, 130).

Consistent with the ATP$_{COST}$ hypothesis, the augmentation in cytosolic ADP accumulation tends to coincide with the augmentation in PCr breakdown during incremental contraction protocols (85, 170), which would be expected to occur if mitochondrial sensitivity to creatine is progressively decreasing. The increase in cytosolic ADP may also explain why these events, as well as the VO$_{2SC}$, coincide and correlate with changes in lactate accumulation, as ADP accumulation within the cytosol will also stimulate greater activation of the glycolytic pathway and may cause a mismatch between the rates of non-oxidative glycolysis and mitochondrial oxidation of cytosolic pyruvate and NADH (94, 204). However, a closer examination of the thermodynamics associated with muscle oxygen consumption during recovery suggest these considerations are unlikely.

Recall that oxygen consumption only occurs when the ETC is active, which requires the ΔG cost of H$^+$ pumping to be lower than the ΔG release of electron shuttling. In short, oxygen consumption indicates that protons are reentering the mitochondrial matrix, but it does not necessarily indicate *how* the protons are reentering this matrix. If the VO$_{2SC}$ is indeed caused by an increased ATP cost of force generation, then the diminished rate of PCr resynthesis following high-intensity contractions should be matched by a rapid decline in muscle oxygen consumption during the recovery period. Consistent with this prediction, Krustrup *et al*. reported similar recovery kinetics for muscle oxygen following low- and high-intensity contractions (111). However, measures were collected on 7 participants, and only 4 of those demonstrated a VO$_{2SC}$ response, suggesting three of the participants did not actually complete high-intensity contractions. Moreover, only the kinetic parameters for the primary recovery component were

reported, making it difficult to ascertain whether the overall rate of muscle oxygen consumption in recovery following the high-intensity contractions was strictly monoexponential or if a slow, secondary, component of elevated muscle oxygen consumption was evident after the primary component.

In contrast, work by Bangsbo *et al*. has shown that following high-intensity contractions, less than 50% of muscle oxygen consumption can be attributed to recovery processes, such as ATP and PCr resynthesis (6–8). These data suggest that while the primary time constants of muscle oxygen consumption may not differ following low- and high-intensity contractions, a slow component of post-exercise oxygen consumption does occur following high-intensity contractions, and therefore represents a large volume of consumed oxygen that must be accounted for. That is, if PCr resynthesis is impaired, then the only explanation that would still support the ATP_{COST} hypothesis is sustained activity of ion-pumping ATPases. However, high-intensity contractions appear to impair the activity of ion-pumping ATPases (56, 137, 138, 147) and maximal Na^+-K^+-ATPase activity only appears to account for ~2 % of total ATP turnover (148). This is a crucial detail, because if PCr resynthesis, ATP repletion, and ATP consumption by ion-pumping ATPases cannot account for the excess muscle oxygen consumption observed following high-intensity contractions, then the only thermodynamically possible explanation is mitochondrial uncoupling. By extension, this suggests that V_{iPCr} can still be used as a gold standard of oxidative ATP synthesis during high-intensity contractions despite the impairing effects of high H^+ and Pi accumulation (205). More work investigating oxygen consumption kinetics during recovery from high-intensity contractions is needed to unravel these differences.

Summary

The mechanisms of the VO_{2SC} and altered control of oxidative phosphorylation during high-intensity contractions are not fully understood. Increased ATP cost of force generation and mitochondrial uncoupling are two leading hypotheses, but myriad experimental limitations have hindered investigations that can distinguish between the two *in vivo*. Both hypotheses offer logical explanations to why skeletal muscle bioenergetics are non-linearly augmented during high-intensity contractions, but their predictions about ATP_{OX} are mechanistically different. The ATP_{COST} hypothesis predicts that ATP_{OX} increases during high-intensity contractions, whereas the mitochondrial uncoupling hypothesis predicts diminished ATP_{OX}.

^{31}P-MRS can be used to measure muscle ATP_{OX} during high-intensity muscle contractions, but most methods are inappropriate for studying the VO_{2SC} because they inherently assume a constant ATP cost (99) or maintained P/O ratio (29, 55, 120, 206). The initial velocity of PCr resynthesis can also be used to measure ATP_{OX}, but this method only yields 1 measurement per bout of contractions, and the metabolic conditions associated with high-intensity contractions appear to impair PCr resynthesis (205). At this time, the excess oxygen consumed by muscle following high-intensity contractions does not appear to be related to a sustained rate of ATP turnover (47, 147, 148). Given the thermodynamic constraints associated with mitochondrial oxygen consumption, these results erode enthusiasm for the ATP_{COST} hypothesis and suggest that V_{iPCr} is not only a valid measure of ATP_{OX} following high-intensity contractions, but that mitochondrial uncoupling is at least partially responsible for the VO_{2SC} (35). The goal of this

dissertation is to provide experimental evidence indicating which of these two hypotheses

may be correct.

CHAPTER 3

METHODS

Study 1 – Oxidative ATP Synthesis During High-Intensity Contractions

Participants

Nine healthy young adults, 25-40 years old, will be recruited from Amherst and the surrounding communities using fliers and word-of-mouth. Individuals who participated in previous studies and indicated they would be interested in participating again in the future will be contacted by phone or email. All participating individuals will be screened by telephone to determine their eligibility (see Telephone Eligibility Screening Form (Study 1, Appendix B) before any visits were scheduled.

Inclusion and Exclusion Criteria

Inclusion criteria for Study 1 are:

- Generally healthy, by self-report

- Ambulatory without the use of walking aids

- Living independently in the community

- Non-smokers; for at least the preceding 2 years

    Exclusion criteria for Study 1 were:

- Metal implants or other contraindications for magnetic resonance studies

- History of major neurological, neuromuscular, cardiovascular pulmonary or

    metabolic disease

- Uncontrolled hypertension (blood pressure > 140/90)

- Moderate to severe lower extremity arthritis or pain (i.e., pain on level walking or that limits activities of daily living such as household ambulation and self-care)

- The use of beta-blockers, sedatives, tranquilizers, or other medication that may impair physical function, such as statins

- Failure to pass the Physical Activity Readiness Questionnaire Plus (PAR-Q+, Appendix D), to be cleared for participation in physical activity

- Pregnancy, as determined by self-report

- An inability to understand written and spoken English

- An inability to follow instructions, as determined by the investigators during the consenting process

Because exercise training improves skeletal muscle oxidative capacity (123, 124, 129), which may affect the muscle fatigue and bioenergetic responses during the oxidative capacity and experimental trials (125), we will exclude participants who report engaging in more than 1 hour of physical activity per day at least 5 days per week.

Paperwork and Experimental Setup

Study one will require one visit lasting 2-3 hours and take place in the Human Magnetic Resonance Center (*h*MRC) at the Institute for Applied Life Sciences on the University of Massachusetts Amherst campus. Upon arriving to the *h*MRC, participants will read an informed consent document (Appendix A) and have any questions answered by the investigator. After agreeing to participate and signing the consent form, participants will fill out a Medical History Form (Appendix D), Physical Activity Readiness Questionnaire Plus (Appendix E), and Magnetic Resonance (MR) Safety Form

(Appendix F). Next, measures of blood pressure, height, and body mass will be obtained. Before entering the magnet room, participants will meet with the MR Operator to review their MR Safety Form, remove all jewelry, empty their pockets, and walked through a metal detector.

Participants will then be escorted to the MR-scanner and positioned on their back with their dominant leg on top of a custom-built knee extension ergometer. The ankle, knee, and thigh will be strapped to the ergometer using Velcro straps. Inelastic straps will also be secured over the participants' hips to prevent unwanted extraneous movement during the experimental protocols. To measure changes in intramuscular phosphate concentrations, a dual-tuned probe (2 copper coil loops for proton and phosphorous, 10.5 x 8 cm) will be secured over the vastus lateralis muscle (VL) using elastic wrap and Velcro straps. Headphones will be provided to limit the amount of noise from the MR scanner and to enable clear communication between the participant and the investigators. The participant's VL will then be positioned in the center of the MR scanner.

Contraction Protocols

To investigate the effect that high-intensity contractions have on the rate of oxidative ATP synthesis (ATP_{OX}; $mM \cdot s^{-1}$) within skeletal muscle, participants will complete multiple trials of a fatiguing knee-extension protocol. The duration of each trial will progressively increase, allowing ATP_{OX} to be measured directly from the initial velocity of PCr resynthesis (V_{iPCr}; $mM \cdot s^{-1}$) at multiple time points. To begin, participants will perform 2-3 maximal voluntary isometric (i.e., 'static') contractions (MVIC), each lasting 3-5 s, to determine their maximal torque. At least 1 minute of rest will be given

between each of these contractions. Participants will then perform 2-3 sets of 3 maximal voluntary isokinetic contractions (MVDC) at a speed of $120°·s^{-1}$ to determine maximal power.

Next, participants will complete an oxidative capacity protocol starting with 90 s of rest, followed by 24 s of isokinetic MVDCs ($120°·s^{-1}$, 1 contraction every 2 s), and 7 minutes of passive recovery. Participants will then complete 3 more trials of isokinetic MVDCs at a speed of $120°·s^{-1}$ (1 contraction every 2 s). Each trial will start with 90 s of rest and be followed by 10 minutes of passive recovery. The duration of the contractile period in these experimental will trials increased from 60 s in trial 1 to 120 and 240 s for trials 2 and 3, respectively.

Measurements of force, velocity, and power produced for each contraction of the oxidative capacity and experimental trials will be recorded by a custom-written MATLAB program (The MathWorks Incorporated, Natick, Massachusetts) and subsequently exported for further analysis in Excel. Contractions will be averaged in 4 s intervals (i.e., 2 contractions) for the first 40 s and 10 s intervals thereafter (i.e., 5 contractions). Total work (Joules), torque-time integral (TTI; Nm·s), and muscle fatigue (% max power) will be compared across all trials (i.e., at 24, 60, 120, and 240 s) to ensure that muscle performance between trials is consistent, thereby allowing us to assume that V_{iPCr} measured at the end of the 24, 60, and 120 s trials is representative of ATP_{OX} during the 240-s trial. When total work or TTI during the 120 and 240 s trials are more than 15% lower than the total work or TTI performed during both the 24 and 60 s trials, the participant will be asked to reperform the 120 and 240 s trials.

Muscle fatigue will be quantified according to Callahan and Kent-Braun (33):

Muscle Fatigue (% max power) = 100 · (avg PP) / (0.5 · ($PP_{baseline}$ + $PP_{protocol}$)) Eq# 1

Where avg PP (peak power) is the average peak power measured over a given time interval of the experimental trial (4 or 10 s), $PP_{baseline}$ is the highest power measured during the baseline isokinetic MVDCs, and $PP_{protocol}$ is the highest power measured during a single contraction at the beginning of the experimental trial.

Before leaving the *h*MRC, participants will be given a uniaxial accelerometer (ActiGraph GT3X, Pensacola, Florida) to quantify habitual physical activity, which will be analyzed to ensure that none of the participants are actively engaged in one or more hours of physical activity per day, as per the exclusion criterion described above. Participants will be instructed to wear the accelerometer on their right hip for 7 days and to record their physical activity in a log book. At the end of the week-long wear period, the accelerometer and physical activity log will be collected by the principal investigator at a time and place that was most convenient for the participant. Accelerometer data will be recorded in 60 s epochs and processed using ActiLife v6.13 software (ActiGraph, Pensacola, FL), with a minimum of 10 hours of wear time being required for a given day to be included in the analysis. Days meeting this criterion will be the analyzed for average daily activity counts and minutes spent in moderate-vigorous physical activity using established thresholds for uniaxial ActiGraph accelerometers (57).

Spectroscopy

Gradient-echo scout images of the thigh will be collected to ensure proper placement of the coil relative to the participant's thigh muscles, and of the muscles relative to the magnetic isocenter of the MR scanner. The homogeneity of the magnetic

field will be optimized by shimming on the proton (^{1}H) signal to minimize the full width at half-maximum of the water peak. Measures of non-localized ^{31}P-MRS will be collected continuously throughout the oxidative capacity and MVDC trials using the following acquisition parameters: 60° nominal hard pulse, 4,000 Hz bandwidth, 2,048 complex points, and a 2s repetition time (TR). A total of 270, 375, 405, and 465 acquisitions will be collected for the oxidative capacity protocol, and 60, 120, and 240 s experimental trials, respectively.

All spectral analyses will be conducted in jMRUI v6.0beta (156). Because the short TR used for the contraction protocols results in partial saturation of the spectra, the first 30 s (15 free induction decays) of every protocol will be excluded from analysis in order to avoid errors in metabolite quantitation due to changes in partial saturation effects during this period. The remaining free induction decays will be averaged to yield temporal resolutions of 60 s at rest, 4 s for all 24 s of the oxidative capacity protocol and the first 40 s of the experimental trials, followed by 10-s temporal resolution thereafter. During recovery, free induction decays will be averaged to yield temporal resolutions of 4 s for the first 20 s of recovery, 8 s for the ensuing 280 s of recovery, and 30 s for the remainder of recovery. The resulting free induction decays will be zero-filled (2,048 points) and apodized using a 1Hz Lorentzian filter. Following Fourier transfrom, spectra will be manually phased and the x-axis will be zeroed on PCr. An ER-Filter will be used to truncate the bandwidth above and below 10 and -6 ppm, respectively. We will use the AMARES algorithm and previously-developed prior knowledge files to linefit peaks corresponding to phosphomonoesters (PME), the Pi doublet (when observeable), phosphodiesters (PDE), PCr, and the γATP doublet (199).

The concentration of γATP at rest will be assumed to equal 8.2 mM and used to normalize γATP during and after all contraction protocols, so that potential changes in [ATP] can be evaluated. The concentrations of Pi, PCr, and PME will be calculated by correcting the measured signal intensities using experimentally-derived saturation correction factors, and assuming the sum of Pi+PCr+PME is equal to 42.5 mM (72). Although most previous studies have used the sum of only Pi and PCr (119, 124, 125), recent work in our lab supports prior work by Bendahan *et al*. that signal loss due to Pi trapping within the glycolytic pathway during high-intensity contractions may result in poor estimations of metabolite concentrations when summing only the Pi and PCr signals (14). Inclusion of the PME peak appears to rectify this inaccuracy (*unpublished data*). Total creatine (TCr) will be assumed to be equal to 42.5 mM and the concentration of free creatine (fCr) will be assumed to be equal to Pi (119, 122, 125). ADP concentration will be calculated based on the creatine kinsae equilibrium (K'_{CK}):

$$[ADP] \text{ (mM)} = ([ATP][Pi]) / ([fCr] \cdot K'_{CK}) \hspace{3cm} \text{Eq\# 2}$$

We will correct K'_{CK} for changes in cytosolic pH according to an exponential equation derived from experimental data reported by Golding *et al*. (65):

$$K'_{CK} = 241147065 \cdot e^{(-2.02 \cdot pH)} \hspace{4cm} \text{Eq\# 3}$$

Muscle pH will be calculated from the chemical shift between Pi and PCr (154), and weighted for each peak when Pi splitting is observed, according to the equation:

$$pH = \text{average } (pH_1 \cdot Pi_{1signal}/\text{Total } Pi_{signal} + pH_2 \cdot Pi_{2signal}/\text{Total } Pi_{signal}) \hspace{1cm} \text{Eq\# 4}$$

The cytosolic phosphorylation potential (CPP) will be calculated as:

$$CPP = ([ADP][Pi])/[ATP] \hspace{5cm} \text{Eq\# 5}$$

Data Analysis – Measurement of Skeletal Muscle k_{PCr}

Baseline oxidative capacity will be determined following the 24-s MVDC protocol by fitting the observed PCr recovery curve with a mono-exponential function:

$$PCr(t) = PCr_{End} + Amp \cdot (1 - Exp^{(-k_{PCr} \cdot t)}) \qquad \text{Eq\# 6}$$

where PCr(t) is the measured [PCr] at time point t, PCr_{End} is the [PCr] at the end of the contraction, Amp is the amplitude of the recovery in mM, and k_{PCr} is the mono-exponential rate constant, which reflects the system's oxidative capacity. Consistent with the alteration of oxygen uptake kinetics during high intensity exercise and recovery (58), PCr recovery following prolonged high-intensity contractions is impaired (28, 193), and does not follow a mono-exponential recovery pattern (71, 193). Consequently, oxidative capacity following the experimental protocols will be calculated by fitting the measured PCr recovery curve with both mono- (Eq 6) and bi-exponential (Eq 7) functions:

$$PCr(t) = PCr_{End} + ((Amp_1 \cdot (1 - Exp^{(-k_{PCr1} \cdot t)})) + (Amp_2 \cdot (1 - Exp^{(-k_{PCr2} \cdot t)})) \qquad \text{Eq\# 7}$$

where PCr(t), Amp, k_{PCr}, and 't' all have their original meanings, and 1 and 2 denote the primary and secondary recovery components, respectively. The function yielding the lowest sum of least squared differences will be used to determine k_{PCr}. An example of improved fitting following a 240-s trial when using a biexponential function compared to a mono-exponential function is demonstrated in Figure 3.1.

Data Analysis – Calculations of ATP Synthesis Rates

Rates of ATP synthesis by the creatine kinase reaction (CK), non-oxidative glycolysis (Glyc), and oxidative phosphorylation will be calculated for each time point

throughout all contraction protocols. ATP synthesis by CK will be calculated from the rate of change in [PCr] over time as:

$$ATP_{CK} \text{ (mM/s)} = \Delta[PCr]/\Delta t \qquad \text{Eq\# 8}$$
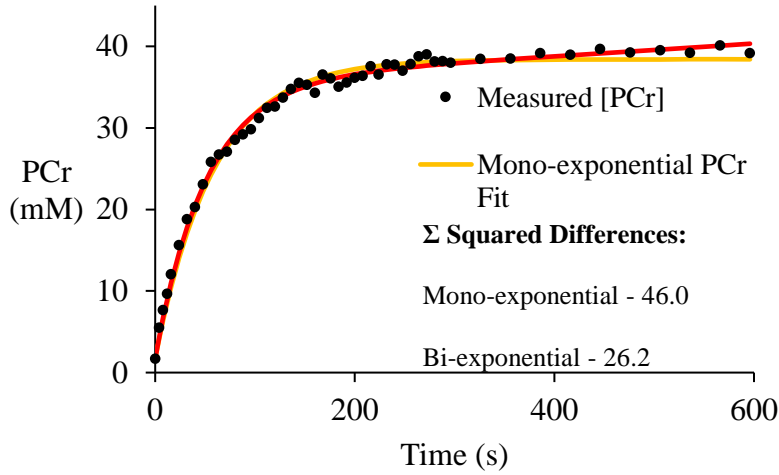
Figure 3.1: Mono- vs. bi-exponential fitting of PCr recovery following high-intensity contractions. The sum (Σ) of the squared differences is much lower for the bi-exponential function, which better captures the delayed recovery of [PCr] back to baseline.

Glycolytic ATP synthesis will be calculated assuming 3 moles of ATP are synthesized for every 2 moles of lactate (82), and that the ratio of lactate:H^+ accumulation is 1:1 (144, 203). The rate of glycolytic ATP synthesis can then be calculated by measuring changes in muscle pH and accounting for H^+ buffering and efflux according to the equation (119, 122):

$$ATP_{Glyc} = 1.5 \ (\theta(\Delta PCr/\Delta t) + -\beta_{tot}(\Delta pH/\Delta t) + V_{Eff}) \qquad \text{Eq\# 9}$$

where $\Delta PCr/\Delta t$ and $\Delta pH/\Delta t$ are the changes in muscle [PCr] and pH between successive time points, respectively, θ is a correction factor for the number of protons consumed by the creatine kinase reaction, β_{tot} is the total muscle buffering capacity in mM H^+/pH unit, and V_{EffExp} is the pH dependent rate of H^+ efflux (mM·s^{-1}) measured during the 240 s trial. θ will be calculated as (96):

$$\theta = 1/(1+10^{pH-6.75}) \qquad \text{Eq\# 10}$$

β_{tot} represents the total buffering capacity of the muscle in slykes (mM H$^+$/pH unit), which takes into account buffering by Pi (β_{Pi}; mM H$^+$/pH unit), PME (β_{PME}; mM H$^+$/pH unit), and the inherent buffering capacity (β_i; mM H$^+$/pH unit):

$$\beta_{tot} = \beta_{Pi} + \beta_{PME} + \beta_i \qquad \text{Eq\# 11}$$

β_{Pi} and β_{PME} will be calculated according to (96):

$$\beta_{Pi} = 2.3 \cdot [\text{Pi}] / ((1+10^{(\text{pH} - 6.75)}) \cdot (1+10^{(6.75 - \text{pH})})) \qquad \text{Eq\# 12}$$

$$\beta_{PME} = 2.3 \cdot [\text{PME}] / ((1+10^{(\text{pH} - 6.2)}) \cdot (1+10^{(6.2 - \text{pH})})) \qquad \text{Eq\# 13}$$

Inherent buffering (β_i; mM H$^+$/pH unit) capacity will be determined by calculating the apparent total buffering capacity (β_{App}; mM H$^+$/pH unit) during the 24-s oxidative capacity protocol and then subtracting the buffering due to Pi and PME (122):

$$\beta_{App} = \theta \cdot ((\Delta PCr/\Delta t)/(\Delta pH/\Delta t)) \qquad \text{Eq\# 14}$$

$$\beta_i = \beta_{App} - \beta_{Pi} - \beta_{PME} \qquad \text{Eq\# 15}$$

where ΔPCr and ΔpH represent the changes in PCr and pH, respectively, and Δt represents the change in time from rest to the peak of the intramuscular alkalosis, which in our lab, occurs about 8-12 s into the contraction period.

The rate of H$^+$ efflux (V_{Eff}; mM·s^{-1}) during 240 s trial will be calculated from the change in muscle pH from baseline (ΔpH). During the initial recovery period intramuscular pH continues to decrease due to H$^+$ release by Pi, after which time, pH tends to recover linearly back to baseline (97, 206). During this linear phase, increases in muscle pH are due to proton efflux from the muscle into interstitial fluid, which, after accounting for H$^+$ release by β_i, β_{Pi}, β_{PME}, and creatine, permits characterization of the relationship between the rate of H$^+$ efflux (V_{Eff}) and the change in muscle pH from baseline (ΔpH). Although this relationship has traditionally been characterized as linear

(122, 206), recent work in our lab suggests the relationship is better characterized by an exponential function (Figure 3.2). Consequently, V_{Eff} during the experimental trials (V_{EffExp}) will be calculated using an exponential function, according to:

$$V_{EffExp} (H^+{\cdot}s^{-1}) = AmpV_{EffExp} \cdot Exp^{(k \cdot \Delta pH)} \qquad \text{Eq\# 16}$$

where $AmpV_{EffExp}$ is the amplitude of the response, k is the rate constant, and ΔpH is the change in pH from baseline at any given time point during the 3rd experimental trial.
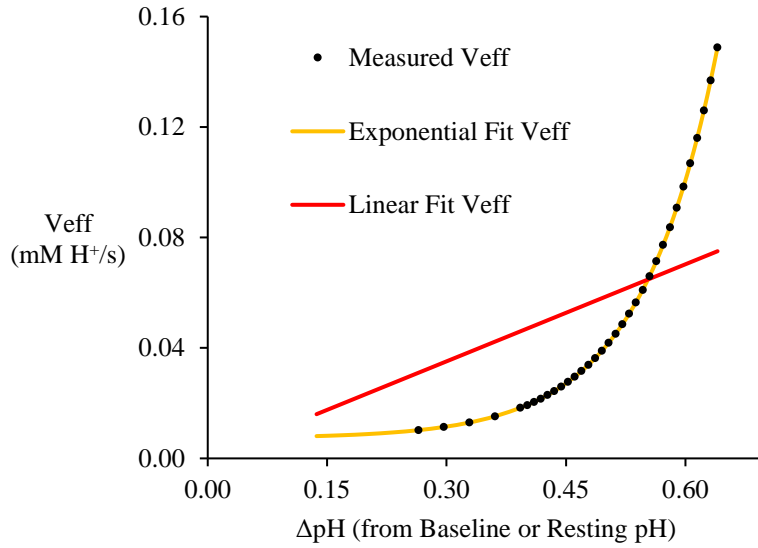
Figure 3.2: V_{Eff} Calculation. The rate of H^+ efflux (V_{Eff}) during recovery, relative to the change in pH from baseline or rest, is better characterized by an exponential function rather than the traditional linear relationship used by others (97, 122, 206).

This exponential equation in Equation 16 will be derived by fitting the calculated rate of V_{Eff} (V_{EffRec}) for each time point during the linear phase of pH recovery against the $\Delta pH_{baseline}$, according to the equation:

$$V_{EffRec} (t) = C - AmpV_{EffExp} \cdot (1-Exp^{(-k \cdot \Delta pHbaseline)}) \qquad \text{Eq\# 17}$$

where C is the maximal measured rate of V_{EffRec}, $AmpV_{EffExp}$ is the amplitude of the change in pH from rest to the end of acidification during recovery, k is the rate constant of the function, and $\Delta pH_{baseline}$ is the measured change in pH from rest for a given time point. V_{EffRec} at any time point (t) will be calculated as:

$$V_{EffRec} \; (H^+ \cdot s^{-1}) = (\Delta\beta_{totRec} \cdot (\Delta pH/\Delta t)) + \theta \cdot (\Delta PCr/\Delta t) \qquad\qquad Eq\# \; 18$$

where $\beta_{totRec} \cdot (\Delta pH/\Delta t)$ and $\theta \cdot (\Delta PCr/\Delta t)$ account for H^+ released by intramuscular buffers and phosphorylation of free creatine, and β_{totRec} is calculated according to the equation:

$$\beta_{totRec} \; (mM \; H^+/pH \; unit) = (\beta_i \cdot \Delta pH_{baseline}) + \beta_{Pi} + \beta_{PME} \qquad\qquad Eq\# \; 19$$

To compare the accuracy of traditional oxidative ATP synthesis (ATP_{OX}) calculations to our new method, ATP_{OX} will be calculated by three methods. The initial rate of PCr resynthesis (V_{iPCr}) will be calculated from the mono- or bi-exponential fitted rate of change in [PCr] observed in the first 4 s of recovery (20, 35). Because PCr resynthesis appears to be an entirely aerobic process (71, 168, 180), and because this method makes no assumptions about changes in ATP_{COST} or mitochondrial uncoupling, V_{iPCr} will be considered the gold standard measurement of ATP_{OX} during the isokinetic MVDC protocols.

The other two ATP_{OX} calculation methods will assume a hyperbolic relationship between ATP_{OX} and cytosolic [ADP] or CPP (29, 119, 122, 129), according to the equation:

$$ATP_{OX} \; (mM/s) = V_{max} \; / \; (1 + (K_m/X)) \qquad\qquad Eq\# \; 20$$

where X is the calculated [ADP] or CPP, K_m is the [ADP] or CPP at $\frac{1}{2}V_{max}$, k_{PCr} is skeletal muscle oxidative capacity, and V_{max} ($mM \cdot s^{-1}$) is the maximal rate of ATP_{OX}, calculated as:

$$V_{max} = k_{PCr} \cdot [PCr]_{baseline} \qquad\qquad Eq\# \; 21$$

The traditional methods for calculating ATP_{OX} from hyperbolic relationships with [ADP] or CPP assume that: 1) ATP_{OX} is in thermodynamic equilibrium with changes in

cytosolic ADP or CPP (i.e., chemical steady state), 2) mitochondrial uncoupling does not occur, and 3) delivery and availability of O_2 and other substrates are not limiting to mitochondrial metabolism. Under these conditions, any increase in [ADP] or CPP is a direct indication that the rate of ATP_{OX} has also increased. However, high-intensity contractions do not always involve steady state conditions, and thus, k_{PCr} (28, 193) and V_{max} may be impaired. Because traditional methods for calculating ATP_{OX} do not adjust for these changes in k_{PCr} and V_{max} (29), their estimations of ATP_{OX} may be inflated. Similarly, a fixed K_m has generally been applied to all participants, instead of measuring the K_m for each individual both before and after high-intensity contractions (29, 119). To overcome these limitations, we will adjust the traditional ATP_{OX} equations to account for changes in k_{PCr}, V_{max}, and K_m measured from baseline to the end of the 240-s experimental trial, according to the equation:

$$ATP_{OX} \text{ (mM/s)} = (V_{max} - (t \cdot \dot{\Delta}V_{max})) / (1 + (K_m - (t \cdot \dot{\Delta}K_m)) / X)) \qquad \text{Eq\# 22}$$

where t is the elapsed time during the 240-s trial and $\dot{\Delta}V_{max}$ and $\dot{\Delta}K_m$ are the linearly scaled rates of change in V_{max} and K_m observed from baseline (i.e., 24-s isokinetic oxidative capacity protocol) to the end of the 240-s experimental trial, according to the equations:

$$\dot{\Delta}V_{max} = (V_{max\text{-baseline}} - V_{max\text{-post240}})/240 \text{ s} \qquad \text{Eq\# 23}$$

$$\dot{\Delta}K_m = (K_{m\text{-baseline}} - K_{m\text{-post240}})/240 \text{ s} \qquad \text{Eq\# 24}$$

A multiparametric analysis (MPA) will also be used to measure V_{max} and K_m after each of the isokinetic MVDC protocols (90, 131). Briefly, MPA methods calculate V_{max}, K_m, and the Hill coefficient (n^H, which indicates the chemical order of control exerted by a metabolite or group of metabolites) by fitting the instantaneous rates of PCr resynthesis,

measured during the recovery period, to the observed [ADP] or CPP using a sigmoidal

function and least-squared differences (90, 131). Although the relationship between

ATP_{OX} and metabolites such as ADP, creatine, and CPP does appear to be sigmoidal, the

time-course of PCr resynthesis, which is being used to estimate ATP_{OX}, is exponential.

Thus, as depicted in Figure 3.3, calculations of V_{max}, K_m, and n^H can be skewed if a large

number of slow PCr resynthesis rates are included in the fitting procedure because

[ADP], CPP, and [creatine] return to resting values much faster than [PCr].
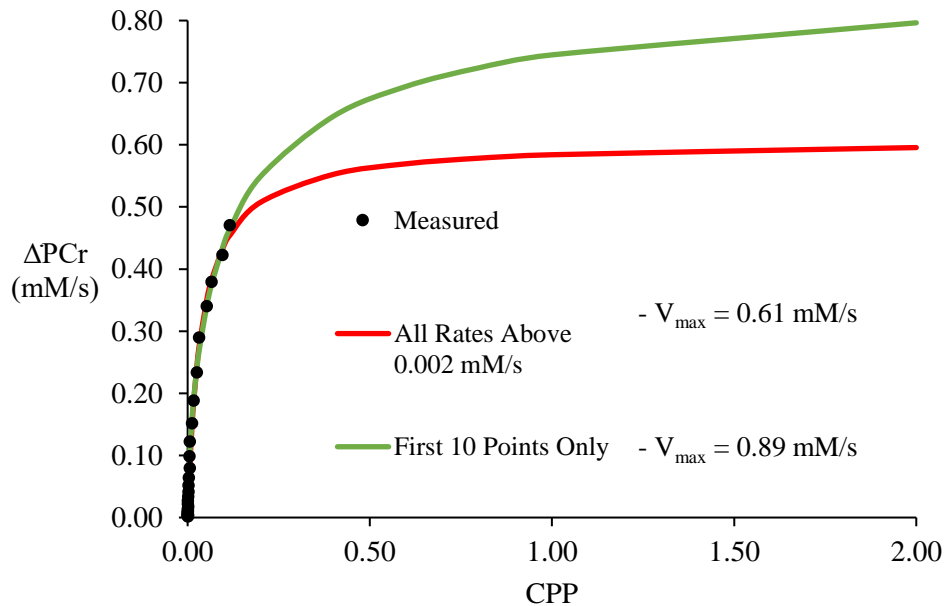
Figure 3.3: Comparison of multiparametric analyses outcomes when using just the first 10 calculated rates of PCr resynthesis vs. rates above 0.002 mM/s. Fitting just the first 10 points (green line) yielded an estimation of V_{max} that was nearly 50% higher than fitting all rates above 0.002mM/s (red line) and resulted in much more accurate estimations of V_{iPCr} when used to calculate ATP_{OX} during the 240-s experimental trial (*data not shown*).

Consequently, V_{max}, K_m, and n^H will be calculated by fitting the first 10 fitted

rates of PCr resynthesis using the least-squared differences and the following hyperbolic

equation:

$\dot{\Delta}PCr \ (mM/s) = V_{max} / (1 + ((X / K_m)^{\wedge nH}))$ Eq# 25

Where V_{max}, K_m, and n^H all have their original meanings, X is the [ADP] or CPP measured at a given time point, and ΔPCr is the corresponding instantaneous rate of PCr resynthesis calculated from the mono- or bi-exponentially fitted PCr recovery curve.

To investigate the effect high intensity exercise has on the ATP cost of contraction (ATP_{COST}; $mM \cdot s^{-1}/W$), the calculated rate of total ATP synthesis (ATP_{tot}) by the 3 main bioenergetic pathways will be divided by work rate (in Watts; W) over the same time period:

$ATP_{COST} = ATP_{tot}$ / Watts   Eq# 26

Where ATP_{tot} ($mM \cdot s^{-1}$) is the summed rate of ATP synthesis by creatine kinase, glycolysis, and oxidative phosphorylation.

The primary outcome variables for this study will be k_{PCr}, V_{max}, K_m, and V_{iPCr} following all 4 of the isokinetic MVDC protocols, as well as the rates of ATP_{OX}, ATP_{tot}, and ATP_{cost} calculated using the traditional and modified methods at 24, 60, 120, and 240 s of the 240-s experimental trial. Secondary outcome measures will include muscle fatigue, total work, total torque-time integral, and changes in intramuscular metabolites. These variables will be compared across all 4 isokinetic MVDC trials to ensure that muscle performance and energetics were consistent across trials, thereby allowing us to assume that the V_{iPCr} measured after the 24, 60, and 120-s trials is representative of the ATP_{OX} rate at those time points during the 240-s trial.

Aims and Hypotheses

Aim 1: Demonstrate that oxidative ATP synthesis is impaired during high-intensity contractions

Hypothesis 1a: Muscle oxidative capacity (k_{PCr}) will decline as the duration of the fatigue trials increase, such that $k_{PCr24} > k_{PCr60} > k_{PCr120} > k_{PCr240}$.

Hypothesis 1b: The rate of ATP$_{OX}$, as measured by V_{iPCr}, will steadily decline beyond the first minute of the fatigue trials, such that $V_{iPCr60} > V_{iPCr120} > V_{iPCr240}$.

Aim 2: Demonstrate that the accuracy of calculating ATP$_{OX}$ during high-intensity contractions can be improved by adjusting traditional ATP$_{OX}$ calculation methods (29, 119, 206) for measured changes in oxidative capacity (i.e., k_{PCr})

Hypothesis 2a: Traditional methods for calculating ATP$_{OX}$ that do not adjust for changes in k_{PCr} and V_{max} will overestimate V_{iPCr} following the 60, 120, and 240-s trials.

Hypothesis 2b: ATP$_{OX}$ at 24, 60 and 120 s of the 240-s trial will not differ from V_{iPCr} following the 24, 60, 120, and 240-s trials when the ATP$_{OX}$ calculations are adjusted to account for changes in k_{PCr} and V_{max}.

Exploratory Aim 1: Compare methods of estimating V_{max} for ATP$_{OX}$ calculations

Hypothesis E1a: V_{max} will be higher when estimated by multiplying $k_{PCr-baseline} \cdot$ [PCr]$_{baseline}$ compared to the ADP and CPP multiparametric analysis methods.

Hypothesis E1b: ATP$_{OX}$ calculations during the 4-minute fatigue protocol will be greater than V_{iPCr} when V_{max} is estimated by multiplying $k_{PCr-baseline} \cdot$ [PCr]$_{baseline}$, but not when using the ADP or CPP multiparametric analysis methods.

Statistical Analyses

Sample size estimations were calculated in G-Power 3.1 (Franz Faul, Kiel University, Germany) assuming α and β levels of 0.05 and 0.8, respectively, and an effect

size of 1.588. Effect size was estimated from the Pillai's Trace value obtained by running a 3x4 repeated measures ANOVA (ATP$_{OX}$ method x time) in SPSS v25.0 (IBM Statistics, Armonk, New York) on a sample of 3 participants that had completed the full protocol. The results of this analysis suggested nine participants should be studied.

All statistical analyses will be conducted using SPSS v25.0 (IBM Statistics, Armonk, New York). Significance will be accepted at the p≤0.05 level. We will report group means and standard errors (SE), 95% confidence intervals, and p-values for differences between means. Hypotheses 1a and 1b will be tested using 1x4 and 1x3 repeated measures ANOVAs, respectively. Hypotheses 2a and 2b will be tested using a 3x4 (ATP$_{OX}$ method x time) repeated measures ANOVA. Exploratory hypotheses E1a and E1b will be tested using a 1x3 (V$_{max}$ method) and 2x4 (V$_{max}$ method x time) repeated measures ANOVA, respectively. If the null hypothesis is rejected for one of the ANOVA tests, a Tukey's post-hoc analyses will be conducted to identify significant differences between dependent variables where appropriate.

Study 2 – Mitochondrial Uncoupling and Oxidative ATP Synthesis During Incremental Knee Extensions

Participants

Eight healthy young adults, 21-40 years old, will be recruited from Amherst and the surrounding local communities. Individuals who participated in previous studies and indicated they would be interested in participating again in the future will also be contacted by phone or email. All individuals will be screened by telephone to determine their eligibility (see Telephone Screening Form, Appendix H) before scheduling any

visits. Inclusion and exclusion criteria will be the same as for Study 1, except that we will also exclude individuals who self-report vascular diseases, such as varicose veins, or deep vein or pulmonary embolisms, to avoid complications from the ischemic procedures used in this study. Unless otherwise noted, all spectroscopy acquisition and post-processing will be the same as in Study 1.

Visit 1 – Paperwork and Familiarization

Visit 1 will take place in the Muscle Physiology Laboratory in the Totman Building. Upon arrival, participants will read an informed consent document (Appendix G) and have any questions answered by the investigator. Next, participants will fill out a Medical History Form (Appendix C), Physical Activity Readiness Plus Questionnaire (Appendix D), and Magnetic Resonance (MR) Safety Form (Appendix E). Measures of blood pressure, height, and body weight will be obtained.

The participants will then be familiarized with the contraction procedures to be completed during Visit 2, which will be described in detail below. Briefly, participants will be strapped into a Biodex 3 dynamometer (Biodex Medical Systems, Shirley, New York) with inelastic straps secured over their ankle, hips, and chest. They will then perform the same series of isometric and dynamic contractions that will be used to measure maximal knee extension torque and oxidative capacity during Visit 2. Participants will also be familiarized with the isotonic incremental knee extension protocol and intermittent ischemia procedures that will be used during Visit 2 to measure the efficiency of oxidative phosphorylation. The intermittent ischemia procedures are described in detail below.

At the end of Visit 1, participants will be given a uniaxial accelerometer (ActiGraph GT3X, Pensacola, FL) to quantify habitual physical activity, which will be analyzed to ensure that none of the participants are actively engaged in more than one hour of physical activity per day for 5 or more days per week, as per the exclusion criterion described above. Accelerometer data will be recorded in 60 s epochs. Participants will be instructed to wear the accelerometer on their right hip for 7 days, and to record their physical activity in a log book. At the end of the week-long wear period, the accelerometer and physical activity log will be collected by the principal investigator at a time and place that is most convenient for the participant. Accelerometer data will be processed using ActiLife v6.13 software (ActiGraph, Pensacola, FL), with a minimum of 10 hours of wear time being required in order for a given day to be included in the analysis. Days meeting this criterion will be analyzed for average daily activity counts and minutes spent in moderate-vigorous physical activity using established thresholds for uniaxial ActiGraph accelerometers (57).

Visit 2 – Incremental Contraction Protocol and Mitochondrial P/O

To investigate the impact that high-intensity contractions may have on mitochondrial uncoupling, we will measure the P/O ratio in the VL after each stage of an incremental knee extension protocol using a new experimental technique adapted from Marcinek *et al*. (145) and Ryan *et al*. (177). Briefly, P/O ratio will be calculated by comparing the rates of PCr resynthesis and deoxymyoglobin appearance during brief periods of ischemia. Although previous ^{31}P MRS and muscle biopsy studies suggest that post-contraction PCr resynthesis does not occur during ischemia (71, 168, 194), our

recent pilot testing has shown that small changes (1-2 mM) can be observed early in the

recovery period (Figure 3.4). This new experimental technique will be used during Visit

2, which will take place at the *h*MRC in the Institute for Applied Life Sciences on the

University of Massachusetts Amherst campus. Upon arriving to the *h*MRC, participants

will meet with the MR Operator to review their MR Safety Form. Before entering the

magnet room, participants will remove jewelry, empty their pockets, and walk through a

metal detector. Participants will then be escorted to the MR scanner and positioned on

their back with their dominant leg on top of a custom-built knee extension ergometer.

The ankle, knee, and thigh will be strapped to the ergometer using Velcro straps. Inelastic

straps will also be secured over the participants' hips to prevent unwanted extraneous

movement during the experimental protocols. To measure changes in intramuscular
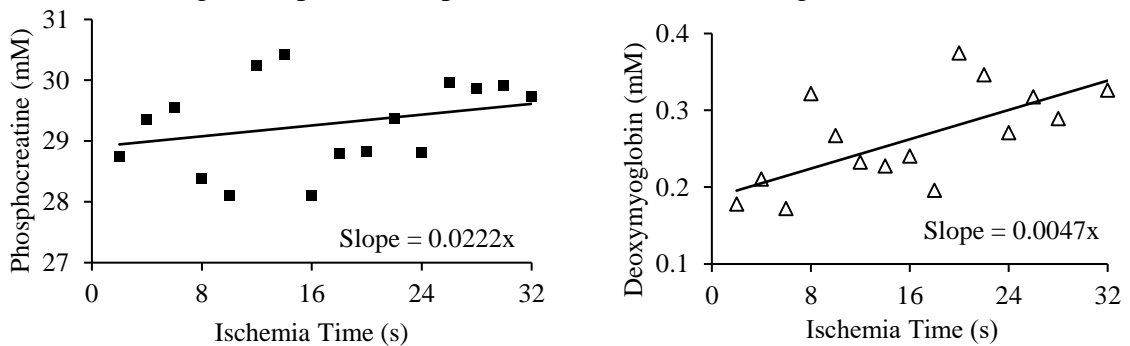
Figure 3.4: Phosphocreatine resynthesis (A) and deoxymyoglobin appearance (B) during 32s of ischemia that followed a 24s MVC. The calculated P/O ratio was 2.33.

phosphate and deoxymyoglobin concentrations, a dual-tuned probe (2 copper coil loops

for proton and phosphorous, 10.5 x 8 cm) will be secured over the vastus lateralis using

athletic wrap and Velcro straps. Headphones will be provided to limit noise from the MR

scanner and enable clear communication with the investigator.

Lastly, two large inflatable blood pressure cuffs, attached to a Hokanson EG20

rapid cuff inflator (D.E. Hokanson Incorporated, Bellevue, Washington) will be wrapped

around the participant's leg, one each around the upper thigh and calf. To ensure that the

inflatable cuffs are comfortable for the participants and positioned correctly, we will perform a familiarization procedure. First, we will inflate the cuffs to a low pressure (~150 mmHg) and then slowly increase the pressure to 240 mmHg, which will be the target pressure during the experimental protocol. Once the participant is comfortable with the cuff placements, we will perform 1-2 rapid inflations (~ 1 s), which will be used to induce ischemia after each stage of the incremental protocol. If necessary, the cuffs will be repositioned after these rapid inflations, to make the participant more comfortable before positioning them in the isocenter of the MR scanner.

Before starting the incremental protocol, participants will complete 2-3 MVICs, each lasting 3-5 s, to determine their maximal torque. One minute of rest will be given between each of these contractions. Two of these contractions must be within 10% of each other in order to confirm a maximal value. Participants will then be refamiliarized with the isokinetic MVDCs by performing 2-3 sets of 3 MVDCs at a speed of $120°·s^{-1}$. Once participants are comfortable with these contractions, they will perform a rest, exercise, recovery protocol to measure baseline oxidative capacity (123, 124). The protocol will begin with 90 s of rest, followed by 24 s of isokinetic MVDCs (0.5 Hz) and 7 minutes of passive recovery.

Participants will then practice a brief series of isotonic contractions before completing an isotonic incremental knee extension protocol. The incremental protocol will consist of 6 stages. Each stage will consist of 1 contraction every 2 s for 3 minutes. Workload will increase with each stage, starting at 10% of the participant's MVIC force, and increasing by 8% for each stage thereafter. Immediately after each stage, we will measure the efficiency of oxidative phosphorylation (i.e., P/O ratio) using an intermittent-

ischemia protocol adapted from Ryan *et al*. (177), which will be performed in the

following sequence:

1- Up to 12 s of rest will be given to allow the muscle to reoxygenate
2- The inflatable cuffs will be rapidly inflated to 240 mmHg
3- The cuffs will remain inflated for up to 40 s while we measure rates of muscle energy production and oxygen consumption
4- The cuff will be rapidly deflated to allow muscles to recover and reoxygenate

Following Step 4 of the intermittent-ischemia protocol, the next 3-minute stage of

contractions will begin. To ensure that our MR-acquisition of ^{1}H and ^{31}P signals remain

time-aligned with the contraction protocol, we will restart MR-acquisition after every

stage, with 30 s of rest added to the beginning of the stage to eliminate the effects of MR-

saturation. After the intermittent ischemia procedures have been completed for Stage 6

(the final stage), participants will complete one more minute of stage 6 isotonic

contractions, followed by a 10 min recovery period, which will allow us to re-measure

the participant's k_{PCr} and accurately calculate rates of ATP$_{OX}$ during the incremental

protocol. This will also provide critical insight into how changes in k_{PCr} relate to changes

in the efficiency of oxidative phosphorylation. After the recovery measures have been

collected at the end of the incremental protocol, the participants will rest quietly during a

10-minute ischemic calibration protocol. This is a standard procedure our lab uses to

determine complete desaturation of myoglobin for use in normalizing (% maximum) the

deoxymyoglobin (dMb) signal during all protocols (121, 194).

Muscle Torque, Power, and Total Work

Torque and power data for each contraction of the isotonic incremental knee-

extension protocol will be collected by a custom MATLAB program (The MathWorks

Incorporated, Natick, Massachusetts) and exported for further processing in Excel. Total work (in Joules) will be summed in 20-s increments and then converted to power (in Watts, Joules/s).

Spectroscopy

Before starting the contraction protocol, gradient-echo scout images of the thigh will be collected to ensure proper placement of the coil relative to the participant's thigh muscles, and the thigh relative to the magnetic isocenter of the MR scanner. The homogeneity of the magnetic field will be optimized by minimizing the full width at half maximum (FWHM) of the water peak using non-localized shimming of the proton (^{1}H-) signal. Absolute quantitation of intramuscular phosphates at rest will be calculated using the non-localized water signal as an internal reference (21, 32, 202). The non-localized water signal will be collected from the ^{1}H-channel using the following acquisition parameters: 60° hard pulse, 2,000 Hz bandwidth, 1,024 complex points, 2 s TR, 0.35 ms echo time (TE), and a total of 70 acquisitions. Non-localized phosphate signals will then be collected from the phosphorous (^{31}P) channel using the following parameters: 60° hard pulse, 4,000 Hz bandwidth, 2,048 complex points, 2 s TR, and a total of 70 acquisitions. Absolute quantitation of muscle creatine will be determined using localized spectroscopy and the water signal as an internal reference (22, 27, 59).

The homogeneity of the magnetic field will then be optimized for a 2x2x2cm voxel centered within the vastus lateralis, and if necessary, parts of the rectus femoris, by minimizing the FWHM of the tissue water signal. The localized water signal will be collected from the ^{1}H-channel using the following parameters: water unsuppressed 90°

hard pulse, 2,000 Hz bandwidth, 2,048 complex points, 2 s TR, 30 ms TE, and a total of 70 acquisitions. The localized creatine signal will be collected from the [1]H-channel using the following parameters: water suppressed 90° hard pulse, 2,000 Hz bandwidth, 2,048 complex points, 2 s TR, 30 ms TE, and a total of 70 measurements.

Lastly, muscle dMb (mM) will be calculated using the non-localized water signal as an internal reference (110). During the intermittent ischemia and ischemic calibration procedures, the non-localized dMb signal will be collected from the [1]H-channel using the following parameters: 90° gaussian pulse, 30,120 Hz bandwidth, 256 complex points, 2 s TR, and 0.35 ms TE. Consequently, to ensure the signal magnitudes are comparable, we will measure the non-localized water signal (a second time) using the following parameters: 90° gaussian pulse, 30,120 Hz bandwidth, 256 complex points, 10 s (fully relaxed) TR, 0.35 ms TE, and 6 acquisitions. This water signal will be acquired following acquisition of the water signal for absolute quantitation of the phosphorous metabolites. The peak dMb signal, which will be used for quantification, will be acquired at the end of the 10-minute ischemic calibration period.

Measures of non-localized ^{31}P-MRS will be collected continuously throughout the oxidative capacity protocol using the following parameters: 60° hard pulse, 4,000 Hz bandwidth, 2,048 complex points, a 2 s TR, and a total of 270 measurements. During the isotonic incremental protocol, measures of non-localized ^{1}H- and ^{31}P-MRS will be collected continuously using an interleaved sequence. For ^{31}P-acquisition, we will use the following parameters: 60° hard pulse, 4,000 Hz bandwidth, 2,048 complex points, a 2 s TR, and a total of 180 measurements. For [1]H-acquisition, we will use the following parameters: 90° gaussian pulse, 30,120 Hz bandwidth, 256 complex points, 40 ms TR,

and 0.35 ms TE. Fifty ^{1}H-FIDs will be acquired during each pass of the ^{1}H signal to yield

a temporal resolution of 2 s per acquisition for a total of 180 measurements. However,

because of the interleaved sequencing, the true temporal resolution for both the ^{1}H and

^{31}P acquisitions will be 4 seconds.

Spectral Analyses

All spectral analyses will be conducted in jMRUI v6.0beta (156). Because of the

short TR (2 s) being used for the contraction protocols, the first 30 s of every acquisition

will be excluded from the oxidative capacity protocol and each stage of the incremental

protocol, to avoid errors in metabolite quantitation due to partial saturation effects. The

remaining free induction decays (FIDs) from the oxidative capacity protocol will be

analyzed as described for Study 1. For the incremental protocol, FIDs will be averaged to

yield temporal resolutions of 20 s during contractions. No averaging will be done for the

FIDs acquired during the 10 s of recovery or intermittent ischemia periods. During the

extra 1 minute of stage 6 contractions, FIDs will be averaged to yield temporal

resolutions of 20 s at rest, 10 s during contractions, 4 s for the first 20 s of recovery, 8 s

for the ensuing 280 s of recovery, and 30 s for the remainder of recovery.

Phosphorous FIDs will be zero-filled (2,048 points) and apodized using a 1 Hz

Lorentzian filter. Following Fourier transfrom, spectra will be manually phased and the

x-axis (frequency in ppm) will be zeroed on PCr. We will use the AMARES algorithm

and prior knowledge files to linefit peaks corresponding to phosphomonoesters (PME),

the Pi doublet (when observeable), phosphodiesters (PDE), PCr, and the γATP doublet

(199). To ensure that the γATP signal is not contaminated by PCr, the ER Filter will also

be used to truncate the bandwidth above and below -1.5 and -6 ppm, respectively, to allow individual linefitting of the γATP peaks.

Proton FIDs will be zero-filled (512 points) and apodized using a 10-Hz Gaussian filter. Following Fourier transform, the x-axis will be referenced on the water peak (4.65 ppm). The water signal will then be filtered out using the Hankel Lanczos Squares Singular Decomposition (17). The resulting spectrum will then be phased manually on the deoxymyoglobin peak at ~78 ppm, and truncated above and below 100 and 60 ppm using the ER Filter. The AMARES algorithm (199) will then be used to linefit the peak corresponding to deoxymyoglobin using a prior knowledge file.

Data Analysis – Metabolite Quantification, k_{PCr}, and ATP Flux

Phosphorous metabolites, total creatine, and dMb will be quantified using the water signal as internal reference and assuming a muscle water concentration of 85.5 M (32, 59, 110). The methods for calculating skeletal muscle k_{PCr}, V_{max}, K_m, n^H and ATP flux through the 3 main bioenergetic pathways will be identical to those described for Study 1.

Data Analysis – Calculating P/O Ratios

The primary outcome variable for this study will be P/O at the end of each stage. The efficiency of oxidative phosphorylation will be calculated from the changes in PCr and dMb measured during the ischemic period following each stage of the incremental protocol. Although previous work has shown that PCr resynthesis appears to be an entirely oxidative process (71, 168), pilot work in our lab suggests PCr resynthesis can

occur early in ischemia provided there is still oxygen bound to myoglobin. Consequently, we will measure the rate of oxidative ATP synthesis ($mM \cdot s^{-1}$) by fitting the PCr recovery signal, measured during ischemia, with a linear regression. Similarly, the dMb signal increases as the partial pressure of intracellular oxygen pO_2 declines Thus, if total dMb content can be estimated then the rate of muscle oxygen consumption can be estimated from the rate of change in the dMb signal ($mM \cdot s^{-1}$). The rates of PCr resynthesis and dMb appearance can then be used to calculate P/O according to the equation:

P/O = $\dot{\Delta}$PCr (mM/s) / $\dot{\Delta}$dMb (mM/s)   Eq# 27

Lastly, I am hypothesizing that mitochondrial uncoupling (i.e., reduced P/O ratio) will only occur during power outputs above an individual's acidic threshold, which will be used as a proxy for the lactate threshold because we will not be able to measure intramuscular lactate directly. Acidic threshold will be calculated for each individual according to Systrom *et al*. (191) as the first workload in which end-stage pH falls below the 95% confidence interval range for resting pH, as determined from the average of resting pH measured at the start of the first 3 stages.

Aims and Hypotheses

Aim: To demonstrate that P/O declines during high-intensity contractions above the acidic threshold.

Hypothesis: During incremental contractions of the knee extensor muscles, skeletal muscle P/O will remain constant for all workloads below the acidic threshold, and progressively decrease as workload increases during stages above the acidic threshold.

Statistical Analyses

Sample sizes were calculated in G-Power 3.1 (program designed by Franz Faul, Kiel University, Germany) assuming α and β levels of 0.05 and 0.8, respectively, and an effect size of 0.5. To the best of my knowledge, there are no data directly measuring mitochondrial P/O ratio following high-intensity contractions *in vivo*. Amara *et al*. reported that mitochondrial P/O ratio in resting skeletal muscle was 40% lower in the flexor digitorum longus of older vs. younger adults (1) but no age-related differences were found for the tibialis anterior muscle. For these reasons, I conservatively estimated a partial eta- (η) squared of 0.2, which resulted in an effect size calculation of 0.5. I also assumed a conservative correlation among repeated measures of 0.5 and a non-sphericity correction of 0.6 (possibility range of 1.0 to 0.2). The resulting sample size calculations indicated eight participants would be needed.

All statistical analyses will be conducted using SPSS v25.0 (IBM Statistics, Armonk, New York). Significance will be accepted at the p≤0.05 level. We will report group means and standard errors (SE), 95% confidence intervals, and p-values for differences between compared means. Hypothesis 1a will be tested using a repeated measures ANOVA to analyze differences in P/O between stages. If the null hypothesis is rejected, a Tukey's post-hoc analysis will be conducted to identify significant differences.

Postori Methodological Amendments

Although I proposed that workload would increase by 8% of MVIC torque between each stage of the step-wise test in study 2, pilot testing indicated that only 2% increments were necessary. Similarly, it was necessary to reduce the starting workload to 8% MVIC torque in some participants to allow them to complete a total of six stages.

Finally, due to circumstances outside of our control, we were unable to develop the interleaved $^1H/^{31}P$-MR sequence needed to perform the intermittent ischemia technique I developed for measuring skeletal muscle P/O ratio after a period of contractions. Consequently, the primary aim of Study 2 was unachievable, and the protocol was adapted to better examine changes in the rate and control of oxidative ATP synthesis above and below the acidic threshold. Specifically, each stage of the stepwise isotonic knee extension test was separated by 3 minutes of passive recovery, which allowed us to perform two critical analyses: 1) calculate rates of oxidative ATP synthesis at the end of each stage from the initial velocity of PCr resynthesis, which Study 1 showed was unaffected by severe decreases in muscle pH, and 2) conduct multiparametric analyses describing the control of oxidative ATP synthesis by cytosolic ADP and phosphorylation potential. Subsequently, our Aims and hypotheses changed as follows:

Study 2 – New Aims and Hypotheses

Aim 1: Examine the relationship between skeletal muscle workload and end-stage changes in cytosolic ADP, phosphorylation potential, and PCr breakdown for workloads above and below the acidic threshold.

Hypothesis 1: The slope of cytosolic ADP, phosphorylation potential, and PCr breakdown, relative to changes in workload, will be greater above the lactate threshold than below.

Aim 2: Examine the relationship between skeletal muscle workload and steady state rates of oxidative ATP synthesis for workloads above and below the acidic threshold.

Hypothesis 2: The slope of oxidative ATP synthesis, relative to changes in workload, will be greater below the lactate threshold than above.

Aim 3: Examine the impact workloads above and below the acidic threshold have on kinetic parameters that describe the control of oxidative ATP synthesis by cytosolic ADP and phosphorylation potential, including V_{max}, K_m, and the Hill coefficient (n^H).

Hypothesis 3: V_{max}, K_m, and n^H will be similar for workloads below the acidic threshold but then become progressively impaired as workload increases above the acidic threshold.

Statistical Analyses

All statistical analyses will be conducted using SPSS v25.0 (IBM Statistics, Armonk, New York). Significance will be accepted at the $p \leq 0.05$ level. We will report group means and standard errors (SE). Hypotheses 1 and 2 will be tested using paired t-tests or the non-parametric equivalent Friendman Test. Hypothesis 3 will be tested using repeated measures ANOVAs. If the null hypothesis is rejected, the estimated marginal means will be used to identify significant differences.

CHAPTER 4

ACCURACY AND VALIDITY OF CALCULATING OXIDATIVE ATP SYNTHESIS DURING HIGH-INTENSITY CONTRACTIONS

Abstract

A full understanding of intracellular bioenergetics during muscular work requires accurate quantitation of the energy (ATP) produced by each metabolic pathway: the creatine kinase reaction, nonoxidative glycolysis, and oxidative phosphorylation. Several methods exist for using ^{31}P-MRS to continuously measure rates of oxidative ATP synthesis (ATP$_{OX}$) during moderate-intensity muscle contractions, but their efficacies have not been validated for high-intensity contractions where relationships between muscle work and oxygen consumption, ADP accumulation, and cytosolic phosphorylation potential are augmented. Specifically, it is unclear whether these augmentations in muscle metabolism are is driven by greater rates of ATP$_{OX}$ due to increases in the ATP cost of force generation (ATP$_{COST}$), or mitochondrial uncoupling, a process that reduces the efficiency of ATP$_{OX}$. To overcome these limitations, we measured phosphate concentrations and muscle pH in the vastus lateralis of 9 young adults during 4 rest-exercise-recovery trials lasting 24, 60, 120, and 240 s. Maximal isokinetic knee extensions (120°·s^{-1}, 1 every 2 s) were performed in a 3 Tesla magnetic resonance system. The initial velocity of phosphocreatine resynthesis (V$_{iPCr}$) following each trial served as the criterion ATP$_{OX}$ measure, and estimated rates of ATP$_{OX}$ calculated from several continuous ATP$_{OX}$ calculation methods were evaluated. Changes in power, metabolites (PCr, Pi, ATP, ADP) and pH were highly reproducible across

trials. V_{iPCr} plateaued from 60-120 s but was reduced following the 240-s trial (p<0.05).

Methods assuming a constant relationship between muscle work and ATP_{COST} were able

to model this behavior but showed poor ability to accurately predict V_{iPCr} across a wide

range of ATP_{OX} values. In contrast, methods that assumed no mitochondrial uncoupling

were considered invalid because they did not model the decline in V_{iPCr}. However,

adjusting these ATP_{OX} calculations for fatigue-induced changes in maximal ATP_{OX}

capacity (i.e., V_{max}) eliminated this error. Subsequently, we identified additional

weaknesses of each ATP_{OX} method and propose solutions for further improving their

accuracies. This study demonstrated that high-intensity contractions impair the capacity

for ATP_{OX} and validates a new, improved methodology for using ^{31}P-MRS to

continuously calculate ATP_{OX}.

Index Terms: muscle, VO_2 slow component, ATP cost, mitochondrial uncoupling,

oxidative phosphorylation

Introduction

During moderate-intensity contractions (i.e., below the lactate threshold), skeletal

muscle oxygen consumption is linearly related to power output and ATP demand is met

largely by oxidative metabolism (2, 58). However, during high-intensity contractions at

power outputs above the lactate threshold, the linear relationship between skeletal muscle

oxygen consumption and power output is augmented (4, 174, 212) and steady-state ATP

turnover is increasingly supplemented by anaerobic metabolism (102, 175). Together,

these observations have become known as the slow component of oxygen uptake kinetics

(VO_{2SC}).

The biochemical mechanisms underlying the VO_{2SC} are not fully understood, but increased ATP cost of force generation (ATP_{COST}) and mitochondrial uncoupling are two leading hypotheses (169, 174). Definitive support for either hypothesis has been hindered by an inability to identify testable predictions that distinguish the two hypotheses from one another *in vivo*. However, one major difference between the two hypotheses is their prediction about the impact high-intensity contractions have on oxidative ATP synthesis (ATP_{OX}). Whereas the increased ATP_{COST} hypothesis predicts that augmentations in muscle oxygen consumption are a direct reflection of increased rates of ATP_{OX}, the mitochondrial uncoupling hypothesis predicts that high-intensity contractions impair the efficiency of oxidative phosphorylation (i.e., decreases the number of ATP produced per dioxygen molecule consumed, or P/O ratio). Thus, it may be possible to distinguish the increased ATP_{COST} and mitochondrial uncoupling hypotheses from one another *in vivo* by directly measuring changes in ATP_{OX} during moderate- and high-intensity contractions.

Yet, where one solution is offered, another limitation presents itself. Under the steady-state conditions of moderate-intensity contractions, 31-phosphorous magnetic resonance spectroscopy (^{31}P-MRS) can be used to continuously calculate rates of ATP_{OX} from changes in muscle force production (99), PCr breakdown (149), cytosolic ADP accumulation (29, 197), or increases in cytosolic phosphorylation potential (CPP) (119, 206). Although prior work has demonstrated most of these methods show good agreement for estimating ATP_{OX} during moderate-intensity contractions (129), their accuracies have not been validated during high-intensity fatigue protocols. Moreover, all these methods are inherently based on an assumption of either constant ATP_{COST} or

mitochondrial coupling, and are therefore all inherently, mathematically biased against one of the two competing hypotheses.

A third method for using ^{31}P-MRS to calculate ATP$_{OX}$ is to measure the initial velocity of PCr resynthesis (V$_{iPCr}$) (19, 35, 158). This method assumes that, glycolysis does not substantially contribute to PCr resynthesis during recovery, and that ATP consumption by ion pumping ATPases is negligible (35, 95). The primary strength of using V$_{iPCr}$ to measure ATP$_{OX}$ during high-intensity contractions is that it makes no assumptions about constant ATP$_{COST}$ or mitochondrial coupling. However, it only yields one measurement of ATP$_{OX}$ per bout of contractions, and therefore cannot be used to study changes in ATP$_{OX}$ over time unless participants perform multiple bouts of exercise that vary in duration. Cannon *et al.* recently used this approach to investigate the VO$_{2SC}$ by having participants perform multiple bouts of moderate- and high-intensity knee extensions lasting 3 and 8 minutes (35). Although V$_{iPCr}$ and ATP$_{COST}$ both appeared to increase from minutes 3-8 during high-intensity contractions, the increases were insufficient to account for the full magnitude of the VO$_{2SC}$, suggesting mitochondrial uncoupling may have also played a role.

There is a clear need to delineate whether high-intensity contractions augment or impair ATP$_{OX}$, as well as to validate methods for using ^{31}P-MRS to continuously measure ATP$_{OX}$ during high-intensity contractions *in vivo*. To address these gaps, we combined experimental approaches from Layec *et al.* (129) and Cannon *et al.* (35). Briefly, participants performed 4 bouts of maximal isokinetic knee extensions, lasting 24, 60, 120, and 240 s. V$_{iPCr}$ was calculated after each trial, yielding 4 gold-standard measurements of ATP$_{OX}$ across time. Subsequently, this allowed us to: 1) examine the impact high-

intensity contractions have on ATP_{OX} via changes in V_{iPCr}, and 2) assess the validity and accuracy of traditional methods for calculating ATP_{OX} during high-intensity contractions by comparing ATP_{OX} estimations obtained during the 240-s trial to V_{iPCr} measurements made at the corresponding timepoints. Here, validity will refer to the ability of an ATP_{OX} method to model changes in V_{iPCr} (i.e., increasing, decreasing, or plateauing), whereas accuracy will refer to the magnitude of separation between pairs of ATP_{OX} estimations and V_{iPCr} measurements.

Our primary hypotheses were that: 1) peak V_{iPCr} would be achieved following either the 60- or 120-s trials, 2) V_{iPCr} would decline from its peak by the end of the 240-s trial, 3) the maximal capacity for ATP_{OX} (i.e., k_{PCr} or V_{max}) would decline from its peak by the end of the 240-s trial, and 4) ATP_{COST} would not change across time. Our secondary hypotheses were: 1) adjusting traditional, continuous ATP_{OX} calculation methods for changes in muscle oxidative capacity (k_{PCr}) or maximal rates of oxidative ATP synthesis (V_{max}, mM·s^{-1}) would improve the accuracy of predicting V_{iPCr} at 24, 60, and 120 s during the 240-s experimental trial, and 2) given that prior work has shown that the different methods for estimating V_{max} *in vivo* yield significantly different values (131), the method used to estimate V_{max} would affect the accuracy of ATP_{OX} calculations.

Methods

Participants

Participants were recruited from Amherst and the surrounding communities using fliers and word-of-mouth. Prior to enrollment, prospective participants were screened by telephone to determine their eligibility and excluded if they reported cardiovascular,

respiratory, or musculoskeletal diseases that would impair their ability to complete the contraction protocol. Subsequently, nine healthy young adults (3 females) were enrolled in the study after providing written informed consent, as approved by the Institutional Review Board at the University of Massachusetts Amherst and in accordance with the Declaration of Helsinki. Because exercise training improves skeletal muscle oxidative capacity (123, 124, 129), which may affect the muscle fatigue and bioenergetic responses during the oxidative capacity and experimental trials (125), we exclude participants who reported engaging in more than 1 hour of physical activity per day at least 5 days per week. Additionally, we quantified habitual physical activity using uniaxial accelerometry (ActiGraph GT3X, Pensacola, Florida). Participants were instructed to wear the accelerometer during all waking hours for a full week and to record their physical activity in a daily logbook. Daily activity (counts·day^{-1}/1000) and minutes spent in moderate-vigorous physical activity (MVPA) were quantified using established thresholds for uniaxial ActiGraph accelerometers (57).

Experimental Approach

To examine the validity and accuracy of traditional methods for continuously calculating ATP_{OX} during high-intensity contractions, participants completed 4 trials of a fatiguing knee-extension protocol inside the bore of a 70 cm 3-Tesla MR system (Siemens, Erlangen, Germany). Phosphate concentrations were measured continuously in the vastus lateralis before, during, and for up to 10 minutes after each trial. The duration of each trial progressively increased (24, 60, 120, and 240 s), thereby allowing ATP_{OX} to be measured from the initial velocity of PCr resynthesis (V_{iPCr}; mM·s^{-1}) following

71

multiple contraction protocol durations. The V_{iPCr} method is considered here as the 'gold standard' measurement of ATP_{OX} that all continuous ATP_{OX} calculation methods were compared to. Total work (Joules), muscle fatigue, and changes in metabolite concentrations such as phosphocreatine (PCr), inorganic phosphate (Pi), and H^+ were compared across all 4 trials to ensure muscle performance and energetics were consistent, thereby allowing us to assume that V_{iPCr} measured after the 24, 60, and 120-s trials were representative of the ATP_{OX} rates occuring at those same timepoints during the 240-s trial. Subsequently, we calculated ATP_{OX} continuously throughout the 240-s trial using several traditional ATP_{OX} calculations (29, 99, 119, 158, 197, 206), and assessed validity and accuracy by comparing ATP_{OX} calculations from each method to the corresponding V_{iPCr} measurements.

Experimental Setup

Participants were positioned supine inside a 3-Tesla MR system (Siemens, Erlangen, Germany) with their dominant leg strapped securely to a custom-built knee-extension ergometer (Jabr *et al*., *submitted*) at the ankle, thigh, and hips, and a dual-tuned $^{31}P/^1H$ surface coil (8 x 10.5 cm) positioned over the vastus lateralis. The knee-extension ergometer's contraction mode, duration, and frequency were all controlled using a custom-written MATLAB program (Mathworks, Natick, Massachusetts). Torque, power, position, and work were recorded for each contraction and exported for post-processing in Excel (Microsoft, Redmond, Washington). The program also provided participants with real-time visual feedback about torque production and muscle fatigue through

display on a non-magnetic digital screen (LCD BOLDscreen, Cambridge Research Systems Ltd., United Kingdom).

Contraction Protocol

Prior to the contraction protocol, participants performed 2-3 maximal voluntary isometric contractions (MVIC), each lasting 3-5 s and followed by at least 1 minute of rest. Participants then performed 2-3 sets of maximal voluntary dynamic contractions (MVDCs) to measure maximal knee-extension power. All MVDCs were isokinetic ($120°·s^{-1}$) and performed at a frequency of 1 contraction every 2 s.

The experimental protocol consisted of 4 trials of isokinetic MVDCs ($120°·s^{-1}$, 1 contraction every 2 s), starting with 90 s of rest, followed by 24, 60, 120, or 240 s of contractions, and 7-10 minutes of quiet recovery. Muscle fatigue, power, and concentric work were calculated for each contraction of all 4 experimental trials and averaged in 4-s intervals (i.e., 2 contractions) for the first 40 s of contractions and 10-s intervals thereafter (i.e., 5 contractions). Muscle fatigue was quantified according to Callahan and Kent-Braun (33):

Fatigue (% max power) = (average PP) / (average ($PP_{baseline}$ + $PP_{protocol}$)) · 100   Eq 1

where PP (peak power) is the peak power achieved during a single MVDC, average PP is the average PP measured across MVDCs over a given time interval (i.e., 4 or 10 s), $PP_{baseline}$ is the greatest PP measured during any of the baseline isokinetic MVDCs, and $PP_{protocol}$ is the greatest PP measured during a single contraction of the experimental trial.

Spectroscopy

Gradient-echo scout images of the thigh were acquired to ensure proper placement of the coil relative to the participant's vastus lateralis and magnetic isocenter of the MR-scanner. The homogeneity of the magnetic field was optimized by shimming on the proton (^{1}H) signal to minimize the full width at half-maximum of the PCr peak (12.1 ±0.3 Hz), with the carrier frequency placed midway between the PCr and phosphodiester peaks. During the 4 experimental trials, non-localized ^{31}P-MRS free-induction decays (FIDs) were collected continuously (60° nominal hard pulse, 4,000 Hz bandwidth, 2,048 complex points, 2 s repetition time) for 90 s of rest, throughout the contractile period (i.e., 24-240 s), and during quiet recovery (7 min for the 24-s trial, 10 min for the 60-, 120-, and 240-s trials).

All spectral analyses were completed in jMRUI v6.0beta (156). The first 30 s (15 FIDs) of each trial were excluded from analysis to avoid partial saturation effects. The remaining FIDs were averaged to yield temporal resolutions of 60 s at rest, 4 s for the first 40 s of the experimental trials, and 10 s for the remainder of the contraction period. During recovery, FIDs were averaged to yield temporal resolutions of 4 s for the first 20 s of recovery, 8 s for the ensuing 280 s of recovery, and 30 s for the remainder of recovery. FIDs were then zero-filled (2,048 points) and apodized using a 1-Hz Lorentzian filter. Following Fourier transfromation, spectra were manually phased and the frequency set to zero at PCr. The AMARES algorithm was used to linefit peaks corresponding to phosphomonoesters (PME), the inorganic phosphate (Pi) doublet, phosphodiesters (PDE), phosphocreatine (PCr), the γ- and α-ATP doublets, and the β-ATP triplet (199).

Millimolar concentrations of phosphorous metabolites were calculated by correcting metabolite signal intensities using experimentally-derived saturation correction factors, and assuming that resting [Pi]+[PCr]+[PME] = 42.5 mM and [ATP] = 8.2 mM (119, 122, 125). Total muscle creatine was assumed to equal 42.5 mM and the concentration of free creatine (fCr) was assumed to be equal to [Pi] (119). Changes in [ATP] during the experimental trials were calculated by comparing the sum of the γ- and α-ATP signal intensities at each timepoint to the sum of the γ- and α-ATP signal intensities at rest, along with a 5-point rolling average to minimize fluctuations due to noise.

[ADP] (mM) was calculated based on the creatine kinase equilibrium (K'_{CK}):

$$[ADP] = ([ATP] [fCr]) / ([PCr] \cdot K'_{CK}) \hspace{3cm} \text{Eq 2}$$

K'_{CK} was corrected for changes in cytosolic pH according to an exponential equation derived from experimental data reported by Golding *et al*. (65). Muscle pH was calculated from the chemical shift between Pi and PCr (154). The cytosolic phosphorylation potential (CPP) was calculated as:

$$CPP = ([ADP][Pi])/[ATP] \hspace{4cm} \text{Eq 3}$$

Adenosine monophosphate (AMP) concentration (mM) was calculated based on the adenylate kinase equilibrium (K'_{AK}):

$$[AMP] = (K'_{AK} \cdot [ADP]^2)/[ATP] \hspace{3cm} \text{Eq 4}$$

K'_{AK} was corrected for changes in cytosolic pH according to an exponential equation derived from experimental data reported by Golding *et al*. (65).

Skeletal Muscle Oxidative Capacity

Baseline skeletal muscle oxidative capacity (k_{PCr}) was determined following the

24 s trial by fitting PCr recovery to a monoexponential function:

$$PCr\ (t) = PCr_{End} + Amp \cdot (1\text{-}Exp^{(-kPCr \cdot t)}) \qquad Eq\ 5$$

where PCr (t) is the calculated [PCr] at time point (t), PCr_{End} is the measured

[PCr] at the end of the 24 s trial, Amp is the amplitude of the recovery in mM, and k_{PCr} is

the mono-exponential rate constant, which reflects the system's oxidative capacity (149,

150). In most cases, PCr recovery following the 60, 120, and 240 s trials did not follow a

mono-exponential recovery pattern (28, 71, 193), and were better fit (i.e., lower sum of

squares) using a bi-exponential function (206):

$$PCr_{Fit}\ (t) = PCr_{End} + ((Amp_1 \cdot (1\text{-}Exp^{(-kPCr1 \cdot t)})) + (Amp_2 \cdot (1\text{-}Exp^{(-kPCr2 \cdot t)})) \qquad Eq\ 6$$

where PCr_{Fit}, (t), Amp, and k_{PCr}, all have their original meanings, and 1 and 2

denote the primary and secondary PCr recovery components, respectively. To avoid

physiologically unrealistic amplitude and k_{PCr} estimations, the sum of Amp1 + Amp2 was

constrained to be no greater than the difference between $[PCr]_{Baseline}$ and $[PCr]_{EndTrial}$.

Subsequently, the overall k_{PCr} of the biexponential function was calculated by weighting

the k_{PCr1} and k_{PCr2} rate constants to their respective amplitudes:

$$\text{Biexponential } k_{PCr} = (k_{PCr1} \cdot (Amp_1/Total\ Amp)) + (k_{PCr2} \cdot (Amp_2/Total\ Amp)) \qquad Eq\ 7$$

Skeletal Muscle ATP Flux

Rates of ATP synthesis by the creatine kinase reaction (ATP_{CK}), adenylate kinase

reaction (ATP_{AK}), non-oxidative glycolysis (ATP_{GLYC}), and oxidative phosphorylation

(ATP$_{OX}$) were calculated at each time point throughout the 240 s experimental trial.

ATP$_{CK}$ (mM·s^{-1}) was calculated from the change in [PCr] between successive timepoints:

$$ATP_{CK} = \Delta[PCr]/\Delta t \qquad\qquad Eq\ 8$$

ATP$_{AK}$ (mM·s^{-1}) was calculated from the change in AMP accumulation between successive timepoints:

$$ATP_{AK} = \Delta[AMP]/\Delta t \qquad\qquad Eq\ 9$$

ATP$_{GLYC}$ (mM·s^{-1}) was calculated assuming 3 moles of ATP are synthesized for every 2 moles of lactate (82) and that the ratio of lactate:H$^+$ accumulation is 1:1 (144, 203). The rate of glycolytic ATP synthesis was then calculated by measuring changes in cytosolic pH and accounting for H$^+$ buffering and efflux according to the equation (119, 122):

$$ATP_{GLYC} = 1.5 \cdot ((\theta(\Delta PCr/\Delta t)) + (-\beta_{tot} \cdot (\Delta pH/\Delta t)) + V_{Eff}) \qquad\qquad Eq\ 10$$

where $\Delta PCr/\Delta t$ and $\Delta pH/\Delta t$ are the changes in muscle [PCr] and pH between successive timepoints, θ is a correction factor for the number of protons consumed by the creatine kinase reaction, β_{tot} is the total muscle buffering capacity in mM H$^+$/pH unit, and V_{Eff} is the pH dependent rate of H$^+$ efflux (mM·s^{-1}) measured following the 240 s trial. θ was calculated as (96):

$$\theta = 1/(1+10^{pH-6.75}) \qquad\qquad Eq\ 11$$

β_{tot} represents the total buffering capacity of the muscle in slykes (mM H$^+$/pH unit), which takes into account buffering by Pi (β_{Pi}), PME (β_{PME}), and other inherent buffers (β_i):

$$\beta_{tot} = \beta_{Pi} + \beta_{PME} + \beta_i \qquad\qquad Eq\ 12$$

β_{Pi} and β_{PME} were calculated according to Kemp and Radda (96):

$$\beta_{Pi} = 2.3 \cdot [Pi] / ((1+10^{(pH - 6.75)}) \cdot (1+10^{(6.75 - pH)})) \qquad \text{Eq 13}$$

$$\beta_{PME} = 2.3 \cdot [PME] / ((1+10^{(pH - 6.2)}) \cdot (1+10^{(6.2 - pH)})) \qquad \text{Eq 14}$$

Inherent buffering capacity (β_i) was determined by calculating the apparent total buffering capacity (β_{App}; mM H^+/pH unit) during the 24-s trial and then subtracting the buffering due to Pi and PME (122):

$$\beta_{App} = \theta \cdot ((\Delta PCr/\Delta t)/(\Delta pH/\Delta t)) \qquad \text{Eq 15}$$

$$\beta_i = \beta_{App} - \beta_{Pi} - \beta_{PME} \qquad \text{Eq 16}$$

where ΔPCr and ΔpH represent the changes in PCr and pH, respectively, and Δt represents the change in time from rest to the peak of intramuscular alkalosis, which occurred 8-12 s into the contraction period.

During the initial phase of PCr recovery, intramuscular pH decreases due to H^+ release by Pi and free creatine, after which time, pH recovers linearly back to baseline (97, 206). During this linear phase of pH recovery, increases in muscle pH are due to H^+ efflux from the muscle into the interstitial fluid, which, after accounting for H^+ release by β_i, β_{Pi}, β_{PME}, and creatine, permits quantification of H^+ efflux (V_{EffRec}) as:

$$V_{EffRec} \, (H^+ \cdot s^{-1}) = (\beta_{totRec} \cdot (\Delta pH/\Delta t)) + \theta \cdot (\Delta PCr/\Delta t) \qquad \text{Eq 17}$$

where $\beta_{totRec} \cdot (\Delta pH/\Delta t)$ and $\theta \cdot (\Delta PCr/\Delta t)$ account for H^+ released by intramuscular buffers and the phosphorylation of free creatine. β_{totRec} (mM H^+/pH unit) was calculated as:

$$\beta_{totRec} = (\beta_i \cdot \Delta pH_{baseline}) + \beta_{Pi} + \beta_{PME} \qquad \text{Eq 18}$$

V_{EffRec} was fit then with a biexponential function across time as:

$$V_{EffRec} \, (t) = C - (AmpV_{EffRec1} \cdot (1\text{-}Exp^{(-k1 \cdot t)})) + (AmpV_{EffRec2} \cdot (1\text{-}Exp^{(-k2 \cdot t)})) \qquad \text{Eq 19}$$

where C is the maximally measured rate of V_{EffRec}, (t) is recovery time in seconds, $AmpV_{EffExp}$ is the amplitude of the V_{EffRec} response, k is the rate constant, and 1 and 2 denote the primary and secondary components. Subsequently, we then calculated the exponential relationship (V_{EffExp}) between V_{EffRec} and the change in muscle pH (ΔpH, from resting baseline) as:

$$V_{EffExp} (H^+ \cdot s^{-1}) = (AmpV_{EffRec1} \cdot Exp^{(k1 \cdot \Delta pH)}) + (AmpV_{EffRec2} \cdot Exp^{(k2 \cdot \Delta pH)}) \qquad \text{Eq 20}$$

where $AmpV_{EffRec}$ and k have their previous meanings, the numbers 1 and 2 denote the primary and secondary components, and ΔpH is the change in pH from rest at any given time point during recovery after the 240 s trial.

Calculating Oxidative ATP Synthesis

The initial velocity of PCr resynthesis (V_{iPCr}) reresents the suprabasal rate of ATP_{OX} achieved at the end of a bout of contractions (35, 95, 158). In this study, V_{iPCr} was calculated as the change in [PCr] measured over the first 4 s of fitted PCr recovery (mono-exponential fit for the 24 s trial and biexponential fit for the 60, 120, and 240 s trials), yielding 4 measurements of ATP_{OX} across time from 24 to 240 s. We then calculated rates of ATP_{OX} throughout the 240 s trial using existing, continuous, ATP_{OX} calculation methods (119, 197, 206), and compared the calculated rates of ATP_{OX} from each method to the corresponding V_{iPCr} measurements at each timepoint.

<u>ATP_{OX} Method 1 – Indirect Method of Calculating ATP_{OX}</u>

The Indirect method (Method 1) for calculating ATP_{OX} (ATP_{OX-M1})inherently assumes that the ATP_{COST} of force generation remains constant (99). Consequently, if muscle force and power production are measured for each contraction, then ATP_{OX} can

be calculated as the difference between the estimated ATP_{COST} ($ATP_{COST-EST}$) of the work performed and the rate of anaerobic ATP synthesis by creatine kinase and glycolysis ($ATP_{ANAEROBIC}$):

$$ATP_{OX-M1} = ATP_{COST-EST} - ATP_{ANAEROBIC} \qquad \text{Eq 21}$$

In the present study, estimated ATP_{COST} (mM·s/Watts) was calculated over the first 12 seconds of the 240-s trial, where rates of ATP_{OX} were lowest, as the average rate of $ATP_{ANAEROBIC}$ divided by the average power output (Watts).

ATP$_{OX}$ Methods 2-6 – Direct Methods of Calculating ATP$_{OX}$

Direct methods of calculating ATP_{OX} assume a constant hyperbolic or sigmoidal relationship between ATP_{OX} and [ADP] or CPP according to the general equation:

$$ATP_{OX} = V_{max} / (1 + (K_m / X)^{nH}) \qquad \text{Eq 22}$$

where X represents [ADP] or CPP, V_{max} is the maximal capacity for ATP_{OX} (mM · s^{-1}), K_m is the concentration of X at which ATP_{OX} is equal to ½V_{max}, and n^H is the Hill coefficient, which describes the order of control ADP exerts over ATP_{OX}. However, on the basis that different methods for calculating V_{max} can produce variable estimations (131), we examined the impact that 5 different methods for calculating V_{max} had on Direct calculations of ATP_{OX} (Methods 2-6), which are summarized in Table 4.1 and then described methodologically below.

ATP$_{OX}$ Method 2 – Linear Model

ATP$_{OX}$ Method 2 estimates V_{max} using the linear analog model described by Meyer (149). Given that the rate constant of PCr recovery (k_{PCr}, s^{-1}) is linearly related to skeletal muscle oxidative capacity (150), V_{max} can be estimated as the product of k_{PCr} and resting [PCr] (119, 207):

$$V_{maxM2} = PCr_{Rest} \cdot k_{PCr}$$

<div align="right">Eq 23</div>

Consistent with its use in previous studies, this method for estimating V_{max} was paired with a CPP model for calculating ATP_{OX} (119, 206):

$$ATP_{OXM2} = V_{maxM2} / (1 + (0.11 / CPP))$$

<div align="right">Eq 24</div>

where V_{maxM2} (M2 – Method 2) and CPP have their original meanings and 0.11 is the K_m for the CPP (206).

ATP_{OX} Method 3 – First-Order ADP Model

ATP_{OX} Method 3 is based on pioneering *in vitro* and *in vivo* works by Chance and colleagues (39–41, 43), and assumes that ADP exerts first-order (i.e., classical Michaelis-Menten hyperbola) control over changes in ATP_{OX}. Subsequently, V_{max} can be estimated as:

$$V_{maxM3} = V_{iPCr} \cdot (1 + (K_m / [ADP]_{End}))$$

<div align="right">Eq 25</div>

where V_{iPCr} is the initial velocity of PCr resynthesis, $K_m = 30\mu M$, and $[ADP]_{End}$ is the concentration of [ADP] at the end of the contractile bout. ATP_{OX} was then calculated as:

$$ATP_{OXM3} = V_{maxM3} / (1 + (K_m / [ADP]))$$

<div align="right">Eq 26</div>

where V_{maxM3} (M3 – Method 3), K_m, and ADP all have their original meanings, and n^H was omitted because $n^H = 1$ (i.e., first-order control).

ATP_{OX} Method 4 – Multiparametric ADP Model-A

Method 4 for estimating V_{max} assumes that the kinetic parameters of Equation 22 can be estimated directly using multiparametric analyses to fit rates of muscle oxygen consumption or V_{iPCr} against changes in [ADP] (90, 218). To maintain consistentcy with other investigations that have compared multiparametric analysis methods for estimating

V_{max} *in vivo* (131), we modeled the control of ATP_{OX} by [ADP] using a least-square technique to fit the function described by Wüst *et al*. (218):

$$V_{PCr} (t) = (V_{maxM4} \cdot [ADP]^{nHM4}) / (K_{mM4} + [ADP]^{nHM4}) \hspace{2cm} \text{Eq 27}$$

where V_{PCr} is the fitted rate of PCr resynthesis ($mM \cdot s^{-1}$) observed at timepoint (t) during recovery, [ADP] is the corresponding concentration of cytosolic ADP, V_{maxM4} (M4 – Method 4) and K_{mM4} have their original meanings, and n^{HM4} is the Hill coefficient describing the sigmoidal relationship between ATP_{OX} and changes in [ADP]. V_{maxM4}, K_{mM4}, and n^{HM4} were all left as unconstrained parameters, and the fitting procedure was conducted on all V_{PCr} rates > 0.02 $mM \cdot s^{-1}$ (90, 131). ATP_{OX} was then calculated as:

$$ATP_{OXM4} = V_{maxM4} / (1 + (K_{mM4} / [ADP])^{nHM4}) \hspace{2cm} \text{Eq 28}$$

where V_{maxM4} (M4 – Method 4), K_{mM4}, n^{HM4}, and ADP all have their original meanings.

ATP_{OX} Method 5 – Second-Order ADP Model-B

Studies that have implemented Method 4 for estimating V_{max} have provided compelling evidence that ADP exerts at least 2nd-order control over ATP_{OX} (90, 131). Based on these results, Method 5 for estimating V_{max} assumes ATP_{OX} is sigmoidally controlled by changes in cytosolic [ADP], but does not use a multiparametric analysis to estimate V_{max}. Instead, V_{maxM5} (M5 – Method 5) is estimated as (29, 197):

$$V_{maxM5} = V_{iPCr} \cdot (1 + ((K_m / [ADP]_{End})^{2.2})) \hspace{2cm} \text{Eq 29}$$

where V_{iPCr} is the initial velocity of PCr resynthesis , $K_m = 30\mu M$, and 2.2 is the set value for the n^H based upon data from Jeneson *et al*. and others (90, 131). Consistent with prior studies that have used this method to calculate V_{max} (29, 197), ATP_{OX} was calculated as:

$$\text{ATP}_{\text{OXM5}} = V_{\text{maxM5}} \: / \: (\: 1 + (K_\text{m} \: / \: [\text{ADP}])^{2.2} \:) \qquad\qquad\qquad\qquad\qquad\qquad \text{Eq 30}$$

where V_{maxM5} (M5 – Method 5), $K_\text{m} = 30\mu\text{M}$, and [ADP] all have their original

meanings and 2.2 is the set value for the n^H.

<u>ATP$_\text{OX}$ Method 6 – Multiparametic ADP-Model</u>

Our preliminary results showed that ATP$_\text{OX}$ Method 2 drastically overestimated

V_iPCr, whereas ATP$_\text{OX}$ Methods 3-5 tended to underestimate V_iPCr. The prior observation

was not surprising given that recent work by Layec *et al*. has shown that V_{maxM2}

significantly overestimates maximal rates of ADP-stimulated respiration *in vitro* (131).

However, the latter observation, that Methods 3-5 underestimated V_iPCr, was less

expected. For Method 4, this error appeared to be influenced by the number of V_PCr data

points being included in the multiparametric fitting procedure. Specifically, V_max

estimations were low when all V_PCr rates > 0.02 mM $\cdot$ s^{-1} were included in the fitting

procedure. Consequently, we adapted the multiparametric analyses described in Method 4

to enhance the accuracy of estimating ATP$_\text{OX}$ (Method 6).

Like Methods 2-5, Method 6 assumes that the control of ATP$_\text{OX}$ by [ADP] can be

estimated using multiparametric analysis. Thus, we followed the approach of Jeneson *et*

al. (90) and elected to estimate V_max using CPP:

$$V_\text{PCr} \: (t) = V_{\text{max-M6}} \: / \: (\: 1 + (K_\text{m} \: / \: \text{CPP} \:)^{\text{nH}} \:) \qquad\qquad\qquad\qquad\quad \text{Eq 31}$$

where V_PCr is one of the first 10 rates of PCr resynthesis (mM $\cdot$ s^{-1}) observed at

timepoint (t) during the mono- or biexponential fit of PCr recovery following an

experimental trial, CPP is the cytosolic phosphorylation potential at the same

corresponding timepoint, and $V_{\text{max-M6}}$ (M6 – Method 6), K_m, and n^H all have their original

meanings. $V_{\text{max-M6}}$ and K_m were left unconstrained and n^H was constrained to all values $\geq$

0.7. We then reperformed the multiparametric analysis against changes in [ADP] by constraining $V_{\text{max-M6}}$ to the value obtained in the CPP-fit and leaving K_{mM6} and n^{HM6} unconstrained according to:

$$V_{\text{PCr}}(t) = V_{\text{max-M6}} / (1 + (K_{\text{mM6}} / [\text{ADP}])^{n\text{HM6}}) \qquad \text{Eq 32}$$

where V_{PCr} is one of the first 10 rates of PCr resynthesis $(\text{mM} \cdot \text{s}^{-1})$ observed at timepoint (t) during the mono- or biexponential fit of PCr recovery following an experimental trial, [ADP] is the cytosolic ADP concentration at the same corresponding timepoint, and V_{maxM6}, K_{mM6}, and n^{HM6} all have their original meanings. Subsequently, ATP_{OX} for Method 6 was calculated as:

$$\text{ATP}_{\text{OX}} = V_{\text{max-M6}} / (1 + (K_{\text{mM6}} / \text{ADP})^{n\text{HM6}}) \qquad \text{Eq 33}$$

Does the Timing of V_{max} Estimations Matter?

Method 2 for estimating V_{max} is well known to be effected by decreases in muscle pH (206), whereas Method 3 appears to be more influenced by the magnitude of metabolic strain (48). The contractile duration of an oxidative capacity protocol can therefore have a significant impact on both the estimation of V_{max} and subsequent calculations of ATP_{OX}. Furthermore, as depicted in Equation 22, Direct ATP_{OX} Methods inherently assume that mitochondrial uncoupling does not occur because V_{max} is held constant throughout a bout of contractions, regardless of contractile intensity. However, if mitochondrial uncoupling does occur, and V_{max} is impaired, then Direct ATP_{OX} calculations could also be affected by *when* V_{max} is calculated (i.e., at baseline or following high-intensity fatiguing exercise) and *how* the final ATP_{OX} calculations account for these changes. Both of these limitations may be surmountable by adjusting

ATP$_{OX}$ calculations for changes in V$_{max}$ observed from baseline to post-fatigue. Consequently, for each of the 5 V$_{max}$ and Direct ATP$_{OX}$ methods described above (Methods 2-6), we calculated ATP$_{OX}$ in 3 ways: 1) V$_{max}$ was measured at baseline (i.e., end of the 24-s trial) and held constant in the calculation of ATP$_{OX}$ throughout the 240-s trial, 2) V$_{max}$ was measured at the end of the 240-s trial and held constant in the calculation of ATP$_{OX}$ throughout the 240-s trial, or 3) V$_{max}$ was measured both at baseline and at the end of the 240-s trial and the value for V$_{max}$ in the calculation of ATP$_{OX}$ was linearly scaled for the observed change in V$_{max}$ according to the equation:

$$ATP_{OX-Adj} = (V_{max24} + (\dot{\Delta}V_{max} \cdot \Delta t)) / (1 + ((K_m/X)^{nH}) \qquad \text{Eq 34}$$

where V$_{max24}$ is the V$_{max}$ measured at baseline following the 24 s trial, Δt is the change in time from 24 s to the respective timepoint of the ATP$_{OX}$ calculation, and $\dot{\Delta}V_{max}$ is the linearly scaled rate of change in V$_{max}$, which was calculated as:

$$\dot{\Delta}V_{max} = (V_{max240s} - V_{max24s}) / 216 \text{ s} \qquad \text{Eq 35}$$

where V$_{max240s}$ and V$_{max24s}$ are the calculated V$_{max}$ values following the 240- and 24-s trials, respectively, and 216 s represents the contractile duration separating the two measurements (i.e., 240 s – 24 s = 216 s). Additionally, because the multiparametric analysis methods (i.e., Methods 4 and 6) also directly estimated K_m and n^H at baseline and at the end of the 240-s trial, these parameters were also adjusted using the same formulas as described for V$_{max}$ (equations 34 and 35), leaving the final ATP$_{OX}$ calculations for Methods 4 and 6 as:

$$ATP_{OX-Adj} = (V_{max24} + (\dot{\Delta}V_{max} \cdot \Delta t)) / (1 + (((K_m + (\dot{\Delta}K_m \cdot \Delta t)) / X)^{(nH+(\dot{\Delta}nH \cdot \Delta t))}) \qquad \text{Eq 36}$$

The ATP cost of force generation (ATP$_{COST}$) was quantified at each timepoint by dividing power output (Watts) by the sum of ATP synthesis rates (mM·s^{-1}) from creatine

kinase, adenylatae kinase, non-oxidative glycolysis, and oxidative phosphorylation. Because [ATP] decreased throughout the 240-s trial, we also incorporated changes in [ATP] between successive timepoints as rates of ATP consumption, leaving our final calculation of ATP_{COST} (W/mM·s^{-1}) as:

$$ATP_{COST} = Watts / (ATP_{CK} + ATP_{AK} + ATP_{GLYC} + ATP_{OX} + \dot{\Delta}[ATP]) \qquad Eq\ 37$$

Finally, to investigate whether high-intensity contractions effect the sensitivity of ATP_{OX} to changes in ADP, the V_{max}, K_m, and n^H that were calculated for each participant, after each trial, using ATP_{OX} Method 6, were subsequently used to estimate rates of ADP-specific ATP_{OX} at set ADP concentrations ranging from 0.01 to 0.5 mM.

Statistical Analyses

All statistical analyses were conducted using SPSS v25.0 (IBM Statistics, Armonk, New York). Data are presented as mean ± SE, with p-values < 0.05 considered statistically significant. Prior to conducting any statistical comparisons, data were tested for normal distrubution using the Shapiro-Wilk test. Normally distributed data were analyzed by t-tests, repeated measures ANOVAs, or Mixed Model ANOVAs. If a significant Trial effect was observed, differences between trials were analyzed from the estimated marginal means. Non-normally distributed data were analyzed using the non-parametric Friedman's test. If a significant Trial effect was observed, differences between Trials were analyzed using individual Wilcoxon signed rank tests, with no corrections made for multiple comparisons. Due to our low sample size, no corrections were made for multiple comparisons.

To evaluate the consistency of muscle performances across trials, changes in metabolite concentrations and power output were compared using repeated measures ANOVAs at 24, 60, and 120 s, as well as at rest. Specifically, data from all 4 trials were compared at rest and 24 s; the 60, 120, and 240-s trials were compared at 60 s; and the 120 and 240-s trials were compared at 120 s. Changes in muscle metabolites and power throughout the 240 s trial were also analyzed using either repeated measures ANOVAs or Friedman's tests.

To test hypotheses 1 and 2, V_{iPCr} measurements were normalized to each participant's V_{max} and then compared across trials using a 1x4 Mixed Model ANOVA. Similarly, to test test hypothesis 3, V_{max} calculations were normalized to V_{max} at baseline and then compared across trials using a 1x4 Mixed Model ANOVA. The same approach was used for change in K_m, n^H, and ADP-specfici ATP_{OX} across trials. To test hypothesis 4, changes in ATP_{COST} across trials were analyzed using a 1x4 Mixed Model ANOVA.

As described above, calculations of ATP_{OX} can be affected by 3 major factors: 1) model selection (i.e., Indirect Model (Method 1) vs. Direct Models (Methods 2-6), 2) the calculation method used to estimate V_{max} (Methods 2-6), and 3) when and how V_{max}, K_m, and n^H are modeled in the ATP_{OX} calculation (Methods 2-6; baseline vs. post-fatigue vs. adjusted for changes observed from baseline to post-fatigue). Collectively, these 3 factors created 16 ATP_{OX} methods that could be compared to V_{iPCr}.

To To test hypotheses 5 and 6, differences between V_{iPCr} and each of the 5 Direct ATP_{OX} Methods that were adjusted for changes in V_{max} were compared using 2x4 Mixed Model ANOVAs (Method x Trial; V_{iPCr} vs. Direct Method; 24, 60, 120, and 240 s). We then calculated intraclass correlations (ICC). To eliminate the repeated measures

component of our ICC (i.e., multiple V_{iPCr} and ATP_{OX} measurements for each participant), we averaged V_{iPCr} and ATP_{OX} values for each participant across the 4 main timepoints (24, 60, 120, and 240 s) and then performed a two-way mixed ICC for absolute agreement. The slope of the ICC between V_{iPCr} and each ATP_{OX} method was also calculated via linear regression with the intercept set to 0. We then constructed Bland-Altman plots and performed one-sample t-tests to analyze whether the average difference between matched measurements of V_{iPCr} and ATP_{OX} calculations were statistically different from 0.

Results

Descriptive data for the participants are listed in Table 4.2. This was a young, relatively active cohort with normal BMIs.

Muscle Fatigue and Metabolites for All Trials

There were no between-Trial differences in muscle fatigue (% peak power) or absolute power output (Watts) at any timepoint (Figure 4.1), but trial effects were observed for muscle metabolites at varying timepoints. The only between-Trial difference observed at rest was a slightly higher PCr concentration at the start of the 120-s trial compared to the 240-s trial (37.8 ± 0.03 vs 36.6 ± 0.6 mM). At 24 s, between-trial differences were found for PCr (24-s trial lower than 240-s trial: 17.0 ± 1.1 vs. 19.4 ± 0.9 mM), Pi (24- and 120-s trials greater than 240-s trial: 22.6 ± 0.9 and 21.4 ± 0.6 vs. 20.0 ± 0.6 mM, respectively), ATP (24-s trials greater than 120-s and 240-s trials: 8.2 ± 0.00 vs. 8.06 ± 0.04 and 8.05 ± 0.06 mM, respectively; and 60-s trial greater than 240-s trial: 8.15

± 0.05 vs. 8.05 ± 0.06), ADP (24- and 120-s trials greater than the 240-s trial: 0.074 ±

0.006 and 0.67 ± 0.003 vs. 0.062 ± 0.003 mM, respectively), and CPP (24- and 120-s

trials greater than the 240-s trial: 0.209 ± 0.022 and 0.179 ± 0.012 vs. 0.155 ± 0.012,

respectively). One difference was also observed at 60 s, with pH being significantly

lower at the end of the 60-s trial compared to 60 s into the 240-s trial (6.81 ± 0.03 vs.

6.86 ± 0.04). No metabolite differences were observed at 120 s between the 120- and

240-s trials.

During the 240-s trial, muscle power (Watts), PCr, and pH all progressively

decreased ($p < 0.05$, all comparisons; Figures 4.1 and 4.2). [ATP] decreased below

resting levels by 60 s and continued to progressively decline thereafter ($60 > 120 > 240$ s,

$p < 0.05$), whereas [ADP] and CPP progressively increased over the first 120 s ($24 < 60 <$

120 s, $p < 0.05$) and then plateaued over the final 120 s ($p = 0.173$).

Comparisons of V_{max} Estimations at Baseline

Estimations of V_{max} from Methods 2-6 are described in Table 4.3. At baseline,

V_{max} estimated by Method 2 was greater than all other Methods ($p < 0.05$). V_{max}

estimated by Methods 4 and 5 were not different from one another ($p = 0.679$) but were

both lower than Methods 3 and 6 ($p < 0.05$). V_{max} estimated by Method 3 was also lower

than Method 6 ($p < 0.05$).

Changes in k_{PCr}, V_{iPCr}, ATP$_{COST}$, and V_{max}

Main effects of trial were found for k_{PCr}, V_{iPCr}, and V_{max} (Table 4.3). Compared to

the 24 s trial, k_{PCr} was slower following the 60, 120, and 240-s trials ($p > 0.05$, all), and

following the 240-s trial compared to the 60-s trial ($p < 0.05$), but did not change from 120 to 240 s ($p = 0.25$). Consistent with our first and second hypotheses, V_{iPCr} peaked following the 60- and 120 s trials but then declined following the 240 s trial (Table 4.3, Figure 4.3). In contrast, and consistent with our fourth hypothesis, we did not observe a main effect of trial for changes in ATP_{COST} across the four timepoints (Figure 4.4, $p = 0.45$).

Consistent with our third hypothesis, trial effects were observed for all 5 methods of calculating V_{max}. For Method 2, V_{max} steadily declined throughout the full protocol ($p < 0.05$, all comparisons). For Method 3, V_{max} following the 240-s trial was lower than all other trials ($p < 0.05$), whereas the only difference observed for Method 4 was between the 240- and 60-s trials. For Method 5, V_{max} following the 60-s trial was faster than the 24-s trial, and V_{max} following the 240-s trial was slower than both the 60- and 120-s trials. For Method 6, V_{max} steadily declined beyond the 60-s trial ($p < 0.05$, all comparisons), but was not different between the 24- and 60-s trials.

No effect of time was found for the Hill coefficient (n^H) using either of the multiparametric analyses (Methods 4 and 6). However, several differences were observed for K_m. For Method 4, K_m was lower following the 120- and 240-s trials compared to the 24-s trial ($p < 0.05$) and following the 120-s trial compared to the 60-s trial ($p < 0.05$). For Method 6, K_m progressively decreased over the first 120 s ($24 > 60 > 120$; $p < 0.05$) but did not change thereafter.

There was a main effect of time for rates of ADP-specific ATP_{OX} at 0.2 mM (Figure 4.5), which was the concentration of ADP at the end of the 240 s trial. No differences were observed between the 24 and 60 s trials. ADP-specific ATP_{OX} was

lower following the 240 s trial than all other trials ($p < 0.01$, all), and following the 120 s

trial compared to the 24 s trial ($p < 0.01$), but no other differences were observed, though

there was a trend for lower values following the 120 s trial compared to the 60 s trial ($p =$

0.07).

Accuracy of ATP$_{OX}$ Calculation Methods

Consistent with our fifth and sixth hypotheses, adjusting traditional calculation

methods for changes in V_{max} improved the accuracy of predicting V_{iPCr} and the method

used to estimate V_{max} had a marked impact on the magnitude of inaccuracy. All six

ATP$_{OX}$ Methods exhibited a significant intraclass correlation when compared to V_{iPCr}

(Table 4.4; $p < 0.01$, all). Methods 1 and 2 exhibited moderate validity, Method 4

exhibited good validity, and Methods 3, 5, and 6 all exhibited excellent validity (108).

However, whereas ATP$_{OX}$ Methods 1, 3, 5, and 6 were not different from V_{iPCr}

across timepoints when analyzed by a Mixed-Model ANOVA ($p > 0.05$), a main effect of

Method was observed for Methods 2 and 4 ($p < 0.05$, both), with Method 2 significantly

overestimating V_{iPCr} and Method 4 underestimating V_{iPCr} (Figure 4.7). Accordingly, V_{max}

estimated by Method 2 were significantly greater than all other Methods at baseline (3-6,

all $p < 0.05$), whereas V_{max} estimated by Methods 4 and 5 were not different from one

another ($p = 0.679$) but were both lower than Methods 3 and 6 ($p < 0.05$; Table 4.3).

Moreover, the average difference between pairs of V_{iPCr} and ATP$_{OX}$ calculations from

Methods 2-5 were all different from zero (1-way t-test; -0.068 ± 0.014, 0.025 ± 0.008,

0.048 ± 0.008, and 0.032 ± 0.007 mM·s^{-1}, respectively; $p < 0.02$, all). These differences

are further illustrated in the Bland-Altman Plots shown in Figure 4.8. Almost every

ATP$_{OX}$ calculation from Method 2 was greater than V$_{iPCr}$, whereas ATP$_{OX}$ calculations

from Methods 3-5 were consistently lower than V$_{iPCr}$. Although the average difference

between V$_{iPCr}$ and ATP$_{OX}$ measurements from Method 1 were not statistically different

from 0 (p=0.803), the difference between matched measurements was not consistent

across all rates of ATP$_{OX}$ (significant Bland-Altman regression, $p < 0.01$), with low rates

of ATP$_{OX}$ consistently undercalculating V$_{iPCr}$ and higher rates of ATP$_{OX}$ consistently

overcalculating V$_{iPCr}$. Method 6 exhibited an excellent ICC with V$_{iPCr}$ (0.948) and the

relationship was stable across the entire range of ATP$_{OX}$ values measured in the present

study (Figure 4.8). Additionally, the average difference between V$_{iPCr}$ and ATP$_{OX}$

calculations from Method 6 were not different from 0 (-0.001 ± 0.010 mM·s^{-1}, $p = 0.96$)

and the ICC slope was identical 1.00, whereas Methods 1-5 exhibited slopes of 1.04,

1.12, 0.96, 0.92, and 0.94, respectively.

Discussion

The global objectives of the present study were to: 1) use multiple measurements

of V$_{iPCr}$ to examine changes in ATP$_{OX}$ and oxidative capacity throughout 4 minutes of

high-intensity contractions, and 2) assess the validity and accuracy of traditional methods

for continuously calculating ATP$_{OX}$ during high-intensity contractions. In agreement with

our first two hypotheses, the most important physiological result of the present study is

that rates of oxidative energy production can decline during high-intensity contractions

despite drivers of oxidative phosphorylation, such as ADP, CPP, or PCr breakdown,

progressively increasing (Figure 4.3). This observation is deductively opposed to the

hypothesis that high-intensity contractions cause an increase in the ATP cost of force

generation but directly aligned with the prediction that high-intensity contractions induce mitochondrial uncoupling. Another critical finding of the present study was that the decline in V_{iPCr} was primarily driven by significant reductions in V_{max} (Table 4.3), which subsequently resulted in substantially reduced rates of ADP-specific ATP_{OX} (Figure 4.5). These latter results are consistent with recent findings from Layec *et al*., who reported lower rates of ADP-stimulated respiration following a 5 km cycling time trial, despite no change in maximal respiratory capacity (127). That is, the capacity for ATP_{OX} was diminished despite no change in the capacity for mitochondrial oxygen consumption. This is critically important, because although mitochondrial uncoupling would be expected to reduce ADP-stimulated respiration by impairing ADP/ATP transport across the inner mitochondrial membrane by adenine nucleotide translocase (105, 117, 159), it would not be expected to have an effect on mitochondrial respiratory capacity. We also found no change in the ATP cost of force generation throughout the 240 s trial (Figure 4.4), which leaves mitochondrial uncoupling as the only remaining explanation for the VO_{2SC} and augmentation of muscle metabolism during all-out exercise protocols in which muscle metabolism remains elevated despite large increases in muscle fatigue.

Our metabolite results are in excellent agreement with previous work in both humans (29, 31, 201) and animal models (155, 221), which have shown that intramuscular metabolic processes, including muscle oxygen consumption (30, 80, 200), remain elevated despite substantial reductions in torque or power generation during all-out contraction protocols. These data have been interpreted as an indication that the VO_{2SC} originates within the fatiguing muscle mass. However, what has remained unclear is whether the sustained elevation of muscle metabolism, despite progressively

diminishing power or torque production, is due to increases in ATP_{COST} or mitochondrial uncoupling. The results of this study suggest that changes in ATP_{COST} do not play a role in the VO_{2SC} during high-intensity, all-out contractions (Figure 4.4). Our results conflict with those of Broxterman *et al*. (29), who reported an increase in the ATP_{COST} of torque generation during an isometric all-out knee extension protocol that was very similar to the dynamic protocol implemented here. However, the method used to calculate ATP_{OX} in that study did not account for changes in V_{max} observed from baseline to the end of fatiguing contractions. In the present study, V_{max} progressively declined beyond the first 60 s, regardless of the calculation method used. Consequently, because Broxterman *et al*. did not measure V_{max} or k_{PCr} at baseline (i.e., before the fatigue protocol), it is possible that the discrepancy in our results may be due to the two different methods used to calculate ATP_{OX}. Specifically, the V_{iPCr} method used in the present study allowed us to observe ATP_{OX} decline over the final 120 s, whereas the ATP_{OX} method employed by Broxterman *et al*. is mathematically unable to model this behavior.

In contrast, Cannon *et al*. also calculated ATP_{OX} from V_{iPCr} measurements and reported that ATP_{COST} increased during 8 minutes of submaximal bilateral knee extensions (35). The reasons for the discrepancy between our results and those of Cannon *et al*. are not immediately clear, but may be due to differences in contraction intensity or protocol duration. For example, as has been discussed previously (18), all-out contraction protocols produce a mirror-like VO_{2SC} response, where muscle VO_2 remains elevated despite decreasing power output or torque generation. In contrast, submaximal square-wave exercise to power outputs above the lactate threshold produce the 'classical' VO_{2SC} response, where VO_2 gradually increases despite constant muscle work due to muscle

fatigue necessitating increases in motor unit recruitment. Consequently, it is possible that we did not observe changes in ATP_{COST} during the present study because motor unit recruitment was likely maximal from the onset of the protocol. Moreover, Cannon *et al.* observed changes in ATP_{COST} over the final 5 minutes of an 8-minute protocol, whereas our protocol lasted only 4 minutes. Thus, we may have observed changes in ATP_{COST} had we extended the protocol to longer durations.

Nevertheless, that we did not observe a change in ATP_{COST} throughout the 240 s trial really should not come as a surprise. High-intensity contractions have repeatedly been shown to impair all three of the major ATPases within skeletal muscle. For example, high-intensity contractions drastically reduce ion pumping activity by both Na^+-K^+- and Ca^{2+}-ATPases (56, 137, 138, 160, 164, 190). Notably, Stienen *et al.* demonstrated that high concentrations of H^+ and inorganic phosphate (Pi), such as those seen here and during other all-out contractions protocols (29, 31, 201), can depress rates of ATP turnover by Ca^{2+}-ATPase by as much as 80% (190). Myosin ATPase is also markedly impaired by high H^+ and Pi (52, 157, 190). Based on these observations, if the rate of ATP turnover progressively decreases with increasing H^+ and Pi accumulation, then skeletal muscle ATP demand, metabolic rate, and oxygen consumption should decrease as well.

If skeletal muscle metabolism is indeed uncoupled from cellular ATP demand during high-intensity, all-out contractions, mitochondrial uncoupling may offer a mechanistic explanation. As Hill and Lupton pointed out nearly a century ago, oxidative metabolism is a recovery process, even during exercise, whereby the end-products of non-oxidative metabolism are recycled to yield gaseous waste products that can be

excreted from the whole organism in copious quantities (79). Mitochondrial uncoupling

directly impairs this recyclative process by dissipating the proton motive force, which

alters the behavior of electrophoretic transport proteins imbedded in the inner

mitochondrial membrane. For example, adenine nucleotide translocase (ANT) catalyzes

the exchange of matrical ATP for ADP in the intermembranous space. The exchange of

ATP and ADP by ANT, as well as the ratio of [ATP]/[ADP] within the matrix vs.

intermembranous space, is dependent upon the magnitude of the electrical potential

energy of the proton motive force. Accordingly, the net consequence of mitochondrial

uncoupling on ANT function is export of ADP from the mitochondrial matrix into the

intermembranous space and cytosol (105, 117, 188). In turn, this should be expected to

cause a right-shift in the cytosolic creatine-kinase equilibrium, thereby augmenting PCr

breakdown and impairing the capacity for PCr resynthesis (192, 193). Thus, whereas

mirror-like augmentations in oxygen uptake and PCr breakdown were initially postulated

as an indication of increased ATP_{COST} (174), the considerations described above suggest

that mitochondrial uncoupling offers an equally plausible explanation.

 Similarly, mitochondrial uncoupling also impairs glutamate-aspartate translocase

(118, 195), the transport protein primarily responsible for driving the malate-aspartate

NADH shuttle. As the magnitude of mitochondrial uncoupling increases, the capacity for

lactate oxidation by the malate-aspartate NADH shuttle is also progressively diminished,

which may explain why the magnitude of the VO_{2SC} is so tightly correlated with

increases in lactate accumulation (175). Moreover, that mitochondrial uncoupling permits

protons to cross the inner mitochondrial membrane passively may also provide a crucial

explanation as to how muscle oxygen consumption can be augmented above the lactate

threshold despite the fact that the acidosis accompanying lactate accumulation should actually inhibit mitochondrial respiration by exogenously contributing to the proton motive force.

Considered *in toto*, mitochondrial uncoupling clearly offers a potential explanation for how muscle oxygen consumption, PCr breakdown, and acidosis can remain suspended in an elevated state despite progressively diminishing muscle power and ATP turnover by cellular ATPases. Specifically, as long as exercise continues, and the stimulus for mitochondrial uncoupling remains present, then regardless of muscle fatigue and intramuscular ATP demand, PCr breakdown and acidosis will remain elevated because uncoupling impairs PCr resynthesis and malate-aspartate NADH shuttle function, and mitochondrial oxygen consumption will remain augmented indefinitely because uncoupled respiration is not controlled by the thermodynamic constraints of H^+ conductance through ATP synthase. However, this now begs two important questions: what causes mitochondrial uncoupling during high-intensity contractions, and why?

Several studies have repeatedly demonstrated that the VO_{2SC} is associated with muscle Type-II fiber content or recruitment (112, 139, 141–143, 220). Not only do Type-II muscle fibers exhibit characteristics that potentiate ROS generation (3), they also exhibit lower antioxidative enzyme concentrations (63, 165) and greater uncoupling protein 3 content (77, 176). Type-II fibers also rely more heavily on the glycerol-3-phosphate NADH shuttle than Type-I fibers (63, 184, 185). This latter detail is notable because unlike the malate-aspartate shuttle, which is driven by the electrical potential energy of the proton motive force (118), the glycerol-3-phosphate shuttle passes electron pairs directly to the quinone pool, and therefore operates fastest when the electron

transport chain is most active (i.e., uncoupled from constraint by ADP-limited control). Moreover, when the proton motive force is high, glycerol-3-phosphate shuttle activity promotes ROS generation by increasing reversed electron flux through complex 1 (26). Given these considerations, it is possible that the VO_{2SC} is caused by a ROS-induced stimulation of mitochondrial uncoupling within Type-II muscle fibers.

However, although mitochondrial uncoupling appears to offer several logical explanations to several components of the VO_{2SC}, results from intricate experiments *in vitro* suggest ROS-stimulation of mitochondrial uncoupling is unlikely during exercise. Gnaiger *et al*. demonstrated that mitochondrial P/O ratio improves as the rate of State-3, ADP-limited respiration increases (64). Similarly, Goncalves *et al*. showed that ROS generation decreases *in vitro* when the respiratory medium mimics conditions seen during exercise (66). Other studies have suggested that the muscle's maximal capacity for ADP-limited respiration exceeds maximal rates of cardiovascular oxygen delivery during whole body exercises (24, 25, 62). That is, skeletal muscle mitochondria appear to exhibit a reserve capacity for oxidative phosphorylation. However, these latter observations are based on assumptions that: 1) maximal rates of state-3 respiration measured *in vitro* under supraphysiological ADP concentrations reflect the muscle's true maximal capacity to consume oxygen *in vivo* under ADP-limited conditions, 2) the maximal rate of state-3 oxygen consumption in a single muscle sample represents the maximal capacity for respiration across the entire muscle mass being studied *in vivo*, and 3) motor unit recruitment and metabolic demand are maximal across the entire muscle mass when measuring maximal oxygen consumption *in vivo*, as this assumption is necessary to normalize calculated rates of absolute muscle oxygen consumption to a measure of

muscle mass (i.e., absolute muscle O_2 consumption in mL O_2/min $\rightarrow$ mL O_2/kg/min). All three of these assumptions are questionable. First, the supramaximal boluses of ADP that are used to stimulate maximal respiration *in vitro* (2 mM or more), are well above the maximal concentrations of ADP observed *in vivo* during all-out contraction protocols (0.2 mM in the present study). There is also marked inter-muscle metabolic heterogeneity even during single-joint exercises (36, 106), suggesting that normalizing *in vivo* measures of absolute muscle oxygen consumption to the whole working muscle mass may lead to underestimation of maximal oxygen consumption rates in the more metabolically active muscle masses.

Additional work is clearly necessary to delineate whether skeletal muscle undergoes mitochondrial uncoupling during high-intensity contractions. Skeletal muscle P/O ratio has been investigated previously by combining ^{31}P-MRS measures of ATP_{OX} with measures of pulmonary oxygen uptake (38, 128), but given that pulmonary oxygen uptake reflects whole body oxygen consumption and not just that of the muscle mass, more direct measures of muscle oxygen consumption would be preferable. Direct, continuous measurement of muscle P/O ratio may be achievable by combining ^{31}P-MRS measures of ATP_{OX} with optical imaging techniques (1, 34, 145), such as near-infrared and diffuse correlation spectroscopy (13, 68), which, if combined with ^{31}P-MRS, may also help expand our understanding of how changes in conduit blood flow and oxygen delivery or extraction effect skeletal muscle oxidative capacity (73, 74, 134).

Changes in ATP_{OX} and V_{max} during High-Intensity Contractions

Another notable finding in the present study is that for V_{max} calculation Methods

3-5, the highest estimations of V_{max} in the vastus lateralis muscle of this group of healthy

young adults tended to occur following the 60-s trial, rather than following the 24-s trial.

Traditionally, skeletal muscle oxidative capacity has been measured following a short

period of contractions, lasting anywhere from 16-30 seconds (124, 132, 207). However,

as demonstrated by Combs *et al*., accurate estimation of skeletal muscle V_{max} requires

sufficient metabolic strain to maximally activate oxidative phosphorylation (48). In the

present study, ADP doubled from 24 to 60 s, suggesting the 24 s trial may have been

insufficient for eliciting maximal estimations of V_{max}. Alternatively, Layec *et al*. showed

that estimations of V_{max} can be improved by augmenting post-exercise conduit blood

flow through reactive hyperemia (134), suggesting that vascular hemodynamics also need

to be considered when measuring skeletal muscle V_{max} *in vivo* from PCr recovery

kinetics. Consequently, the faster V_{max} observed following the 60 s trial in the present

study could have been due to improved vascular conductance. Additional work is needed

to identify contraction protocols that are optimized for measuring skeletal muscle V_{max}

using ^{31}P-MRS. Given previous work, optimal protocols will vary depending on: 1) the

population or species being studied, 2) the calculation method used to estimate V_{max}, 3)

the muscle group being investigated (124, 135), and 4) whether the investigation

implements isometric or dynamic contractions (48, 178).

Calculating ATP$_{OX}$ Continuously during High-Intensity Contractions

The second goal of this study was to examine the validity and accuracy of

traditional methods for calculating ATP$_{OX}$ continuously. The traditional methods for

calculating ATP$_{OX}$ were separated by: 1) inherent assumptions of constant ATP$_{COST}$

(Method 1) or mitochondrial coupling (Methods 2-6); 2) the calculation method used to estimate V_{max}, K_m, or n^H (Methods 2-6); and 3) how changes in V_{max} are accounted for in the final estimation of ATP_{OX} (Methods 2-6). Methods 2-6 were deemed invalid if they only measured V_{max} at baseline or at the end of the fatigue protocol because they were inherently, mathematically unable to model the decline in V_{iPCr} (Figure 4.6). However, consistent with our fifth hypothesis, this mathematical limitation was overcome by adjusting Methods 2-6 to account for changes in V_{max} measured from baseline to the end of a fatigue protocol (Figure 4.7). Thus, Direct Methods 2-6 that only measured V_{max} at baseline or at the end of the fatigue protocol were excluded from the accuracy analysis, thereby narrowing down the total pool of traditional ATP_{OX} methods from 16 to 6.

In the present study, we defined accuracy as the difference between pairs of V_{iPCr} and ATP_{OX} calculations. Although Method 1 was accurate at the group mean level (Figure 4.7), the significant linear-regression slope in the Bland-Altman plot (Figure 4.8) showed that this method is inaccurate across a wide range of ATP_{OX} values. Adjusting ATP_{OX} calculations for changes in V_{max} observed from baseline to post-fatigue improved the validity of all 5 Direct Methods (i.e., Methods 2-6). However, consistent with our sixth hypothesis, the improvement was dependent on the calculation method used to estimate V_{max}. As has been shown previously (131), the greatest estimations of V_{max} came from Method 2, whereas V_{max} calculations from Methods 4 and 5 tended to be lowest. Accordingly, ATP_{OX} calculations from Method 2 drastically overestimated V_{iPCr}, whereas ATP_{OX} calculations from Methods 4 and 5 tended to underestimate V_{iPCr} (Figures 4.7 and 4.8).

These observations led us to develop a new method for estimating V_{max}, which

was based on the multiparametric approach described by Jeneson *et al.* and Wust *et al.* (89, 90, 218) but limited the multiparametric fitting procedure to just the first 10 rates of PCr resynthesis. This modification improved the accuracy of predicting V_{iPCr} across the entire 240 s trial. Like Methods 3 and 5, Method 6 exhibited an excellent ICC with V_{iPCr}. However, the average difference between V_{iPCr} and ATP_{OX} calculations from Method 6 was not different from zero, and the slope of the ICC regression for Method 6 was identical to 1.0. The Bland-Altman plot in Figure 4.8 further demonstrates that Method 6 also provides accurate estimations of V_{iPCr} across a wide range of ATP_{OX} values.

Consequently, a crucial finding of the present study is that valid, accurate measurements of ATP_{OX} can be obtained continuously during high-intensity contraction protocols by adjusting ATP_{OX} calculations for the changes in V_{max} observed from baseline to the end of the fatiguing protocol. This holds true despite substantial reductions in skeletal muscle oxidative capacity (k_{PCr} and V_{max}, Table 4.3), muscle pH, and [ATP]. Not only does this eliminate the need to have participants perform several bouts of contractions to measure changes in ATP_{OX} over time, but the ability to continuously measure ATP_{OX} accurately during high-intensity fatigue protocols will further permit continuous calculations of ATP_{COST}, which will allow future investigations to study the biochemical mechanisms underlying the VO_{2SC} in greater depth.

Limitations

There are multiple notable limitations to the present study. First, we assumed that the post-contraction responses (i.e., measurements of k_{PCr}, V_{iPCr}, V_{max}, etc.) from each trial could all be merged into one continuous measurement across time as long as muscle

metabolic demand was similar between trials and across each timepoint. As shown in Figures 4.1 and 4.2, the four trials were indeed well matched for changes in muscle power and metabolites, and in many cases, the responses from each trial were superimposed on one another. Although there was a cluster of metabolite differences between the 240-s trial and the 24-s trial at 24 seconds, no other consistent differences in muscle power or metabolites were observed. Consequently, we were confident that the metabolic demands were matched well enough between trials to permit treating measurements of k_{PCr}, V_{iPCr}, and V_{max} from each trial as a single set of continuous measurements changing over time.

The second critical assumption made during this study was that V_{iPCr} measured at the end of each trial accurately reflects the suprabasal rate of ATP_{OX} at the end of contractions. This assumption is, in and of itself, predicated on two additional assumptions about the recovery period: 1) that non-contractile ATP turnover is negligible, and 2) glycolytic ATP synthesis does not contribute to PCr resynthesis. First, prior work has shown that ATP consumption by Na^+-K^+-ATPase only accounts for ~2-5 % of total ATP turnover during maximal exercise (9, 148), and post-activation uptake of Ca^{2+} into the sarcoplasmic reticulum by Ca^{2+}-ATPase is completed in under 1 s, even under fatiguing conditions (160, 210). Moreover, as described above, given that high-intensity contractions impair Na^+-K^+-ATPase and Ca^{2+}-ATPase (56, 137, 138, 160, 164, 190), it seems highly unlikely that these enzymes could have consumed ATP at a fast enough rate to substantially reduce V_{iPCr}, or at the very least, the effects should have been similar between the 120- and 240-s trials. Previous work has also demonstrated that PCr resynthesis does not occur during ischemia (71, 168), suggesting glycolysis does not

contribute to V_{iPCr}, or that any contribution would be negligible.

Another potential limitation to the present study is that our calculations of V_{iPCr} and V_{max} could have been affected by the large decreases in intramyocellular pH. Previous studies have repeatedly demonstrated a positive relationship between decreases in cytosolic pH and decreases in skeletal muscle k_{PCr} (28, 135). Walsh *et al*. also reported that low pH reduces submaximal rates of creatine-stimulated respiration *in vitro* (205). However, the results of the present study, as well as others (207), suggest that while k_{PCr} may be affected by acidosis, calculations of V_{iPCr} are not. Walter *et al*. reported that acidosis (end-exercise pH = 6.45) had no effect on estimations of V_{iPCr} and V_{max} when using a first-order ADP calculation method (i.e., Method 3 in the present study) (207). Accordingly, in the present study, changes in V_{iPCr} and acidosis were not temporally aligned: Whereas muscle pH decreased substantially from 60 to 120 seconds, V_{iPCr} plateaued. Then, V_{iPCr} decline from 120 to 240 s despite little to no change in muscle pH. Finally, although k_{PCr} tended to steadily decrease throughout the protocol, methods that did not use k_{PCr} to estimate V_{max} (i.e. V_{max} Methods 3-6) exhibited minimal changes over the first 120 s, where decreases in muscle pH were most apparent. Together, these observations suggest V_{iPCr} and V_{max} Methods 3-6 are not directly affected by acidosis and can therefore be used to investigate changes in the capacity for ATP_{OX} over time during high-intensity contractions.

Another limitation of the present study is that we did not collect any measures of oxygen utilization. Although previous studies have shown that $\dot{V}O_2$ rapidly achieves $\dot{V}O_{2max}$ and then plateaus during all-out whole-body exercise (30, 80, 200), we cannot rule out the possibility that the decline in V_{iPCr} observed over the final 2 minutes of the

240-s trial was not matched by a proportional drop in pulmonary or muscle $\dot{V}O_2$, and therefore cannot definitively conclude whether or not muscle mitochondrial P/O ratio declined. Future studies should replicate the protocol described here while also collecting direct measures of muscle $\dot{V}O_2$, such that changes in P/O ratio can be measured directly. Alternatively, given that the majority of pulmonary $\dot{V}O_{2SC}$ emanates from the working muscle mass (111, 167), preliminary studies may consider calculating P/O ratio by combining ^{31}P-MRS with pulmonary $\dot{V}O_2$. This approach has been used previously to measure P/O ratio during moderate-intensity contractions (38, 128), but to the best of my knowledge, has not been performed during an all-out contraction protocol like the one used in this study.

Conclusions

In summary, during all-out contractions, the VO_{2SC} does not appear to be caused by augmented rates of ATP_{OX} due to increases in the ATP cost of force generation. Instead, high-intensity contractions progressively diminish V_{max} and ADP-specific rates of ATP_{OX} while not affecting ATP_{COST}. These findings suggest that high-intensity contractions induce mitochondrial uncoupling, though the mechanism for how this process would be stimulated during exercise *in vivo* remains unclear. Given the maximal intensity of the protocol implemented in this study, additional work is needed to investigate whether similar observations are also observed during submaximal high-intensity contractions (i.e., at power outputs between the lactate threshold and $\dot{V}O_{2max}$). Future investigations should also seek to better characterize the impact that mitochondrial uncoupling has on creatine kinase and NADH shuttle activity *in vivo*.

We also demonstrated that traditional methods for calculating ATP_{OX} during high-intensity contractions are invalid unless they account for changes in V_{max} observed from baseline to the end of the fatigue protocol. Moreover, the calculation method for estimating V_{max} also has a significant impact, with Method 2 leading to overestimations of ATP_{OX}, and Methods 3-5 tending to underestimate ATP_{OX}. In contrast, Method 1, though accurate at the group-mean level, showed poor accuracy across a wide range of ATP_{OX} values, and is therefore an unreliable method for calculating ATP_{OX} during dynamic high-intensity contractions. The new method we developed for calculating ATP_{OX} overcame all of these limitations and demonstrated both high validity and strong accuracy across a wide range of ATP_{OX} values throughout the 240-s trial. This method can be used to accurately calculate changes in ATP_{COST} over time during high-intensity fatigue protocols, which may help further unravel the mechanisms underlying the VO_{2SC} and augmentation of skeletal muscle metabolism at power outputs above the lactate threshold.

V_{max} Estimation Model	ATP$_{OX}$ Method #	Equation	Sources
Linear Model	2	$V_{max} = k_{PCr} \cdot [PCr]_{Rest}$	(45, 124, 162)
ADP-1st Order Control	3	$V_{max} = V_{iPCr} \cdot (1 + (K_m / [ADP]_{End}))$	(55, 207)
ADP-MPA*	4	$V_{PCr} (t) = (V_{max} \cdot [ADP]_t^{nH}) / (K_m^{nH} + ADP_t^{nH})$	(89, 90, 218)
ADP-2nd Order Control	5	$V_{max} = V_{iPCr} \cdot (1 + (K_m / [ADP]_{End})^{2.2})$	(29, 197)
ADP-MPA	6	$V_{PCr} (t) = V_{max} / (1 + (K_m / [ADP]_t)^{nH})$	

Table 4.1: Calculations for Estimating ATP$_{OX}$-V$_{max}$ *In Vivo*. Methods 2-6 calculate ATP$_{OX}$ based upon first- or second-order changes in ADP and vary in the method used to calculate V$_{max}$. The multiparametric equation listed below for Method 4 (*), is from Wüst *et al*. (218). A different equation was presented by Jeneson *et al*. (89, 90), but was not tested here. The multiparametric analysis in Method 6 is presented as a development that emerged from this study.

Age (years)	27.3 ± 1.0
Height (cm)	172.9 ± 4.2
Body Mass (kg)	70.4 ± 4.4
BMI (kg/m^2)	23.4 ± 0.6
PA (counts·day^{-1}/1000)	294.3 ± 29.4
MVPA (minutes·day^{-1})	44.9 ± 4.9
Torque (Nm)	274.1 ± 24.2
Power (Watts, 120°·s^{-1})	255.4 ± 22.4

Table 4.2: Study 1 Participant Characteristics. Data are presented as means ± SE.

Measure	Trial 1 (24 s)	Trial 2 (60 s)	Trial 3 (120 s)	Trial 4 (240 s)
k_{PCr} ($\cdot s^{-1}$) †	0.025 ± 0.001 #,‡,§	0.021 ± 0.001 *,§	0.019 ± 0.001*	0.017 ± 0.001 *,#
V_{iPCr} (mM·s⁻¹) †	0.491 ± 0.031 #,‡	0.603 ± 0.020 *,§	0.602 ± 0.032 *,§	0.524 ± 0.037 #,‡
V_{max} M2 (mM·s⁻¹) †	0.91 ± 0.03 #,‡,§	0.79 ± 0.03 *,‡,§	0.72 ± 0.05 *,#,§	0.62 ± 0.05 *,#,‡
V_{max} M3 (mM·s⁻¹) †	0.70 ± 0.03 §	0.73 ± 0.02 §	0.67 ± 0.05 §	0.61 ± 0.05 *,#,‡
V_{max} M4 (mM·s⁻¹) †	0.57 ± 0.03	0.62 ± 0.02 §	0.59 ± 0.03	0.51 ± 0.04 #
V_{max} M5 (mM·s⁻¹) †	0.57 ± 0.03 #	0.62 ± 0.02 *,§	0.61 ± 0.03 §	0.53 ± 0.04 #,‡
V_{max} M6 (mM·s⁻¹) †	0.81 ± 0.03 ‡,§	0.77 ± 0.02 ‡,§	0.70 ± 0.04 *,#,§	0.61 ± 0.05 *,#,‡
K_m M4 (µM) †	26.5 ± 1.0 ‡	24.5 ± 1.0 ‡	21.1 ± 1.2 *,#	22.1 ± 1.1 *
K_m M6 (µM) †	46.0 ± 2.0 #,‡,§	35.8 ± 1.7 *,‡,§	28.2 ± 1.9 *,#	29.9 ± 1.7 *,#
n^H M4	1.72 ± 0.07	1.59 ± 0.06	1.71 ± 0.08	1.68 ± 0.06
n^H M6	1.17 ± 0.03	1.03 ± 0.02	1.05 ± 0.03	1.04 ± 0.04

Table 4.3: Changes in ATP$_{OX}$ parameters as the duration of high-intensity knee extensions increase. Significant effect of Trial (†), Significantly different from Trial 1 (*), significantly different from Trial 2 (#), significantly different from Trial 3 (‡), significantly different from Trial 4 (§). Data are presented as means ± SE.

	ICC	ICC Classification	Linear Reg. Slope	Average Difference (V_{iPCr}-ATP$_{OX}$, mM·s^{-1})
Method 1	0.593 *	Moderate	1.04	-0.013 ± 0.049
Method 2	0.706 *	Moderate	1.12	-0.068 ± 0.014, #
Method 3	0.929*	Excellent	0.96	0.025 ± 0.008, #
Method 4	0.838 *	Good	0.92	0.048 ± 0.008, #
Method 5	0.905 *	Excellent	0.94	0.032 ± 0.007, #
Method 6	0.948 *	Excellent	1.00	-0.001 ± 0.010

Table 4.4: Relationship between measurements of V_{iPCr} and calculations of ATP$_{OX}$.
Measurements of V_{iPCr} and ATP$_{OX}$ were averaged across time (n = 4 each) to eliminate repeated measures within each participant (n = 9). Significant ICC (*), Average difference between matched pairs of V_{iPCr} and ATP$_{OX}$ significantly different from 0 (1-way t-test, #). ICC classifications are from Koo and Li (108). Data are presented as means ± SE.
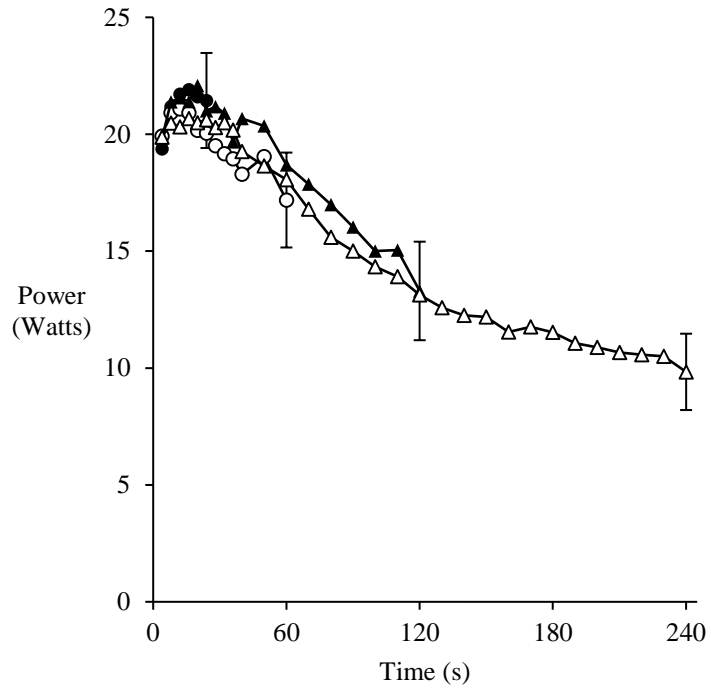
Figure 4.1 – Changes in muscle power output between trials. To avoid congestion, error bars are only presented for the final datapoint in each trial. Data are presented as means ± SE.
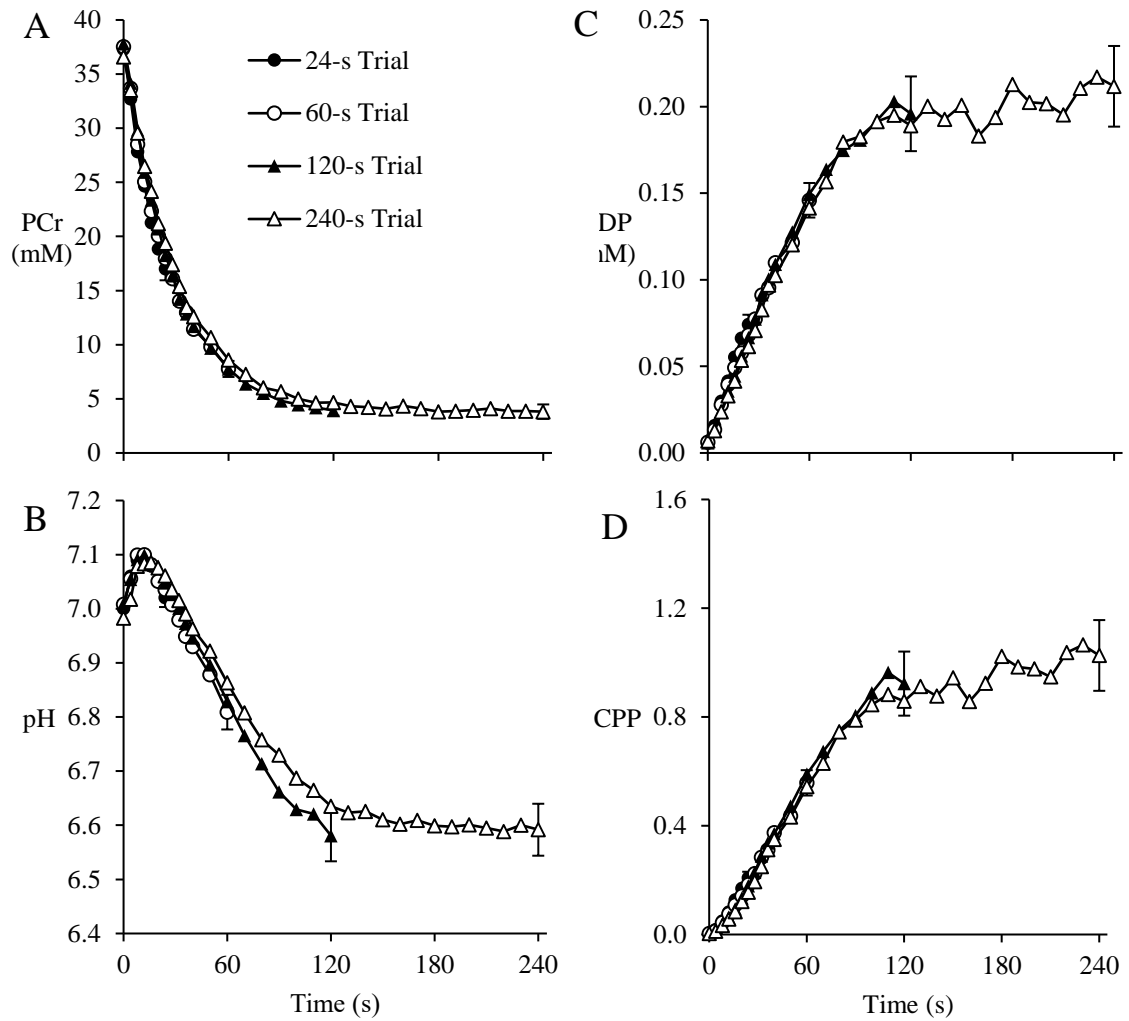
Figure 4.2 – Changes in muscle metabolites between trials. Changes in PCr (*A*), pH (*B*), ADP (*C*), and CPP (*D*) across time for each trial. Filled circles represent the 24-s trial, open circles represent the 60-s trial, filled triangles represent the 120-s trial, and open triangles represent the 240-s trial. To avoid congestion, error bars are only presented for the final datapoint in each trial. Data are presented as means ± SE.
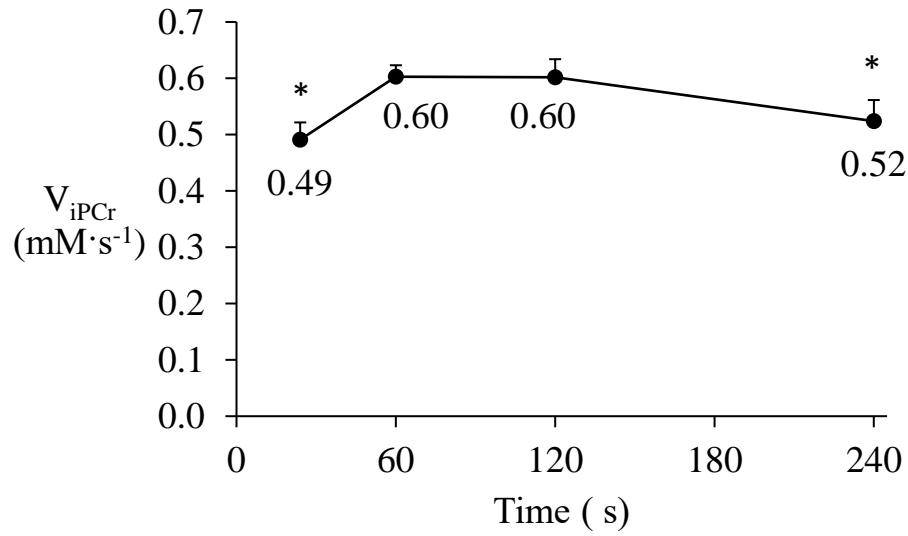
Figure 4.3 – Changes in V_{iPCr} during 240 s of maximal isokinetic knee extensions. V_{iPCr} was calculated after each trial from the change in [PCr] observed over the first 4 s of mono- or biexponentially fitted PCr-recovery. V_{iPCr} increased rapidly at the onset of contractions and plateaued from 60-120 s. However, by the end of the 240-s trial, V_{iPCr} decreased by 15%, despite cytosolic ADP and phosphorylation potential remaining elevated (*see Figure 4.2*).
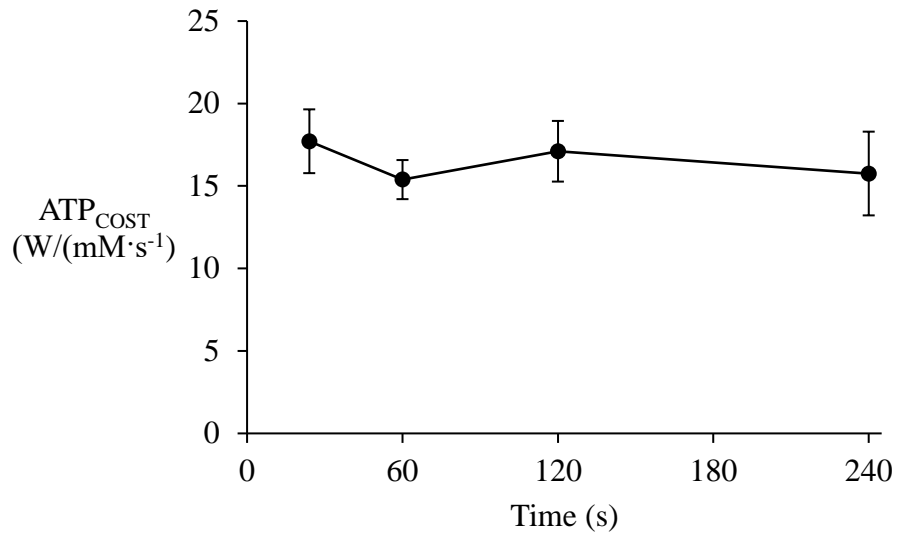
Figure 4.4 – Changes in ATP$_{COST}$ throughout 240 s of high-intensity knee extensions.
ATP$_{COST}$ (W/mM·s^{-1}) was calculated by dividing power output (Watts) by the sum of ATP synthesis by the creatine kinase, non-oxidative glycolytic, and oxidative phosphorylation pathways. Because [ATP] significantly declined during the 240 s trial, we also calculated rates of ATP consumption from the decline in [ATP] between successive timepoints, as well as rates of ATP synthesis by the adenylate kinase reaction. However, these latter two processes only contributed ~ 0.17% and 0.0005% to the total rate of ATP consumption throughout the 240 s trial.
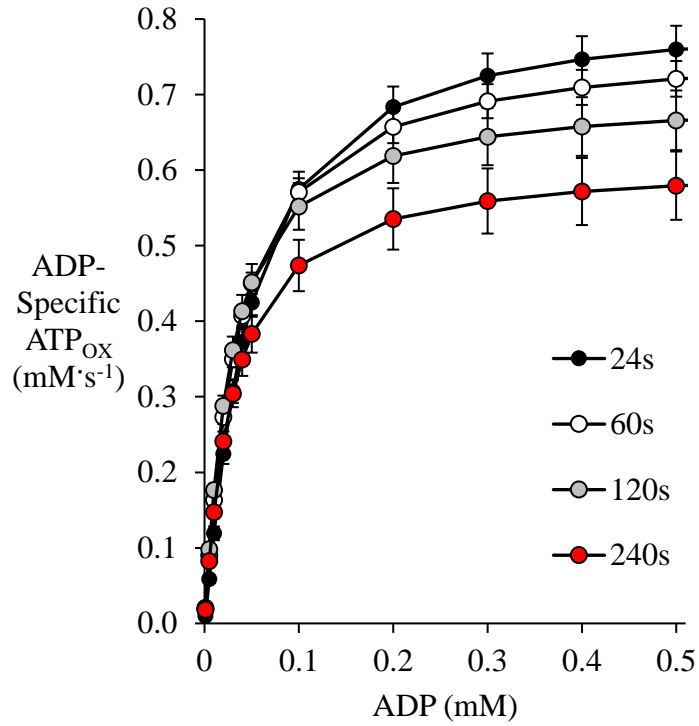
Figure 4.5 – Changes in ADP-specific rates of ATP$_{OX}$ over time. ADP-specific rates of ATP$_{OX}$ were calculated using the V$_{max}$, K_m, and n^H values derived from the multiparametric analysis of ATP$_{OX}$ Method 6, which was selected because it exhibited the most accurate estimations of V$_{iPCr}$ across the entire 240-s protocol. As depicted above, the sensitivity of ATP$_{OX}$ to changes in [ADP] was progressively diminished as the duration of high-intensity contractions progressed.
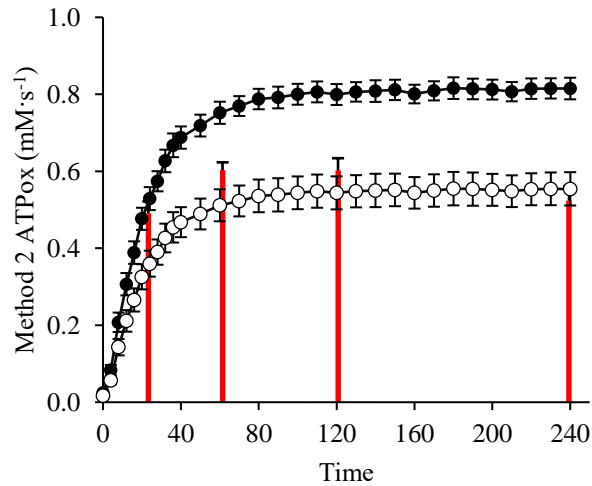
Figure 4.6 – Impact of not adjusting ATP$_{OX}$ calculations for changes in V$_{max}$. Regardless of whether V$_{max}$ was calculated at baseline or after the 240-s trial, not adjusting for changes in V$_{max}$ observed from baseline to post-fatigue resulted in poor estimations of V$_{iPCr}$. In the image below, filled and open circles represent ATP$_{OX}$ calculations from Method 2 when V$_{max}$ is measured only at baseline or post-fatigue, respectively, and the red bars indicate V$_{iPCr}$ measured at 24, 60, 120, and 240 s. Data are presented as means ± SE.
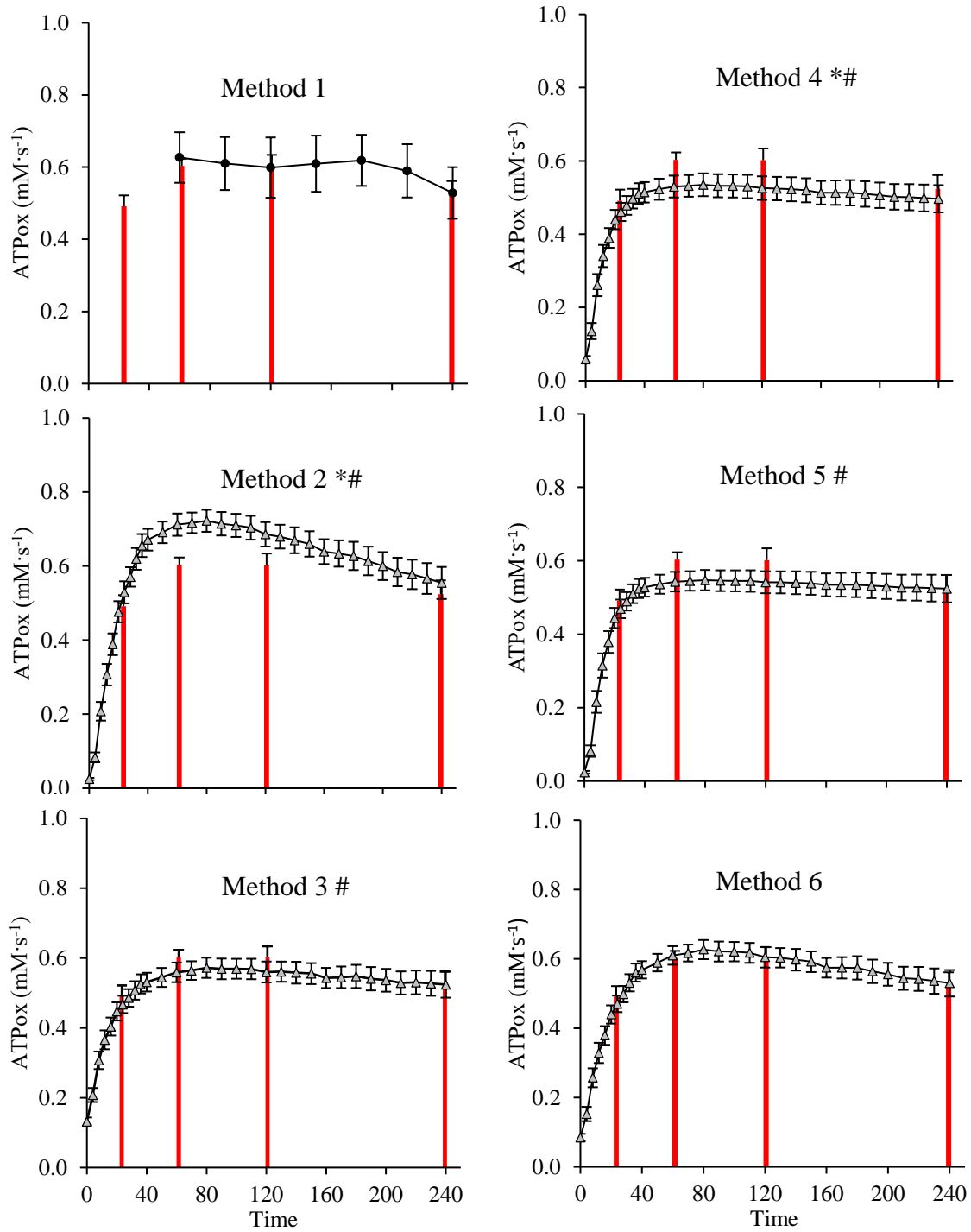
Figure 4.7 – Calculations of ATP$_{OX}$ using Method 1 and all 5 Direct Methods (Methods 2-6) when V$_{max}$ is adjusted for changes observed from baseline to the end of the 240-s trial. Bars indicate V$_{iPCr}$ at 24, 60, 120, and 240 s. Significantly different than V$_{iPCr}$ by Mixed-Model ANOVA (*). Significantly different than V$_{iPCr}$ by 1-way t-test (#). Data are presented as means ± SE.
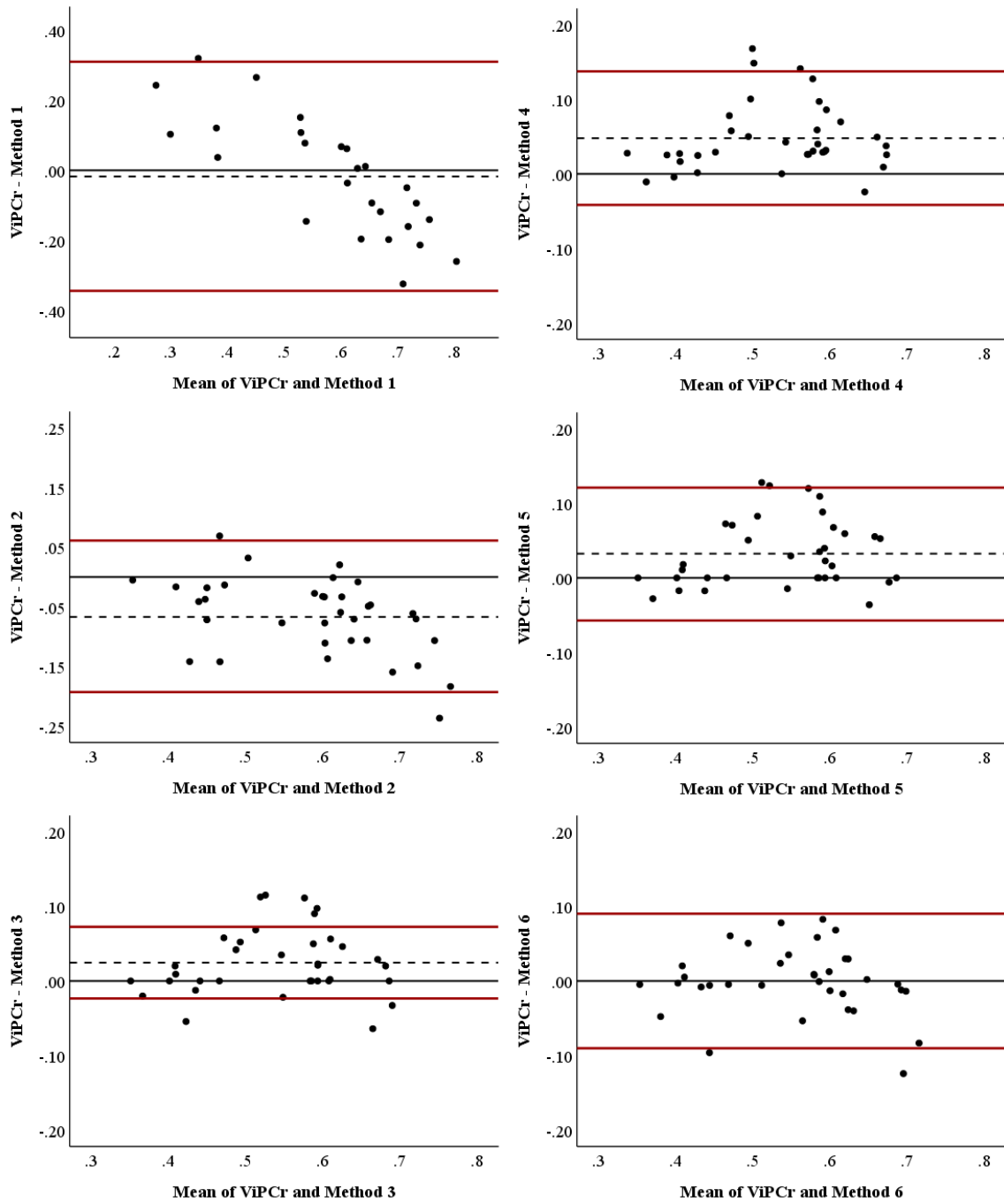
Figure 4.8 – Bland-Altman Plots of ATP$_{OX}$ Calculations vs. V$_{iPCr}$: Comparisons of V$_{iPCr}$ measurements and ATP$_{OX}$ calculations from Methods 1-6. Solid lines indicate 0 on the y-axis. Dashed lines indicate the mean difference between V$_{iPCr}$ measurements and ATP$_{OX}$ calculations, and the maroon bold lines indicate the 95% confidence interval for the mean difference between V$_{iPCr}$ measurements and ATP$_{OX}$ calculations.

CHAPTER 5

RATES OF OXIDATIVE ATP SYNTHESIS IN HUMAN QUADRICEPS ARE NOT AUGMENTED ABOVE THE pH THRESHOLD DURING AN ISOTONIC STEPWISE PROTOCOL

Abstract

Skeletal muscle metabolism and oxygen consumption are augmented during high-intensity contractions above the lactate threshold, but it is unclear whether these augmentations are caused by increases in the ATP cost of force generation (ATP_{COST}) or impairments in the efficiency of oxidative ATP synthesis (ATP_{OX}). Although recent evidence suggests that maximal contraction protocols impair muscle's capacity for ATP_{OX} (i.e., V_{max}), other studies suggest ATP_{COST} plays a greater role during submaximal high-intensity contractions (i.e., at power outputs above the lactate threshold but below maximal oxygen uptake). Consequently, we used ^{31}P-MRS to measure changes in muscle phosphates, ATP_{OX}, and ATP_{COST} during a stepwise knee extension protocol. For workloads above and below the muscle pH threshold (pH_T; used here as a proxy for the lactate threshold), we calculated slopes relating stepwise changes in muscle work to changes in muscle phosphates, ATP_{OX}, and V_{max}. Changes in muscle phosphates and ATP_{OX} were linearly related to workload below the pH_T. However, above the pH_T, changes in muscle phosphates were augmented ($p<0.05$), whereas increases in ATP_{OX} were attenuated ($p<0.05$) and V_{max} declined ($p<0.05$). ATP_{COST} did not change throughout the stepwise test ($p=0.10$). Consistent with results from maximal contraction protocols, these results suggest ATP_{COST} is unchanged during submaximal high-intensity contractions. Instead, augmentations in muscle metabolism observed during high-

intensity contractions at workloads above the pH or lactate threshold appear to be caused by reductions in V_{max} and ATP_{OX} efficiency, which we postulate may be caused by mitochondrial uncoupling due to its impact on ADP-ATP exchange by adenine nucleotide translocase.

Index Terms: muscle energetics, stepwise, incremental, oxidative phosphorylation, mitochondrial uncoupling

Introduction

Much is still unknown about the mechanisms that control oxidative phosphorylation during high-intensity exercise. For workloads below an individual's lactate threshold, changes in muscle metabolism and oxygen consumption are linearly related to stepwise increases in muscle work. However, for workloads above an individual's lactate threshold, skeletal muscle metabolism and oxygen consumption are augmented (2, 10, 85, 102, 104, 174), a phenomenon known as the slow component of oxygen uptake kinetics (VO_{2SC}). Presently, it is unclear whether the VO_{2SC} is caused by increases in the ATP cost of force generation (29, 35, 174), or impairments in the efficiency of oxidative ATP synthesis (ATP_{OX}) due to mitochondrial uncoupling (*Chapter IV*). Although recent evidence suggests that mitochondrial uncoupling may contribute to the VO_{2SC} during maximal exercise protocols (*Chapter IV*))(127), data from heavy-intensity protocols (i.e., at power outputs above the lactate threshold but below maximal oxygen uptake) suggest that ATP_{COST} may play a greater role. For example, Cannon *et al*. reported augmentations in ATP_{OX} and ATP_{COST} during 8-minutes of heavy bilateral knee extensions (35). However, the magnitude of the increase in ATP_{OX} was

insufficient to account for the full magnitude of the VO_{2SC}, suggesting mitochondrial uncoupling may have played a role during this submaximal high-intensity protocol as well.

Similarly, several models have been proposed to explain how changes in cytosolic metabolites control the rate of oxidative ATP synthesis (ATP_{OX}) within skeletal muscle during steady state contractions: including first- and second-order control mechanisms by cytosolic [ADP] (40, 41, 90), first-order control by changes in cytosolic phosphocreatine (PCr) or free creatine (fCr^-) (15, 140), and linear nonequilibrium control by changes in the cytosolic phosphorylation potential (CPP; ADP·Pi/ATP) (149). However, a common link between each of these models is that they assume a constant relationship between increases in ATP_{OX} and stepwise changes in cytosolic ADP, fCr^-, or CPP. This assumption is invalid under conditions of mitochondrial uncoupling because dissipation of the proton motive force alters the electrophoretic behavior of adenine nucleotide translocase (105, 117), which causes a net efflux of ADP from the mitochondrial matrix into the intermembranous space and cytosol. Not only would this augment cytosolic ADP and CPP, but it would also cause a right-shift in the creatine kinase equilibrium, thereby leading to greater PCr breakdown as well. Consequently, while previous observations of a PCr-slow component during high-intensity contractions have traditionally been attributed to a greater ATP_{COST} of contraction (174, 211), it is also possible that the PCr-slow component is a function of uncoupling-induced alterations in the distribution of adenine nucleotides across the inner mitochondrial membrane. That is, under conditions of mitochondrial uncoupling, increases in cytosolic [ADP], CPP, and PCr breakdown do not necessarily reflect concomitant increases in ATP_{OX}.

Consequently, there is a need to further delineate the contributions that increased ATP_{COST} and mitochondrial uncoupling contribute to augmentations in [ADP], CPP, and PCr breakdown during submaximal high-intensity contractions. To address this issue, we used 31-phosphorous magnetic resonance spectroscopy (^{31}P-MRS) to measure changes in muscle phosphates and ATP_{OX} during a stepwise contraction protocol similar to that described by Binzoni *et al.* (16). Briefly, the protocol consisted of 6 stages of isotonic knee extensions. Each stage lasted 3 minutes and was followed by 3-10 minutes of recovery, which allowed us to measure ATP_{OX} from the initial velocity of PCr resynthesis, and kinetic parameters controlling ATP_{OX} using multiparametric analyses (V_{max}, K_m, and n^H; described below). We specifically selected this approach to examine the relationship between changes in muscle phosphates, ATP_{OX}, and ATP_{COST} across multiple workloads above and below the muscle pH threshold (pH_T; used here as a proxy for the lactate threshold), which was calculated in each participant using a bilinear fitting procedure (102). We predicted that changes in muscle [ADP], CPP, PCr breakdown, and ATP_{OX} would be linearly proportional to changes in workload for all stages at intensities preceding the pH_T. However, consistent with our previous mitochondrial uncoupling hypothesis (*Chapter IV*), we predicted that changes in [ADP], CPP, and PCr breakdown would be augmented for workloads above the pH_T, whereas changes in ATP_{OX} would be attenuated. We further predicted that the capacity for ATP_{OX} (i.e., V_{max}) and substrate-specific rates of ATP_{OX} would progressively decline above the pH_T, whereas the ATP cost of force generation (ATP_{COST}) would remain unchanged, thereby supporting the concept that mitochondrial uncoupling is responsible for the VO_{2SC} (i.e., the

augmentation of skeletal muscle oxygen consumption and metabolism during high-intensity contractions at workloads above the pH and lactate thresholds).

Methods

Participants

Eight healthy young adults (25.2 ± 1.3 years, 3W) were recruited from the local community using fliers and word-of-mouth. All prospective participants were free of cardiovascular, respiratory, and musculoskeletal disease and provided written informed consent, as approved by the Institutional Review Board at the University of Massachusetts Amherst and in accordance with the Declaration of Helsinki. Because exercise training improves skeletal muscle oxidative capacity (123, 124, 129), which may affect the muscle fatigue and bioenergetic responses during the oxidative capacity and experimental trials (125), we excluded participants who reported engaging in more than 1 hour of physical activity per day at least 5 days per week. Additionally, we quantified habitual physical activity using uniaxial accelerometry (ActiGraph GT3X, Pensacola, Florida). Participants were instructed to wear the accelerometer during all waking hours for a full week and to record their daily physical activity in a logbook. Daily activity (counts·day^{-1000}) and minutes spent in moderate-vigorous physical activity (MVPA) were quantified using established thresholds for uniaxial ActiGraph accelerometers (57).

Experimental Approach

To examine changes in the control of oxidative phosphorylation at workloads above and below the pH_T, participants completed 6 stages of a stepwise knee extension

protocol. Each stage consisted of 3 minutes of isotonic contractions at 0.5 Hz, followed by 3 minutes of passive recovery. The rate of ATP_{OX} at the end of each stage was measured from the initial velocity of PCr resynthesis (V_{iPCr}, mM·s^{-1}) by fitting PCr recovery to either a mono- or biexponential function. Subsequently, changes in the control of ATP_{OX} by ADP or CPP were examined after each stage using multiparametric analysis to derive V_{max}, K_m, and n^H, as described previously (*Chapter 4*). This allowed us to calculate ATP_{OX} throughout each stage, which, when combined with measures of ATP synthesis by creatine kinase and non-oxidative glycolysis, permitted estimation of ATP_{COST} throughout each stage as well.

Experimental Setup

Participants were positioned supine inside the bore of a 70 cm 3-Tesla MR-scanner (Siemens, Erlangen, Germany) running on VE11c platform. A dual-tuned $^{31}P/^{1}H$ surface coil (8x10.5 cm) was positioned over the vastus lateralis (VL) of the participant's dominant leg and secured using athletic wrap and Velcro straps. Next, the participant's leg was securely strapped to a custom-built knee-extension ergometer at the ankle, thigh, and hips using inelastic straps and positioned inside the bore of the magnet such that the surface coil and VL were located within the scanner's isocenter. The knee-extension ergometer's contraction mode, duration, and frequency were all controlled using a custom-written MATLAB program (Mathworks, Natick, Massachusetts). Torque, position, and work were recorded for each contraction and exported for post-processing in Excel (Microsoft, Redmond, Washington). The program also provided participants

with real-time visual feedback about each contraction through display on a non-magnetic digital screen (LCD BOLD screen, Cambridge Research Systems Ltd., United Kingdom).

Contraction Protocol

The contraction protocol began with 2-3 maximal voluntary isometric contractions (MVIC), each lasting 3-5 s and followed by at least 1 minute of rest. Participants then performed 2-3 sets of maximal voluntary isokinetic contractions (MVDCs) to measure maximal knee-extension power. All MVDCs were isokinetic ($120°·s^{-1}$) and performed at a frequency of 0.5 Hz. Next, participants completed a rest-contract-recover protocol that began with 90 s of rest, followed by 24 s of MVDCs, and 7 minutes of passive recovery in order to measure baseline skeletal muscle oxidative capacity (k_{PCr}, $·s^{-1}$), as described previously (*see Chapter 4*).

Participants then completed the stepwise contraction protocol, which began with 3 minutes of rest, followed by 6 stages of isotonic knee extensions. Each stage lasted 3 minutes and was followed by 3 minutes of passive recovery (Figure 5.1), except for stage 6, which was followed by 10 minutes of recovery. The starting workload was set to 8-10% of the participant's MVIC torque (Nm) and increased by 2% MVIC each stage thereafter. Concentric work (Joules) was recorded for each contraction by the custom-written MATLAB program and subsequently exported for further analysis in Excel.

Spectroscopy

Gradient-echo scout images of the thigh were acquired to ensure proper placement of the coil relative to the participant's vastus lateralis and magnetic isocenter

of the MR scanner. The homogeneity of the magnetic field was optimized by manual

shimming on the proton (^{1}H) signal to minimize the width at half-maximum of the water

peak, followed by frequency optimization on the phosphorous (^{31}P) signal to minimize

the width at half-maximum of PCr (12.5 ± 0.6 Hz). Non-localized ^{31}P-MRS free-

induction decays (FIDs) were collected continuously throughout the oxidative capacity

and stepwise contraction protocols using a nominal $60°$ hard pulse, 4,000 Hz bandwidth,

2,048 complex points, and 2-s repetition time. For the oxidative capacity protocol, FIDs

were acquired during 90 s of rest, throughout the 24 s contractile period, and during 7

minutes of passive recovery. For the stepwise contraction protocol, FIDs were acquired

during 3 minutes of rest and throughout all contractile and recovery periods of the

stepwise exercise test (43 minutes).

All FIDs were analyzed using jMRUI v6.0beta (156). The first 30 s (15 FIDs) of

acquisition were excluded from analysis to avoid partial saturation effects. For the

oxidative capacity protocol, the remaining FIDs were averaged to yield temporal

resolutions of 60 s at rest, 4 s during the contractile period, 4 s for the first 20 s of

recovery, 8 s for the ensuing 280 s of recovery, and 30 s for the remainder of recovery.

For the stepwise protocol, FIDs were averaged to yield temporal resolutions of 150 s at

rest, 10 s during contractions, 4 s for the first 20 s of recovery, 8 s for the ensuing 280 s

of recovery, and 30 s for the remainder of recovery. FIDs were then zero-filled (2,048

points) and apodized using a 1Hz Lorentzian filter. Following Fourier transform, spectra

were manually phased and the frequency was zeroed on PCr. The AMARES algorithm

was used to linefit peaks corresponding to phosphomonoesters (PME), inorganic

phosphate (Pi), phosphodiesters (PDE), phosphocreatine (PCr), the γ- and α-ATP doublets, and the β-ATP triplet (199).

Millimolar concentrations of phosphorous metabolites were calculated by correcting metabolite signal intensities using experimentally-derived saturation correction factors that were collected on a separate sample of 12 young adults (5 women), and assuming [Pi]+[PCr]+[PME] is equal to 42.5 mM (72). Total muscle creatine was also assumed to equal 42.5 mM and the concentration of free creatine (fCr) was assumed to be equal to [Pi] (104, 119). [ATP] was assumed to equal 8.2 mM at rest (119, 122, 125) and changes in [ATP] during the experimental trials were calculated by comparing the γ-ATP signal intensity at each timepoint to the γ-ATP signal intensity at rest. We then conducted linear regressions of [ATP] vs. time to determine if [ATP] declined in any given stage. [ADP] was calculated based on the creatine kinsae equilibrium (K'_{CK}):

$$[ADP] \ (mM) = ([ATP][Pi]) \ / \ ([fCr] \cdot K'_{CK}) \hspace{3cm} Eq \ 1$$

K'_{CK} was corrected for changes in cytosolic pH according to an exponential equation derived from experimental data reported by Golding *et al*. (65). Muscle pH was calculated from the chemical shift between Pi and PCr (154). Muscle pH_T and Pi/PCr thresholds were determined for each participant using a bilinear fit, as described previously (102).

Skeletal Muscle Oxidative Capacity

Baseline skeletal muscle oxidative capacity (k_{PCr}, $\cdot s^{-1}$) was calculated following 24 s of MVDCs by fitting the observed PCr recovery to a mono-exponential function:

$$PCr_{Fit} \ (t) = PCr_{End} + Amp \cdot (1 - Exp^{(-kPCr \cdot t)}) \hspace{2.5cm} Eq \ 2$$

Where PCr_{Fit} is the calculated [PCr] at time point (t), PCr_{End} is the measured [PCr] at the end of the 24 s trial, Amp is the amplitude of the recovery in mM, and k_{PCr} is the mono-exponential rate constant, which reflects the system's oxidative capacity (149, 150). This process was then repeated following each stage of the stepwise protocol. For stages above the pH_T, PCr recovery did not always follow a mono-exponential pattern (71, 193). In these cases, PCr recovery was modelled using a biexponential function:

$$PCr_{Fit} (t) = PCr_{End} + ((Amp_1 \cdot (1\text{-}Exp^{(-kPCr1 \cdot t)})) + (Amp_2 \cdot (1\text{-}Exp^{(-kPCr2 \cdot t)})) \qquad Eq\ 3$$

where PCr_{Fit}, (t), Amp, and k_{PCr}, all have their original meanings, and 1 and 2 denote the primary and secondary PCr recovery components, respectively. To avoid physiologically unrealistic amplitude and k_{PCr} estimations, the sum of (Amp1 + Amp2) was constrained to be no greater than the difference between the concentration of PCr observed at the end of the trial and the greatest concentration of PCr observed in recovery. Subsequently, the overall k_{PCr} of the biexponential function was calculated by weighting the k_{PCr1} and k_{PCr2} rate constants to their respective amplitudes:

$$Biexponential\ k_{PCr} = (k_{PCr1} \cdot (Amp_1/Total\ Amp)) + (k_{PCr2} \cdot (Amp_2/Total\ Amp)) \qquad Eq\ 4$$

Rates of oxidative ATP synthesis (ATP_{OX}) at the end of each stage were calculated from the initial velocity of PCr resynthesis (V_{iPCr}, $mM \cdot s^{-1}$). V_{iPCr} was calculated as the change in [PCr] measured over the first 4 s from the fitted PCr recovery estimation, using a mono-exponential fit for workloads prior to the pH_T and a biexponential fit for workloads beyond the pH_T. Consistent with our previous work (*Chapter 4*), we then calculated kinetic parameters of ATP_{OX} using multiparametric analysis. Briefly, the first 10 rates of PCr resynthesis after each stage were fit against CPP to derive V_{max}, K_{mCPP}, and $n^{H\ CPP}$ according to the equation:

$$V_{PCr} \ (mM \cdot s^{-1}) = V_{max} / \ (\ 1 + (K_{m\text{-}CPP} / CPP)^{nHCPP} \ ) \tag{Eq 5}$$

where V_{PCr} is one of the first 10 rates of PCr resynthesis, V_{max} is the maximal rate of ATP_{OX} $(mM \cdot s^{-1})$, $K_{m\text{-}CPP}$ is the CPP at which V_{max} is half-maximal, n^{HCPP} is the Hill coefficient. This process was then repeated while fitting the first 10 rates of PCr resynthesis against [ADP]:

$$V_{PCr} \ (mM \cdot s^{-1}) = V_{max} / \ (\ 1 + (K_{m\text{-}ADP} / [ADP])^{nHADP} \ ) \tag{Eq 6}$$

where V_{PCr}, $K_{m\text{-}ADP}$, and n^{HADP} all have their original meanings, and V_{max} is constrained to the value obtained from the CPP multiparametric analysis to avoid physiologically unrealistic estimations, as previously (*Chapter IV*).

pH and Pi/PCr Thresholds

Thresholds for intracellular pH and Pi/PCr were calculated for each participant using a bilinear model described by Kent-Braun *et al*. (102):

$$y = m_1 * W + b_1 \qquad \text{for} \qquad 0 < W \leq \text{ip} \tag{Eq 7}$$

$$y = m_2 * W + b_2 \qquad \text{for} \qquad \text{ip} \leq W \tag{Eq 8}$$

$$b_2 = (m_1 - m_2)\text{ip} + b_1 \tag{Eq 9}$$

where 'ip' is the inflection point, m_1 and m_2 represent the slopes of the equations defining workloads below (Eq# 7) and above (Eq# 8) the inflection point, and b_1 and b_2 represent the respective intercepts. To examine whether changes in end-stage metabolite concentrations and V_{iPCr} were similar above and below the pH_T, separate linear slopes were fit for each variable of interest against workload. End stage metabolite concentrations were averaged over the final 30 s of each stage.

Statistical Analyses

All statistical analyses were conducted using SPSS v25.0 (IBM Statistics, Armonk, New York). Unless noted otherwise, data are presented as mean±SE, with p-values < 0.05 considered statistically significant. Prior to conducting any statistical comparisons, all data were tested for normal distrubution using the Shapiro-Wilk test. Changes in end-stage metabolite concentrations, V_{iPCr}, kinetic parameters of ATP$_{OX}$, and ATP$_{COST}$ across stages were compared using repeated measures ANOVAs or the non-parametric Friedman test, with estimated marginal means or Wilcoxon signed-rank tests to determine individual differences, respectively. Slopes describing stepwise changes in muscle work and: 1) end-stage metabolite concentrations, 2) V_{iPCr} , and 3) kinetic parameters of ATP$_{OX}$ above and below the pH$_T$ were compared using paired t-tests. Finally, to ensure that V_{iPCr} calculated at the end of each stage in the stepwise test was not confounded by the shortened recovery period (i.e., 3 minutes), we conducted Pearson correlations between V_{iPCr} measurements obtained by fitting all of recovery after the baseline oxidative capacity protocol (7 minutes) and the final stage of the stepwise test (10 minutes) to measurements of V_{iPCr} obtained by fitting only the first 3 minutes of recovery.

Results

Descriptive data for the participants are listed in Table 5.1. This was a young, moderately active cohort with normal BMIs. Representative data from one participant showing the work done for each contraction of a single stage are shown in Figure 5.1A. Figure 5.1B depicts the mean work done for each contraction of the entire stepwise

protocol for all participants. Changes in cytosolic pH, PCr, and ADP throughout the protocol are shown in Figure 5.2. None of the participants exhibited decreases in [ATP] ($p > 0.05$) but end-stage values for pH, PCr, ADP, and CPP changed across all stages (all, $p < 0.01$).

The workloads corresponding to the pH_T and Pi/PCr threshold were not different from one another (23.6 ± 2.4 vs. 23.3 ± 2.2 Joules, respectively; $p = 0.44$). Group mean slopes above and below the pH_T are described in Table 5.2. As shown in Figure 5.3, the slopes of cytosolic [ADP] and CPP vs. workload were greater above the pH_T than below it ($p < 0.02$), but this was not the case for PCr ($p = 0.78$). V_{iPCr} also increased linearly with workload for the first 4 stages but plateaued thereafter (Figure 5.4), resulting in the slope above the pH_T being significantly lower than that observed below the pH_T ($p = 0.03$).

Results from the multiparametric analyses for ADP- and CPP-specific ATP_{OX} are presented in Table 5.3. There was no main effect for changes in V_{max} across stages ($p = 0.135$) but the slope for changes in V_{max} above the pH_T was lower than the slope observed below ($p = 0.045$, Table 5.2 and Figure 5.5). Similarly, no main effect of stage was observed for $K_{m\text{-}ADP}$, $K_{m\text{-}CPP}$, or n^{HCPP}, although n^{HADP} did exhibit a main effect of stage ($p = 0.001$), with post hoc analysis indicating that n^{HADP} progressively declined across stages, except for stage 2 compared to stage 3 ($p = 0.19$), and stage 6 compared to stages 4 and 5 ($p = 0.081$ and $p = 0.704$, respectively). A main effect of stage was also observed for both ADP- and CPP-specific ATP_{OX} ($p < 0.05$, both; Figure 5.6). For ADP-specific ATP_{OX}, Stage 6 was lower than Stages 2-4, and Stage 5 was lower than Stages 2 and 4. For CPP-specific ATP_{OX}, Stages 5 and 6 were both lower than Stages 2 and 4.

Finally, there was no change in ATP_{COST} across stages throughout the stepwise test (Figure 5.7; $p = 0.10$).

Discussion

The main finding of the present study is that augmentations in cytosolic ADP and CPP during high-intensity contractions at workloads above the pH_T are not accompanied by concomitant increases in ATP_{OX}. In accordance with our main hypothesis, changes in cytosolic [ADP], CPP, PCr breakdown, and V_{iPCr} were linearly related to workload for stages below the pH_T (Figure 5.3). However, for workloads above the pH_T, changes in cytosolic [ADP] and CPP were augmented, whereas V_{iPCr} tended to plateau after stage 4 (Figure 5.4). Moreover, V_{max} began to decline after stage 4 (Figure 5.5), which lead to declines in both ADP- and CPP-specific ATP_{OX} (Figure 5.6). Furthermore, consistent with our second hypothesis, we did not observe a change in ATP_{COST} throughout the protocol (Figure 5.7). Consequently, the results of this study suggest that the VO_{2SC} is caused by impairments in the capacity for ATP_{OX}, possibly due to mitochondrial uncoupling.

Our stepwise test produced most of the stage-stage changes in muscle work and metabolites that we expected to see. As demonstrated in Figure 1, within-stage muscle work performances were stable and increased linearly across all 6 stages. The pH_T occurred after stage 2 in one participant, after stage 3 in 5 participants, and after stage 4 in 2 participants, thereby allowing us to compare changes in muscle phosphates, ATP_{OX}, and ATP_{COST} above and below the pH_T in all participants. Consistent with previous work, changes in muscle phosphates were linearly related to changes in muscle work for

132

workloads below the pH_T but augmented thereafter (10, 85, 102, 104). However, we did not observe a significant augmentation in PCr breakdown above the pH_T (Figure 5.3). This null finding appeared to be due to a floor-effect, as PCr breakdown reached 70% of the baseline resting level by the end of stage 4 and only decreased an additional 15% thereafter, which may have been a consequence of the high energy cost of overcoming inertia associated with isotonic contractions. Nevertheless, the augmentation of cytosolic [ADP], CPP, and proton (H^+) accumulation indicated that muscle metabolism was indeed augmented above the pH_T. Subsequently this allowed us to examine whether the augmentations in muscle metabolism were caused by increases in ATP_{COST} or mitochondrial uncoupling-induced alterations in the capacity for ATP_{OX}.

Consistent with our primary hypothesis, V_{iPCr} was not augmented above the pH_T. This finding is deductively opposed to the hypothesis that augmentations in muscle oxygen consumption during high-intensity contractions reflect increased rates of ATP_{OX} caused by increases in the ATP_{COST} of force generation (29, 35, 174, 211). Moreover, we saw no change in ATP_{COST} throughout the stepwise test (Figure 5.7). These results contrast those of Cannon *et al*. (35), who observed increases in V_{iPCr} and ATP_{COST} during high-intensity bilateral knee extensions. One possible explanation for this discrepancy is the duration of the two contraction protocols. Whereas Cannon *et al*. calculated changes in ATP_{COST} over the final 5 minutes of an 8-minute bout of contractions, our stages were only 3 minutes. Consequently, we cannot rule out the possibility that our 3-minute stages were not long enough to permit changes in ATP_{COST} to develop. That this is the second time we have reported no change in ATP_{COST} using contraction protocols that last 3-4 minutes per bout, strongly suggests that additional work is necessary to identify whether

the observations reported here, and previously (*Chapter IV*), are replicable during longer stepwise stage durations and all-out contraction protocols.

Collectively, the results presented here suggest that contraction intensities above the pH_T are associated with impairments in the capacity for ATP_{OX}, which is consistent with the notion that high-intensity contractions stimulate mitochondrial uncoupling (*Chapter IV*) (35). However, another notable finding of the present study is that although increases in V_{iPCr} relative to workload were attenuated above the pH_T, the relationship was not immediately impaired. Stage 4 was above the pH_T in six of the eight participants, but the increase in V_{iPCr} continued to follow the linear relationship observed for workloads below the pH_T. Rates of ADP- and CPP-specific ATP_{OX} were also well maintained. Consequently, it is possible that mitochondrial uncoupling does not immediately impair ATP_{OX} provided respiration by the electron transport chain can increase sufficiently to compensate for the passive proton conductance. Put another way, mild mitochondrial uncoupling may alter P/O ratio and the behavior of electrophoretic transport proteins (105, 117, 118), but if proton pumping by the electron transport chain can increase sufficiently to account for H^+ conductance by both mitochondrial uncoupling and ATP synthase activity, then ATP_{OX} may not necessarily be compromised. Consistent with this notion, mitochondria appear to exhibit a reserve capacity for respiration, as peak rates of mitochondrial oxygen consumption *in vitro* tend to occur when respiration is uncoupled from thermodynamic constraint by ATP synthase and matrical phosphorylation potential (54, 87, 126, 127, 163). This latter observation adds to the symmorphosis concept described by Gifford *et al*. (62). Specifically, multiple studies have reported that State-3 respiratory capacity *in vitro* exceeds oxygen delivering

capacity *in vivo* (24, 25, 62), the paradox being why skeletal muscle would develop such a large capacity for ATP_{OX} if the capacity is physiologically unachievable *in vivo*. Possibly even more perplexing, however, is how and why uncoupled respiratory capacity would be greater than State-3 respiratory capacity if oxygen delivery by the cardiovascular system only barely matches the muscle's capacity for *in vivo* State-3 respiration in the first place.

In light of this latter symmorphosis, perhaps we need to start considering the possibility that, in healthy young adults, oxygen delivery and availability may not be limiting to oxidative phosphorylation *in vivo*. Instead, perhaps the true limit to oxidative phosphorylation *in vivo* is not oxygen availability or respiratory capacity, but rather the mitochondria's intrinsic capacity for ATP synthesis (i.e., phosphorylation capacity). If this were the case, the magnitude of the proton motive force would always remain high and intramuscular oxygenation would always, theoretically, be excessive, or hyperoxic, because respiration would always be under State-3, phosphorylative control. In turn, this may lead to greater rates of reactive oxygen species generation, which could stimulate mitochondrial uncoupling to attenuate oxidative stress.

Although this scenario may appear radical at first, it becomes much more tenable when one considers that the VO_{2SC} is associated with the recruitment of Type-II muscle fibers (114, 141, 143), which tend to exhibit a lower mitochondrial content and oxidative capacity than Type-I fiber (63, 67, 86, 115), as well as lower antioxidative capacities (63, 165) and greater uncoupling protein 3 content (77, 176). Moreover, this hypothesis also provides an explanation for why the VO_{2SC} is attenuated following endurance training, as improvements in mitochondrial phosphorylation capacity would improve the muscle's

135

capacity to utilize oxygen for ATP_{OX}, thereby attenuating the magnitude of hyperoxia and reducing the generation of ROS that stimulated mitochondrial uncoupling prior to the endurance training regimen. Thus, perhaps we need to consider the possibility that for healthy young adults, high-intensity exercise at workloads above the lactate threshold are associated with *hyper*-oxia, rather than *hypo*-oxia.

Limitations

There are two major limitations to the present study that need to be addressed in the near future. First, we did not measure muscle or pulmonary oxygen consumption during the present study, and therefore cannot say for certain that the plateauing of V_{iPCr} after stage 4 was strictly due to changes in the efficiency of oxidative ATP synthesis. Indeed, V_{iPCr} would also be expected to plateau if the muscle achieved VO_{2max} by stage 4. Consequently, we cannot say for sure that mitochondrial uncoupling was occurring in skeletal muscle during stages above the pH_T. Follow-up studies should address this limitation by combining ^{31}P-MRS measures of ATP_{OX} with pulmonary oxygen uptake (38, 128) or direct measures of muscle oxygen consumption (13, 49, 68, 145).

Second, from an applied physiology perspective, another factor we have to consider is that oxygen delivery by the cardiovascular system is less limiting to oxidative metabolism during single-leg knee extensions than during whole body exercises (24, 25, 62). Consequently, it is possible that if mitochondrial uncoupling does occur *in vivo*, it may only present during high-intensity single-joint contraction protocols, and not whole-body exercises, such as cycling or treadmill running where cardiovascular oxygen delivery may not be able to match intramuscular demand. To overcome this limitation,

future investigations should continue to implement large muscle mass protocols inside magnetic-resonance scanners, such as bilateral knee extensions (35, 174) or cycling (91), to investigate whether whole-body exercises induce similar impairments in V_{iPCr} and V_{max} that we have observed here and in our previous investigation (*see Chapter IV*). Indeed, Jeneson *et al*. developed an MR-compatible cycle ergometer that elicited heart rates of ~150 beats per minute, 80% PCr breakdown, and pH values of 6.7 at the end of an incremental exercise test (91); values that are consistent with the results reported in this study.

Conclusions

In conclusion, we have demonstrated that oxidative ATP synthesis, measured from the initial rate of PCr resynthesis, is not augmented during high-intensity submaximal contractions at workloads above the pH_T, despite significant augmentations in two key driving factors for mitochondrial energy production: cytosolic [ADP] and CPP. Instead, the capacity for ATP_{OX}, as well as ADP- and CPP-specific rates of ATP_{OX}, are diminished above the pHT, though these impairments do not present immediately. Notably, we also observed no change in the ATP_{COST} of contraction across a range of workloads, including those above the pH_T, suggesting that mechanical efficiency is not impaired during high-intensity contraction in healthy young adults. Collectively, these results add to the growing body of evidence suggesting that mitochondrial uncoupling is the mechanism responsible for the VO_{2SC} and augmentations in muscle metabolism during high-intensity exercise at workloads above the pH_T. Future studies should look to collect measures of muscle oxygen consumption simultaneously with ^{31}P-MRS measures

of ATP_{OX} to determine more directly whether mitochondrial P/O ratio is decreasing during high-intensity contractions. Additionally, in contrast to the single-leg knee extension model used here, it would be advantageous to develop and employ MR-compatible ergometers that can mimic whole-body exercise models inside MR-scanners (35, 91), where oxidative metabolism and exercise performance are more likely to be centrally limited by the cardiovascular system's oxygen delivering capacity.

Age (years)	25.2 ± 1.3
Height (cm)	175.7 ± 3.5
Body Mass (kg)	74.4 ± 5.0
BMI (kg/m^2)	23.9 ± 0.8
PA (counts·day^{-1}/1000)	284.4 ± 25.5
MVPA (minutes·day^{-1})	46.7 ± 4.6
Peak isometric torque (Nm)	251.5 ± 20.0
Peak power (Watts, 120°·s^{-1})	277.4 ± 34.4

Table 5.1: Study 2 Participant Characteristics. Data were collected on 8 healthy young adults (3F). Data are presented as means $\pm$ SE.

	Stages < pH Threshold	Stages > pH Threshold
PCr Breakdown (ΔmM/ΔJ)	-1.07 ± 0.13	-1.28 ± 0.28
ADP (ΔmM/ΔJ)	0.005 ± 0.001	0.016 ± 0.003 *
CPP (ΔCPP/ΔJ)	0.021 ± 0.005	0.081 ± 0.014 *
V_{iPCr} (ΔmM·s^{-1}/ΔJ)	0.019 ± 0.005	0.000 ± 0.005 *
V_{max} (ΔmM·s^{-1}/ΔJ)	0.002 ± 0.008	-0.020 ± 0.003 *

Table 5.2: Slopes for changes in muscle metabolites, V_{iPCr}, and V_{max} vs. muscle work (J) at intensities above or below the pH_T. After determining each participant's pH_T, slopes were calculated by using a linear estimation to fit Δvariable/Δmuscle work for stages above and below an individual's pH_T respectively. * Denotes a significantly different slope above the pH_T compared to below. Data are presented as mean ± SE.

	Stage 1	Stage 2	Stage 3	Stage 4	Stage 5	Stage 6
k_{PCr} ($\cdot s^{-1}$) *	0.025 ± 0.002 [e,f]	0.024 ± 0.002 [c-f]	0.022 ± 0.002 [b,e,f]	0.021 ± 0.002 [b,e,f]	0.018 ± 0.002 [a-d]	0.018 ± 0.002 [a-d]
V_{max} ($mM \cdot s^{-1}$)	0.73 ± 0.04	0.79 ± 0.06	0.75 ± 0.06	0.76 ± 0.07	0.69 ± 0.08	0.65 ± 0.08
K_m-ADP (mM)	0.037 ± 0.004	0.040 ± 0.003	0.039 ± 0.002	0.039 ± 0.002	0.035 ± 0.002	0.030 ± 0.002
n^H ADP *	1.30 ± 0.08 [b-f]	1.17 ± 0.05 [a,d-f]	1.10 ± 0.04 [a,d-f]	1.02 ± 0.03 [a,c,e]	0.96 ± 0.02 [a-d]	0.97 ± 0.02 [a-c]
K_m CPP	0.085 ± 0.014	0.098 ± 0.010	0.094 ± 0.007	0.101 ± 0.008	0.091 ± 0.007	0.080 ± 0.005
n^H CPP	0.79 ± 0.04	0.74 ± 0.02	0.72 ± 0.01	0.71 ± 0.01	0.70 ± 0.00	0.73 ± 0.02

Table 5.3: Oxidative kinetics at the end of each stage of the stepwise test. k_{PCr} declined throughout the contraction protocol. V_{max} was not different across stages when analyzed by repeated measures ANOVA, but the slope of V_{max} above the pH threshold was different from the slope below the acidic threshold (p=0.045, see text for details). The only other parameter that changed across stages was n^H-ADP (*, $p < 0.001$). [a] – significantly different from stage 1; [b] – significantly different from stage 2, [c] – significantly different from stage 3, [d] – significantly different from stage 4, [e] – significantly different from stage 5, [f] – significantly different from stage 6.
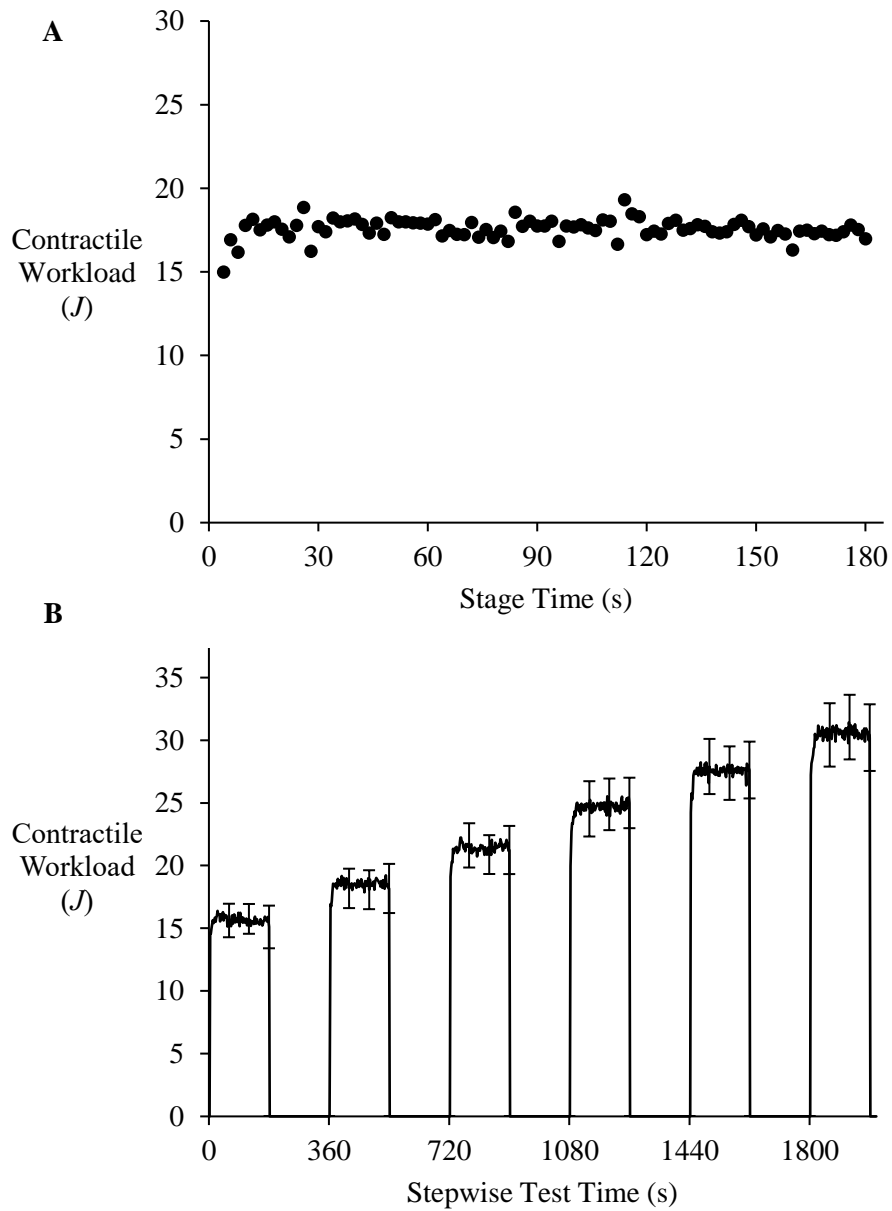
Figure 5.1: Muscle performances during the stepwise knee extension protocol. The representative data in panel *A* illustrate the work (Joules) performed for each contraction of a single stage in one participant. Panel *B* illustrates group mean data for all contractions performed throughout the stepwise protocol. Data are presented as mean ± SE, with error bars shown at the end of each minute.
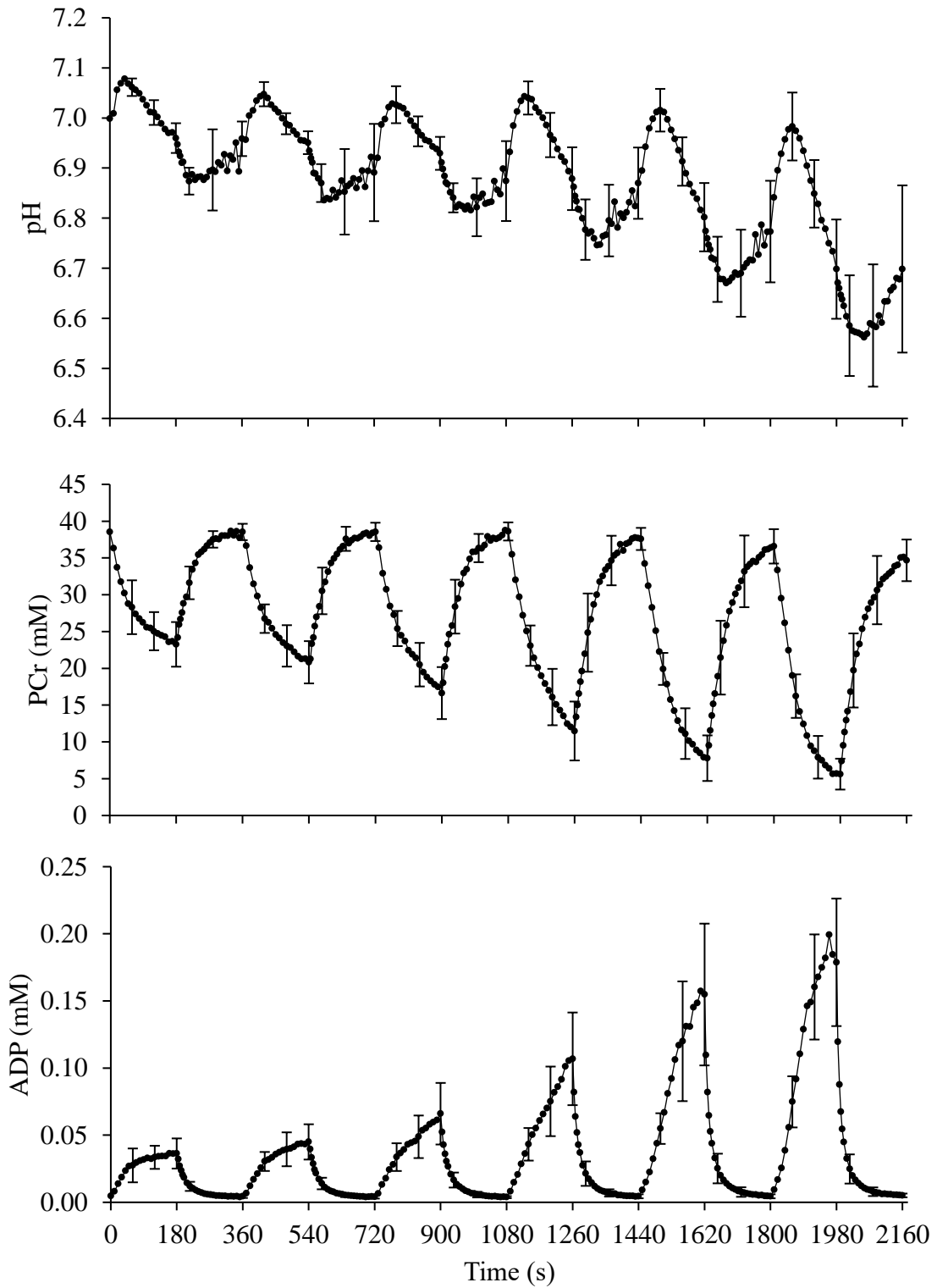
Figure 5.2: Changes in muscle metabolites throughout the stepwise contraction protocol. Muscle pH, PCr, and ADP for six 3-minute stages of isotonic contractions and 3 minutes of recovery are shown. Data are presented as mean ± SD, with error bars shown intermittently.
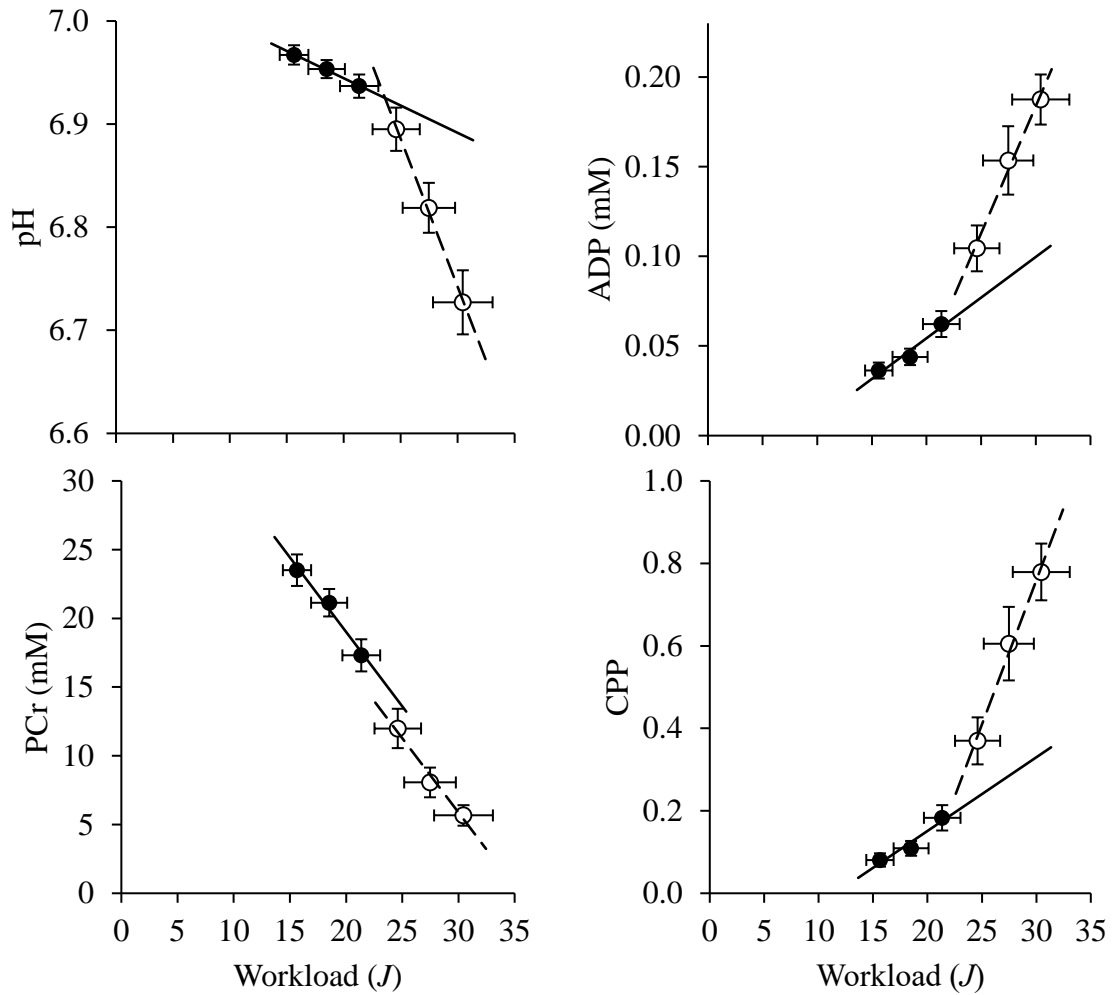
Figure 5.3: End-stage changes in muscle metabolites. Metabolites during the final 30 s of each stage. Open and filled circles represent variables at the end of workloads above and below the pH_T, respectively. The dashed and solid lines illustrate the mean linear relationships observed for changes in metabolites relative to workload above and below the pH_T, respectively. Data are presented as mean ± SE.
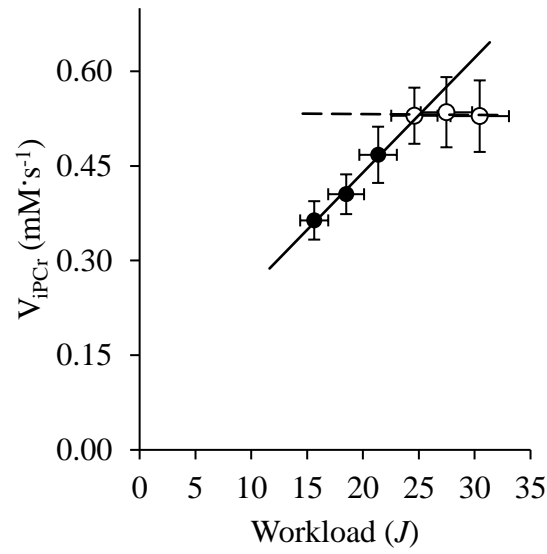
Figure 5.4: Changes in V_{iPCr} across stages. As expected, V_{iPCr} increased linearly with workload below the acidic threshold, but beyond stage 4, the increase in V_{iPCr} was attenuated relative to the increase in workload. Data are presented as mean ± SE.
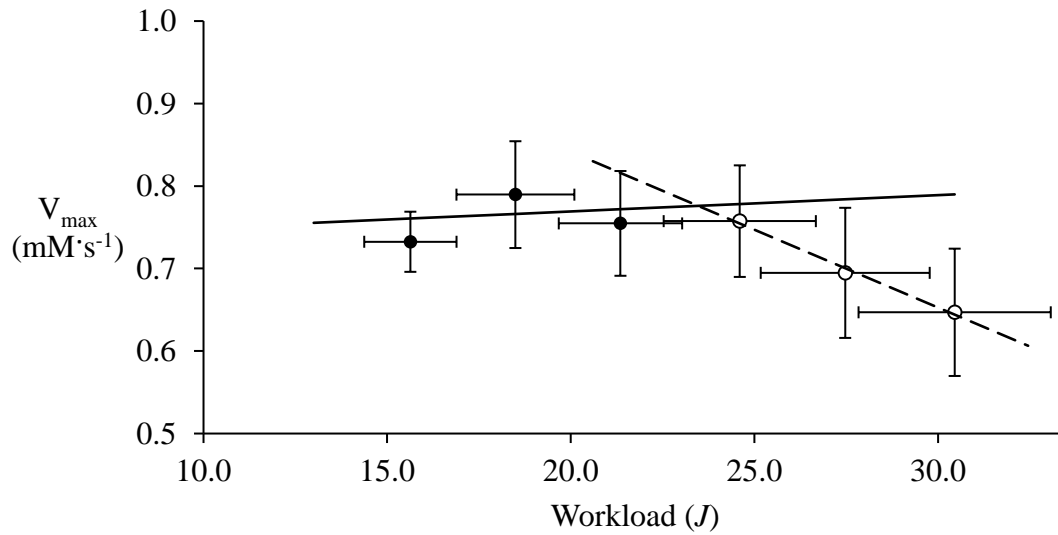
Figure 5.5: Estimations of V_{max} across stages. There was little to no change in V_{max} across the first 4 stages (slope < pH_T = 0.002 mM·s^{-1}/J), but after stage 4, V_{max} steadily declined (slope > pH_T = -0.020 mM·s^{-1}/J). Data are presented as mean ± SE.
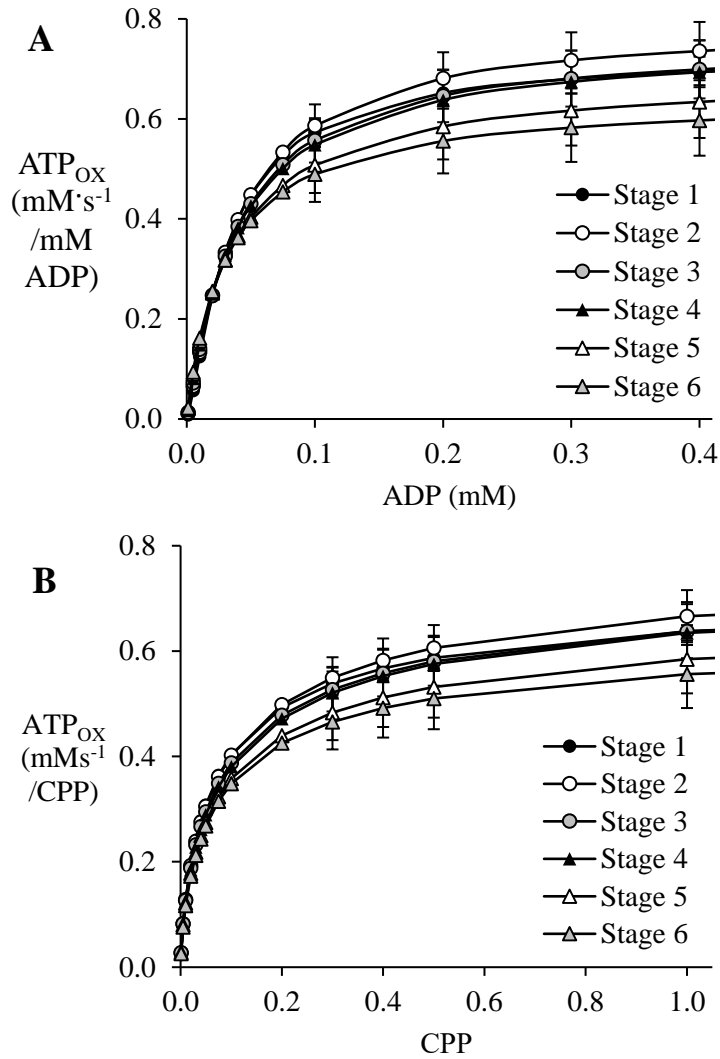
Figure 5.6: End-stage rates of substrate-specific ATP$_{OX}$. Rates of substrate-specific ATP$_{OX}$ were calculated after every stage for each participant. Substrate-specific ATP$_{OX}$ remained similar across the first 4 stages but tended to be lower following stages 5 and 6 for both ADP (*A*) and CPP (*B*) (*see Results for more details*). Data are presented as mean ± SE. Error bars are shown for the final 4 substrate levels for clarity.
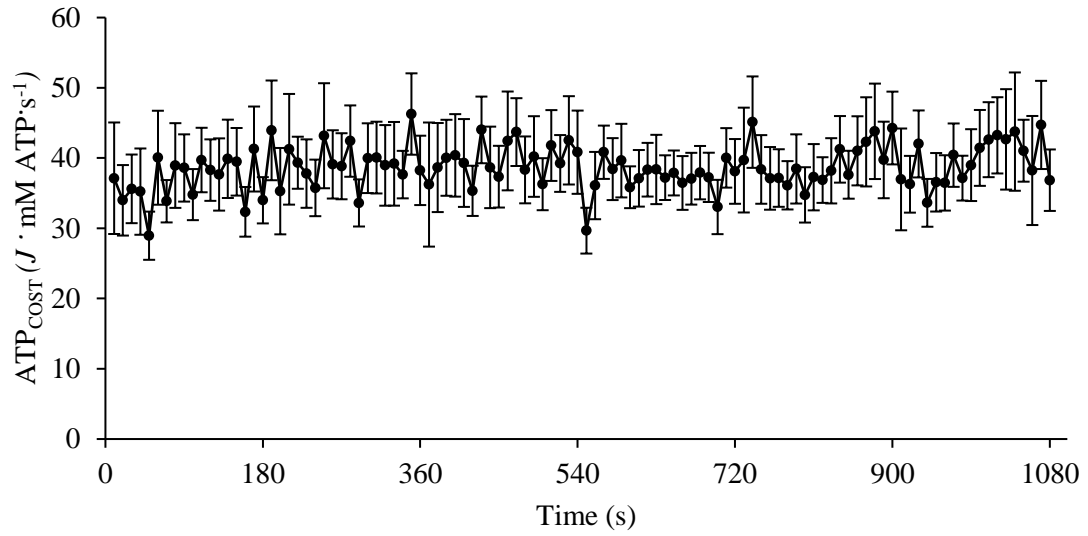
Figure 5.7. Changes in ATP$_{COST}$ during the stepwise knee extension protocol. Mean ATP$_{COST}$ (J·mM ATP·s^{-1}) was calculated for each stage by averaging all timepoints (10-s resolution) in each stage and did not change throughout the stepwise contraction protocol (p = 0.10). Mean ATP$_{COST}$ for each timepoint throughout the full protocol are shown. Data are presented as mean ± SE.

CHAPTER 6

DISSERTATION SUMMARY

Current models of oxidative phosphorylation sufficiently describe skeletal muscle energetics during moderate-intensity contractions because ATP demand is met mainly by oxidative ATP synthesis (ATP_{OX}) and steady-state muscle metabolism is linearly related to the rate of muscle work. These metabolic conditions allow researchers to use 31-phosphorous magnetic resonance spectroscopy (^{31}P-MRS) and basic principles of chemical thermodynamics to calculate rates of ATP_{OX} from known relationships with cytosolic free creatine, [ADP], or the phosphorylation potential (CPP) (19, 95, 98, 119, 120, 129, 149, 158).

However, the mechanisms that limit and control oxidative phosphorylation *in vivo* during square-wave high-intensity contraction protocols (i.e., above the lactate threshold) are not fully understood. Not only is steady-state metabolism delayed until 5-6 minutes into exercise (58, 212, 213, 219), or unachievable, but the linearity between skeletal muscle metabolism and power output is distorted (58, 109). Specifically, the oxygen cost of high-intensity contractions is greater than would be predicted by the linear relationship observed during moderate-intensity contractions, and is accompanied by greater changes in phosphocreatine (PCr) breakdown, acidosis, [ADP], and the free energy of ATP hydrolysis (10, 44, 83, 85, 104, 170, 174, 191).

Previously, researchers postulated that the augmentation of skeletal muscle oxygen consumption during high-intensity contractions was driven either by: 1) increases in the ATP cost of force generation (174), or 2) decreases in the efficiency of ATP_{OX} due to mitochondrial uncoupling. However, methodological limitations had hindered a

definitive evaluation of either hypothesis *in vivo*. Specifically, although several methods exist for using ^{31}P-MRS to calculate rates of ATP$_{OX}$, all of these methods assume that the ATP cost of force generation does not change (99) or that mitochondrial uncoupling does not occur (29, 119). Given that these two assumptions formulate the basis of the two hypotheses that have been put forth to explain why skeletal muscle oxygen consumption is augmented above the lactate threshold (35, 169, 174), they cannot be used to study changes in the control of oxidative phosphorylation. Consequently, the objective of this dissertation was to unravel the mechanisms that alter the control of oxidative ATP synthesis during contractions at workloads above the lactate threshold by measuring changes in ATP$_{OX}$ from the initial velocity of PCr resynthesis (V$_{iPCr}$). Because V$_{iPCr}$ yields only one measure of ATP$_{OX}$ per bout of contractions, a secondary objective was to develop and validate new methods for calculating ATP$_{OX}$ continuously during high-intensity contractions.

Study 1 allowed us to achieve both of these objectives. Participants performed repeated bouts of maximal voluntary dynamic contractions lasting 24, 60, 120, and 240 s that were matched for changes in power and metabolites. V$_{iPCr}$ increased over the first 60 to 120 s but then declined over the final 120 s. The decrease in V$_{iPCr}$ from 120 to 240 s occurred despite elevated cytosolic ADP, CPP, and PCr breakdown. That cytosolic ADP, CPP, and PCr breakdown remained elevated over the final two minutes indicates that the decline in V$_{iPCr}$ was not a function of muscle fatigue and motor unit dropout, as this would have caused each of these metabolic measures to partially recover before the end of the 240-s trial. Instead, the decline in V$_{iPCr}$ over the final 2 minutes appeared to be caused by a diminished capacity for ATP$_{OX}$. Multiparametric analyses performed after

each trial to calculate V_{max}, K_m, and n^H confirmed this suspicion, with V_{max} being

significantly lower after the 120- and 240-s trials than the 24-s trial. Together, these data

strongly suggest that augmentations in oxidative metabolism during high-intensity

contractions are caused by mitochondrial uncoupling. Regretably, however, we did not

collect any measures of oxygen consumption, and therefore cannot conclude without a

doubt that mitochondrial uncoupling affected ATP_{OX} in this study.

On the other hand, we did calculate ATP_{COST} throughout the 240-s trial and found

that ATP_{COST} did not change across any timepoints. These findings conflict with those of

Broxterman *et al*. (29), who reported an increase in the ATP_{COST} of torque generation

during a maximal isometric contraction protocol in the knee extension muscles of healthy

young adults. However, the method for calculating ATP_{OX} in that study did not account

for changes in V_{max} from baseline to the end of fatiguing contractions, which the second

half of Study 1 in this dissertation (*described below*) showed is necessary for accurate

calculation of ATP_{OX}. Consequently, it is possible that the increase in ATP_{COST} observed

in that study was a function of inaccurate ATP_{OX} calculation.

The ATP_{COST} results of Study 1 also conflict with those of Cannon *et al*. (37),

who reported increased ATP_{COST} during 8 minutes of submaximal bilateral knee

extensions. Notably, although Cannon *et al*. calculated ATP_{OX} from V_{iPCr}, it is unclear if

they fit PCr recovery to a monoexponential following both the 3- and 8-minute trials, or

if biexponential fitting was used when PCr recovery did not follow a mono-exponential

pattern. As shown in Figure 3.1, this methodological consideration is one that requires

greater investigation to ensure that calculations of k_{PCr}, V_{iPCr}, V_{max}, and ATP_{OX} are

accurate and consistent across labs using ^{31}P-MRS to investigate skeletal muscle

energetics. Alternatively, the discrepancy between our results could have been due to differences in contraction intensity and protocol duration. Although we saw no change in ATP_{COST} throughout the stepwise contraction protocol in Study 2, where changes in muscle metabolites were augmented for several workloads above the pH threshold, we cannot rule out the possibility that changes in ATP_{COST} may have been observed if we had extended the duration of our stages to 6 minutes or longer.

The second major finding of Study 1 was that ATP_{OX} can be calculated continuously during high-intensity, non-steady state contractions by adjusting for changes in V_{max}. That is, ATP_{OX} can be calculated continuously, regardless of the contraction intensity, by measuring V_{max}, K_{m}, and n^{H} at baseline following an oxidative capacity protocol, and then again during the recovery period immediately after the bout of contractions. The ATP_{OX} method I developed and presented in this dissertation, which was a modification of traditional Direct ATP_{OX} methods, should help pave the way for future investigations of skeletal muscle bioenergetics during high-intensity contractions in both healthy young adults, as well as in clinical populations that are easily fatiguable and would not be able to perform repeated bouts of contractions.

Subsequently, the purpose of Study 2 to follow up on Study 1 by measuring changes in ADP, CPP, PCr breakdown, and parameters of ATP_{OX} (V_{iPCr}, V_{max}, K_{m}, and n^{H}) after each stage of a stepwise, or incremental, isotonic contraction protocol. Similar to previous studies (40, 101), muscle metabolites and ATP_{OX} increased linearly with workload for all workloads below the pH threshold (pH_{T}). Calculations of V_{max}, K_{m}, and n^{H} were also consistent across stages, indicating the capacity for ATP_{OX}, and control by ADP or CPP, were not affected by the contractions. For workloads above the pH_{T},

however, changes in muscle metabolites were augmented relative to workload, yet this was not accompanied by an augmentation in ATP_{OX}. Instead, ATP_{OX} plateaued, and V_{max} declined (slope above pH_T < slope below pH_T), over the final 2 stages, leading to decreases in substrate-specific phosphorylation rates of ATP_{OX} by ADP and CPP (stages 5 and 6 lower than stages 2-4 for ADP specific ATP_{OX}, and stages 2 and 4 for CPP-specific ATP_{OX}). Moreover, there was no change in ATP_{COST} throughout the protocol, suggesting once again that augmentations in muscle metabolism during high-intensity contractions are not caused by greater rates of ATP demand due to increased ATP cost of force generation.

Collectively, these results suggest that the declines in V_{iPCr} and V_{max} observed in Study 1 were not simply a function of the all-out, maximal intensity and high energy demand of the contaction protocol. Instead, the impairment of V_{max} during high-intensity contractions appears to be a function of both intensity (i.e., the magnitude of the workload above the pH_T) and duration (i.e., length of the contraction protocol). However, we did not collect any measures of oxygen consumption, such as pulmonary oxygen uptake, during Study 2, and therefore cannot conclude beyond a reasonable doubt that these obervations were definitively caused by mitochondrial uncouping. However, that ATP_{OX} was not augmented above the pH_T strongly refutes the suggestion that augmentations in skeletal muscle oxygen consumption during high-intensity contractions are caused by increased rates of ATP_{OX}, leaving mitochondrial uncoupling as the only viable hypothesis remaining.

Prospective Considerations

My undergraduate mentor, Dr. Robert Lehnhard, once told me; "the only limitation to science is the inability to ask the right questions…". In Chapter II, I explained how mitochondrial uncoupling offers as valid an explanation to the slow component of oxygen uptake kinetics (VO_{2SC}) as does increases in the ATP cost of force generation. Yet, mitochondrial uncoupling rarely garners significant attention as a potential explanation for the VO_{2SC} because there is no clear mechanistic hypothesis that explains both ***how*** and ***why*** it would occur during high-intensity exercise, which precludes the development of testable predictions that permit deductive separation of mitochondrial uncoupling from increases in ATP_{COST} *in vivo*. As I have mentioned several times throughout this dissertation, there are numerous metabolic and bioenergetics aspects of high-intensity exercise that the increased ATP_{COST} hypothesis cannot reconcile, and, in my opinion, the only reason this hypothesis has persisted for so long is because there has never been a viable alternative hypothesis to clearly oppose it.

In my opinion, the presentation of an alternative mechanistic hypothesis is the single most important next step to unraveling the mechanisms that limit oxidative phosphorylation *in vivo* and alter its control during high-intensity contractions. Although I have developed a theoretically comprehensive hypothesis to address this gap, which posits that phosphorylation capacity is the true limit to oxidative phosphorylation *in vivo* and that hyperoxic mitochondrial uncoupling is responsible for the VO_{2SC}, as well as many other unresolved metabolic and bioenergetic phenomena, such as the lactate paradox and excess post-exercise oxygen consumption, I will wait to unveil its complete description until each component of the hypothesis can be organized and explained in a

single unadulterated manuscript without being diminished by the novel observations and methodologies presented in this dissertation.

Moving forward, researchers should look to collect measures of skeletal muscle oxygen consumption alongside ^{31}P-MRS measures of ATP$_{OX}$, which should permit calculation of the P/O ratio and direct demonstration of mitochondrial uncoupling. Changes in mitochondrial coupling within skeletal muscle could also be examined by measuring changes in muscle metabolites that are distributed in the matrical and cytosolic compartments according to the proton motive force (117, 118, 159). That is, conditions of oxygen-limited metabolism could be separated from conditions of mitochondrial uncoupling by identifying specific 'biochemical signatures' for each condition. However, to the best of my knowledge, this has not been investigated comprehensively. Future studies should also look to combine other techniques with ^{31}P-MRS, such as near-infrared spectroscopy (46, 172, 177), diffuse correlation spectroscopy (5, 171, 198), and surface fluorimetry (42, 92), which will provide additional insight into the role oxygen availability plays in limiting or altering the regulation of oxidative phosphorylation within skeletal muscle during moderate- and high-intensity contractions.

INFORMED CONSENT DOCUMENT (STUDY I)

INFORMED CONSENT DOCUMENT
University of Massachusetts
Amherst, MA 01002

Project Title: *Calculating Oxidative Energy Production during Non-Steady State Contractions*
Principal Investigator: Jane A. Kent, PhD
Co-Investigators: Rajakumar Nagarajan, PhD, Miles F. Bartlett, Liam F. Fitzgerald, Joseph A. Gordon, Julia D. Miehm

Your written informed consent is required before you can participate in this project. Please read this document carefully and then sign your name on the last page if you agree to participate. This document is in accordance with regulations for the Protection of Human Research Subjects (45 CFR 46). You are encouraged to ask questions at any time before, during or after participating.

Purpose: Aerobic energy production in skeletal muscles can be measured during moderate-intensity contractions, but this becomes difficult during high-intensity contractions. We recently developed a new method for calculating aerobic energy production in contracting skeletal muscles that appears to overcome the limitations of previous methods, and so the purpose of this study is to test the validity of our new method.

Eligibility: To participate in this study you must be healthy and between 25-40 years of age. You may not have any: neurological or neuromuscular disease; a history of stroke, peripheral vascular disease, cardiac or pulmonary disease; be a smoker; or have a history of any metabolic diseases/disorders. You may not be pregnant. You may not have any metal implants or anything that would prevent you from undergoing a magnetic resonance imaging (MRI) exam.

Procedures: Prior to your first visit, you will be screened by telephone interview for general health, medical history, current medications, usual physical activity habits, and eligibility for the study. If you are qualified and agree to participate, you will be invited to the Human Magnetic Resonance Center (HMRC) at the University of Massachusetts Amherst for one visit.

Paperwork and Muscle Contraction Protocol (~2 hours)
　　　Upon arriving to the HMRC, you will read the informed consent document and have any questions answered by the investigator. After agreeing to participate and signing the consent form you will fill out the following documents (attached):
　　　　　　- Physical Activity Readiness Questionnaire
　　　　　　- Medical History Form

- Magnetic Resonance (MR) Safety Form

Next, measures of blood pressure, height, and body weight will be obtained. Before entering the magnet room, you will empty your pockets and walk through a metal detector. We will then escort you to the MR scanner and position you on your back with your dominant leg on top of our custom-built leg exercise apparatus. The lower leg (shin) will be strapped to the apparatus just above the ankle, and at the knee using Velcro straps. Inelastic straps will also be secured over your hips to prevent unwanted movement during the muscle contractions. A specially designed copper coil encased in a plastic box will be secured over the thigh muscles using Velcro straps. This coil will be used to measure changes in muscle biochemistry during the contractions. Headphones will be provided to limit the amount of noise from the MR scanner, and to enable clear and constant communication between you and the investigators. We will talk with you and explain each set of measures as we go along. These measures are described next.

First, we will position you in the center of the MR scanner and "tune" the magnet to the thigh muscles. We will then take resting measures of your muscle biochemistry. During this time, you will lay quietly for about 10-15 minutes. Next, you will complete 2-3 maximal isometric (i.e., 'static') contractions, each lasting 3-4 seconds, to determine your maximal strength. You will be given 1-2 minutes of rest between each of these contractions. Then, you will repeat this effort, but this time you will maintain the maximal isometric contraction for 24 seconds, after which you will rest quietly without moving for up to 10 minutes. This procedure will be used to determine your muscle's "aerobic" capacity.

You will then perform 2-3 sets of 3 rapid, maximal dynamic contractions (i.e., "with movement"). The dynamic contractions will all be isokinetic; that is, the speed of the contraction will be limited by our custom-built exercise apparatus. These contractions will be used to determine your maximal dynamic strength. You will be given 1-2 minutes of rest between each of these sets.

Next, you will perform our experimental protocol, which will include 4 sets of dynamic knee extensions. You will perform one contraction every 2 seconds by kicking as hard and as fast as you can. The duration of each set will vary, beginning with 24 seconds for set 1 and increasing to 60, 120, and 240 for sets 2, 3, and 4, respectively. Up to 10 minutes of rest will be given between each set.

Lastly, before leaving, we will give the you a uniaxial accelerometer, which is a small activity monitor that will record the amount and intensity of physical activity you perform over the next 7 days. You will be instructed on how and when to use it and how to keep a simple physical activity log book. At the end of the week-long wear period, a member of the Muscle Physiology Laboratory will collect the accelerometer and log book at a time that is most convenient for you.

Subject Enrollment/Length of Study: We expect to enroll 10-20 participants in this study. Your participation will include 1 visit lasting approximately 2 hours.

Possible Risks and Discomforts: There are minimal risks associated with the procedures used in this research study. You may experience soreness in your muscles in the days following the testing, but this would be a normal response and should be

temporary. Injury is possible if you have any metal in or on you during the magnetic resonance testing, but we will check you beforehand to detect any such metal.

Magnetic Resonance Spectroscopy (MRS) and Imaging (MRI) – The United States Food and Drug Administration (FDA) has established guidelines for magnet strength and exposure to radio waves, and we carefully observe those guidelines. No ill effects have been reported for the radio wave exposure associated with this protocol. Some people may feel uncomfortable or anxious while in the MR scanner, which is a large magnet. If this happens to you, you may ask to stop the study at any time and we will take you out of the MR scanner. On rare occasions, some people might feel dizzy, get an upset stomach, have a metallic taste, feel tingling sensations, or experience muscle twitches. These sensations usually go away quickly but please tell the research staff if you have them.

MRI and MRS pose some risks for certain people. If you have a pacemaker or certain types of metal objects inside your body, you may not be in this study because the strong magnet used for these MR studies might harm you. Another risk is a metallic object flying through the air toward the magnet and hitting you. To reduce this risk we require that all people involved with the study remove all metal from their person and all metal objects from their pockets. Nothing metal can be brought into the magnet room at any time. Also, once you are in the magnet, the door to the room will be closed so that no one accidentally bring a metal object near the magnet while you are in it.

Please read the Magnetic Resonance Safety Form and complete it very carefully. Those questions are for your safety. Take a moment now to be sure that you have read this Form and be sure to ask any questions and tell us any information you think might be important. **Even if you think that it is probably okay, we would rather have you ask us to make sure.**

If you experience significant claustrophobia during the MR testing, you will be removed immediately. You will be positioned feet-first in the magnet and your head will remain near the opening in order to minimize claustrophobia.

What if there is an unexpected finding on my MRI scan? The investigators for this research project are not licensed or trained diagnosticians or clinicians. The testing performed in this project is not intended to find abnormalities, and the images or data collected do not comprise a diagnostic or clinical study. However, occasionally in the process of research, investigators may perceive an abnormality, the health implications of which may not be clear. When this occurs, UMASS Amherst researchers will consult with a radiologist. If the radiologist determines that an additional inquiry is warranted, the researcher will then contact you regarding the radiologist's opinion of the unexpected finding(s).

In such a case, you are advised to consult with a licensed physician to determine whether further examination or treatment would be prudent. Although the images collected for this research project do not comprise a diagnostic or clinical study, the images can be

made available to you for clinical follow-up. The costs for any care that will be needed to diagnose or treat an unexpected finding(s) would not be paid for by University of Massachusetts, Amherst. These costs would be your responsibility. If you have further tests done by your licensed physician, those results will then become part of your medical record, which may affect your current and future health or life insurance.

Regardless of the health implications, the discovery of an unexpected finding(s) may cause you to feel anxious or worried. You may wish to talk to your physician or a qualified mental health clinician. You can contact the Center for Counseling and Psychological Health (CCPH) at (413) 545-2337 (Mon-Fri from 8-5pm) - on weekends or after 5pm, call (413) 577-5000 and ask for the CCPH clinician on call. You can also contact the Psychological Services Center at 413-545-0041 (Monday-Friday 8am-5pm) or psc@psych.umass.edu. In a serious emergency, remember that you can also call 911 for immediate assistance.

Confidentiality: Steps are taken to protect the identities of you and the data collected in this study. The Informed Consent, Physical Activity Readiness Questionnaire, and MR Safety Form (all of which will have your name on them) will be stored and locked in a filing cabinet within a locked office. All other data collection sheets will be coded with your participant number and the study name instead of your name, so that no potential identifiers can be linked back to you. Data collection sheets and lists of participant codes and names are kept separate from all other study materials. Paper documents with names or codes will be stored in separate locked filing cabinets located in a locked office. All electronic data will be kept on a password-protected computer in a locked office. Any data that are published or used in a presentation will not include any names or identifiers that could link back to you.

In Case of Injury: In the unlikely event of an injury resulting directly from participation in this study, we will do everything we can to assist you in seeking medical treatment. The University of Massachusetts does not have a program for compensating subjects for injury or complications related to human subject research.

Benefits: You will receive no direct benefit from participating in this study.

Costs and Reimbursement: There is no cost to participate in this study. To compensate you for your participation, we will give you $10 cash for completing all of the contraction protocols, and another $10 for completing all of the physical activity measures.

Withdrawal from Participation: Participation in this research is voluntary. You have the right to refuse to continue or withdraw from the study at any point, without prejudice.

Alternative Procedures: The procedures described above are non-invasive techniques that are commonly used in muscle research. There are no other non-invasive techniques that can be used to obtain the information necessary in this study.

Request for Additional Information: You are encouraged to ask questions about the study. The investigators will attempt to answer all of your questions to the best of their knowledge. The investigators fully intend to conduct the study with your best interest, safety, and comfort in mind. Please address any questions regarding the study to the Muscle Physiology Laboratory. Our phone number is (413) 545-5305. We can also be reached by email at umassmplab@umass.edu. You may also address questions to Prof. Kent by calling her at (413) 545-9477 or by emailing her at jkent@kin.umass.edu. If you would like to speak with someone not directly involved in the research study, you may contact the Human Research Protection Office at the University of Massachusetts via email at humansubjects@ora.umass.edu; telephone (413) 545-3428; or mail at the Human Research Protection Office, Research Administration Building, University of Massachusetts Amherst, 70 Butterfield Terrace, Amherst, MA 01003-9242.

Subject Statement of Voluntary Consent: By signing this form, I am agreeing to voluntarily enter this study. I understand that, by signing this document, I do not waive any of my legal rights. I have had a chance to read this consent form, and it was explained to me in a language that I use and understand. I have had the opportunity to ask questions and have received satisfactory answers. A copy of this signed Informed Consent Form will be given to me.

_____

Participant's name   Address

_____

Signature   Phone Number   Date

STUDY REPRESENTATIVE STATEMENT:

The investigator has read and understands the federal regulations for the Protection of Human Research Subjects (45 CFR 46) and agrees to comply with all of its clauses to the best of her ability. The investigator also pledges to consider the best interests of the subject beyond the explicit statement contained in the aforementioned federal regulations and to exercise professional expertise to protect the rights and welfare of the subject.

_____

Signature of Person Obtaining Consent   Date

TELEPHONE ELIGIBILITY SCREENING SCRIPT (STUDY 1)

Calculating Oxidative Energy Production during Non-Steady State Contractions

<u>Telephone Screening Script</u>

"Hello, my name is _____ and I'm calling from the Muscle Physiology Lab at the University of Massachusetts Amherst. I am contacting you today because you have expressed interest in participating in our study about muscle metabolism. If now is a good time, I can explain the study to you, answer any questions you may have, then ask you a few questions about yourself to see if you would qualify.

Before we begin, what is your age?"

- *If the participant is not 25-40 years of age we will inform them that they do not qualify for the study, and ask if they would like to be contacted for future studies. If their age falls within these ranges, we will move onto the script below.

  "As I describe the study to you, feel free to ask any questions that you may have."

  "In this study, we are investigating how high intensity exercise affects aerobic, or oxidative, metabolism within contracting skeletal muscles. Oxidative energy production can be measured during moderate intensity exercise because skeletal muscle metabolism reaches a plateau. However, the precision and accuracy of these methods are reduced during high intensity exercise because this metabolic plateau is altered or not reached. We recently developed a new method for calculating oxidative energy production that appears to overcome this limitation. Thus, the purpose of this study is to investigate the validity of our new method."

  "The study involves one visit and will take about 2 hours in total. We will provide free parking, if needed. All testing will take place at the Human Magnetic Resonance Center in the new Life Sciences Lab Building. Upon arriving, you will read an Informed Consent document and have any questions you might have answered by the investigators. Following completion of this consenting procedure, you will be asked to fill out a Medical History Form, Physical Activity Readiness Questionnaire, and Magnetic Resonance Safety Form. We will then measure your blood pressure while you are seated, and obtain your height and weight. Next, we will review your Magnetic Resonance Safety Form, have you remove all jewelry, and change into paper pants for the study. We will also ask you to walk through a metal detector for your safety. You will be escorted to the Magnet Room, where you will be positioned in the scanner on your back with your dominant leg on our non-magnetic leg exercise apparatus, which is similar to a knee extension machine you would use at a gym. Your leg will be strapped to the apparatus just above your ankle and at your knee using Velcro straps. Straps will also be secured

over your hips. A specially designed copper coil encased in plastic will be secured over your thigh muscles using Velcro straps. This coil will non-invasively measure changes in your muscle biochemistry while you exercise **(if they ask: non-invasively means we will not be poking into you)**. Headphones will be provided to you to limit the amount of noise from the scanner, and to enable clear and constant communication between you and the investigators."

"We will then determine your strength during 2-3 maximal static contractions, each lasting 3-4 seconds. For these, you will attempt to straighten your leg as quickly and forcefully as possible, but the exercise apparatus will not let your leg move. You will be given 1-2 minutes of rest between each of these contractions. Next, we will have you repeat this effort, but this time you will maintain your strongest contraction for 24 seconds, after which you will rest quietly without moving for up to 10 minutes. This procedure will be used to determine your muscle's "aerobic" capacity."

"You will then perform 2-3 sets of 3 rapid, maximal dynamic contractions to determine your maximal dynamic strength. The dynamic contractions will all be isokinetic; that is, the speed of the contraction will be limited by our custom-built exercise apparatus. You will be given 1-2 minutes of rest between each of these 2 sets. You will then perform the experimental protocol, which will include 4 sets of maximal dynamic ('with movement') knee extensions. During each of these sets, you will be asked to kick your leg out as hard and fast as you can once every 2 seconds. The duration of each set will vary, beginning with 24 seconds for set 1 and increasing to 60, 120, and 240 seconds for sets 2, 3, and 4, respectively. Up to 10 minutes of rest will be given between each set."

"Lastly, before you leave, you will be given a small accelerometer, which is an activity monitor that will record the amount and intensity of physical activity you perform over the next 7 days. You will be instructed on how and when to use it and how to keep a simple physical activity log book. At the end of the week-long wear period, a member of the Muscle Physiology Laboratory will collect the accelerometer and log book at a time that is most convenient for you. To compensate you for your participation, we will give you $10 cash for completing all of the contraction protocols, and another $10 for completing all of the physical activity measures."

"None of these tests will cause permanent damage and any discomfort that you may feel will go away shortly. You may have some muscle soreness in the 2-3 days following the study, but that will also go away. Do you have any questions?"

"If you don't mind, I am now going to ask you a few questions about your medical history to determine if you are eligible for the study. Any information I receive today and all information collected during the study will be kept private and locked in a filing cabinet within a locked room. If you do not qualify for the study and are not interested in participating in further studies, your information will be destroyed. We follow careful procedures to make sure your privacy is protected at all times. Do you have any questions?"

- *Complete 'Telephone Eligibility Screening Form' and 'MR Safety Form.'*
  "Do you have any other questions? Thank you very much for your time. We will get back to you once we determine if you are eligible. If you are eligible, we schedule your first visit."

TELEPHONE ELIGIBILITY SCREENING FORM (STUDY 1)

Screened by:_____ Date:_____
Status:_____

TELEPHONE SCREENING FORM: MR STUDIES

1) Name_____

2) Phone # (Circle preferred contact):   Best time/day to contact: ____

      a. Home _____   Message?   Yes   No ____

      b. Work _____   Message?   Yes   No ____

      c. Cell _____   Message?   Yes   No ____

3) Email: _____

4) Age_____   Sex_____   Height ___   Weight _____   BMI _____

  (calculate)

5) How did you find out about this

  study?_____ _

6) Have you ever participated in a research study

  before?_____

      a. Are you currently participating in any other research studies right now?_____

          i. If yes, describe:_____

         ii. End date: _____

7) Current health status (general)_____

8) Do you have any physical limitations?_____

9) Are you pregnant?_____

10) Do you, or have you ever had, any of the following:

    a. Stroke?_____

    b. Peripheral vascular disease?_____

    c. Cardiac disease?_____

    d. Pulmonary disease?_____

    e. Neurological disease?_____

    f. Arthritis in the lower leg?_____

    Have you used ambulatory devices during the last month (i.e., ankle-foot

    orthotic, cane, wheelchair,

    etc.)?_____

11) Do you smoke or have you ever smoked before?____ For how long?_____Quit?_____

12) Do you have any allergic reactions?_____

13) Do you have any significant past medical history? (e.g. hypertension, CAD, etc.)

_____

14) Current medications:

Drug Name	Classification	Dosage	Frequency	Duration	Prescribed for?

    a. Do you take any Statins?_____ If yes, please describe:_____

_____

b. Do you take any beta-blockers, sedatives, tranquilizers, or other medication that may impair physical function?_____ If yes, please describe:_____

15) Current physical activity level (regular exercise, none, athlete, etc.)_____

_____

16) Has your Doctor ever told you not to exercise?_____If yes, please

describe:_____

17) What was the date of your last doctor's visit?_____

18) Is fatigue a problem for you?_____ Leg fatigue?_____

19) What type of transportation will you be using?_Will you need a parking pass? _____

20) Would you like to be contacted again for future studies?   Yes   No

21) Comments:_____

_____

_____

22) Go through Magnetic Resonance Safety Questionnaire:

APPENDIX D

MEDICAL HISTORY FORM

Medical History Form

Please fill out and sign below in ink. This record is confidential.

Medical History
Do you take any prescribed or over-the-counter medications? Please include vitamins, herbs, or other dietary supplements. If yes please list the dose, frequency and duration of use.

_____ Do you take any statins? If yes, please indicate name and dose:_____

Have you ever been told by a physician that you should not exercise?
Yes _____   No _____   If yes, please explain:

Do you have or have you EVER had any of the following problems? Check if YES and provide details below.

_____ Heart disease/rheumatic fever	_____ Thyroid disorder	_____ Asthma
_____ High blood pressure	_____ Claustrophobia	_____ Allergies
_____ Elevated Cholesterol	_____ Anemia	_____ Stroke
_____ Epilepsy or seizure disorder_____	_____ Diabetes	_____ Dizziness

_____ Blurred or double vision
_____ Orthopedic or joint problems (e.g., arthritis)
_____ Shortness of breath or difficulty in breathing
_____ Phlebitis, blood-clots, varicose veins, peripheral vascular disease
Details, if relevant:

Lifestyle

Do you smoke cigarettes?	Yes _____	No _____
Do you drink alcohol?	Yes _____	No _____
Do you get regular exercise?	Yes _____	No _____
	If yes, number of times per week _____	
Have you had surgery?	Yes _____	No _____
	If yes, when was this? _____	

Is there any other information that you feel we should know about before you participate in the study? If yes please explain in the space below.

Signature: _____   Date: _____

167

PHYSICAL ACTIVITY READINESS QUESTIONNAIRE

2016 PAR-Q+

The Physical Activity Readiness Questionnaire for Everyone

The health benefits of regular physical activity are clear; more people should engage in physical activity every day of the week. Participating in physical activity is very safe for MOST people. This questionnaire will tell you whether it is necessary for you to seek further advice from your doctor OR a qualified exercise professional before becoming more physically active.

GENERAL HEALTH QUESTIONS

Please read the 7 questions below carefully and answer each one honestly: check YES or NO.	YES	NO
1) Has your doctor ever said that you have a heart condition ☐ OR high blood pressure ☐?	☐	☐
2) Do you feel pain in your chest at rest, during your daily activities of living, **OR** when you do physical activity?	☐	☐
3) Do you lose balance because of dizziness **OR** have you lost consciousness in the last 12 months? Please answer **NO** if your dizziness was associated with over-breathing (including during vigorous exercise).	☐	☐
4) Have you ever been diagnosed with another chronic medical condition (other than heart disease or high blood pressure)? **PLEASE LIST CONDITION(S) HERE:** _____	☐	☐
5) Are you currently taking prescribed medications for a chronic medical condition? **PLEASE LIST CONDITION(S) AND MEDICATIONS HERE:** _____	☐	☐
6) Do you currently have (or have had within the past 12 months) a bone, joint, or soft tissue (muscle, ligament, or tendon) problem that could be made worse by becoming more physically active? Please answer **NO** if you had a problem in the past, but it *does not limit your current ability* to be physically active. **PLEASE LIST CONDITION(S) HERE:** _____	☐	☐
7) Has your doctor ever said that you should only do medically supervised physical activity?	☐	☐

☑ **If you answered NO to all of the questions above, you are cleared for physical activity.**
Go to Page 4 to sign the PARTICIPANT DECLARATION. You do not need to complete Pages 2 and 3.

▶ Start becoming much more physically active – start slowly and build up gradually.

▶ Follow International Physical Activity Guidelines for your age (www.who.int/dietphysicalactivity/en/).

▶ You may take part in a health and fitness appraisal.

▶ If you are over the age of 45 yr and **NOT** accustomed to regular vigorous to maximal effort exercise, consult a qualified exercise professional before engaging in this intensity of exercise.

▶ If you have any further questions, contact a qualified exercise professional.

🔴 **If you answered YES to one or more of the questions above, COMPLETE PAGES 2 AND 3.**

⚠ **Delay becoming more active if:**

✓ You have a temporary illness such as a cold or fever; it is best to wait until you feel better.

✓ You are pregnant - talk to your health care practitioner, your physician, a qualified exercise professional, and/or complete the ePARmed-X+ at **www.eparmedx.com** before becoming more physically active.

✓ Your health changes - answer the questions on Pages 2 and 3 of this document and/or talk to your doctor or a qualified exercise professional before continuing with any physical activity program.

OSHF

2016 PAR-Q+

FOLLOW-UP QUESTIONS ABOUT YOUR MEDICAL CONDITION(S)

1. Do you have Arthritis, Osteoporosis, or Back Problems?

If the above condition(s) is/are present, answer questions 1a-1c   If **NO** ☐ go to question 2

1a.	Do you have difficulty controlling your condition with medications or other physician-prescribed therapies? (Answer **NO** if you are not currently taking medications or other treatments)	YES☐ NO☐
1b.	Do you have joint problems causing pain, a recent fracture or fracture caused by osteoporosis or cancer, displaced vertebra (e.g., spondylolisthesis), and/or spondylolysis/pars defect (a crack in the bony ring on the back of the spinal column)?	YES☐ NO☐
1c.	Have you had steroid injections or taken steroid tablets regularly for more than 3 months?	YES☐ NO☐

2. Do you currently have Cancer of any kind?

If the above condition(s) is/are present, answer questions 2a-2b   If **NO** ☐ go to question 3

2a.	Does your cancer diagnosis include any of the following types: lung/bronchogenic, multiple myeloma (cancer of plasma cells), head, and/or neck?	YES☐ NO☐
2b.	Are you currently receiving cancer therapy (such as chemotheraphy or radiotherapy)?	YES☐ NO☐

3. Do you have a Heart or Cardiovascular Condition? *This includes Coronary Artery Disease, Heart Failure, Diagnosed Abnormality of Heart Rhythm*

If the above condition(s) is/are present, answer questions 3a-3d   If **NO** ☐ go to question 4

3a.	Do you have difficulty controlling your condition with medications or other physician-prescribed therapies? (Answer **NO** if you are not currently taking medications or other treatments)	YES☐ NO☐
3b.	Do you have an irregular heart beat that requires medical management? (e.g., atrial fibrillation, premature ventricular contraction)	YES☐ NO☐
3c.	Do you have chronic heart failure?	YES☐ NO☐
3d.	Do you have diagnosed coronary artery (cardiovascular) disease and have not participated in regular physical activity in the last 2 months?	YES☐ NO☐

4. Do you have High Blood Pressure?

If the above condition(s) is/are present, answer questions 4a-4b   If **NO** ☐ go to question 5

4a.	Do you have difficulty controlling your condition with medications or other physician-prescribed therapies? (Answer **NO** if you are not currently taking medications or other treatments)	YES☐ NO☐
4b.	Do you have a resting blood pressure equal to or greater than 160/90 mmHg with or without medication? (Answer **YES** if you do not know your resting blood pressure)	YES☐ NO☐

5. Do you have any Metabolic Conditions? *This includes Type 1 Diabetes, Type 2 Diabetes, Pre-Diabetes*

If the above condition(s) is/are present, answer questions 5a-5e   If **NO** ☐ go to question 6

5a.	Do you often have difficulty controlling your blood sugar levels with foods, medications, or other physician-prescribed therapies?	YES☐ NO☐
5b.	Do you often suffer from signs and symptoms of low blood sugar (hypoglycemia) following exercise and/or during activities of daily living? Signs of hypoglycemia may include shakiness, nervousness, unusual irritability, abnormal sweating, dizziness or light-headedness, mental confusion, difficulty speaking, weakness, or sleepiness.	YES☐ NO☐
5c.	Do you have any signs or symptoms of diabetes complications such as heart or vascular disease and/or complications affecting your eyes, kidneys, **OR** the sensation in your toes and feet?	YES☐ NO☐
5d.	Do you have other metabolic conditions (such as current pregnancy-related diabetes, chronic kidney disease, or liver problems)?	YES☐ NO☐
5e.	Are you planning to engage in what for you is unusually high (or vigorous) intensity exercise in the near future?	YES☐ NO☐

OSHF

2016 PAR-Q+

6. Do you have any **Mental Health Problems or Learning Difficulties?** *This includes Alzheimer's, Dementia, Depression, Anxiety Disorder, Eating Disorder, Psychotic Disorder, Intellectual Disability, Down Syndrome*

If the above condition(s) is/are present, answer questions 6a-6b   If **NO** ☐ go to question 7

6a.	Do you have difficulty controlling your condition with medications or other physician-prescribed therapies? (Answer **NO** if you are not currently taking medications or other treatments)	YES ○ NO ○
6b.	Do you have Down Syndrome **AND** back problems affecting nerves or muscles?	YES ○ NO ○

7. Do you have a **Respiratory Disease?** *This includes Chronic Obstructive Pulmonary Disease, Asthma, Pulmonary High Blood Pressure*

If the above condition(s) is/are present, answer questions 7a-7d   If **NO** ☐ go to question 8

7a.	Do you have difficulty controlling your condition with medications or other physician-prescribed therapies? (Answer **NO** if you are not currently taking medications or other treatments)	YES ○ NO ○
7b.	Has your doctor ever said your blood oxygen level is low at rest or during exercise and/or that you require supplemental oxygen therapy?	YES ○ NO ○
7c.	If asthmatic, do you currently have symptoms of chest tightness, wheezing, laboured breathing, consistent cough (more than 2 days/week), or have you used your rescue medication more than twice in the last week?	YES ○ NO ○
7d.	Has your doctor ever said you have high blood pressure in the blood vessels of your lungs?	YES ○ NO ○

8. Do you have a **Spinal Cord Injury?** *This includes Tetraplegia and Paraplegia*

If the above condition(s) is/are present, answer questions 8a-8c   If **NO** ☐ go to question 9

8a.	Do you have difficulty controlling your condition with medications or other physician-prescribed therapies? (Answer **NO** if you are not currently taking medications or other treatments)	YES ○ NO ○
8b.	Do you commonly exhibit low resting blood pressure significant enough to cause dizziness, light-headedness, and/or fainting?	YES ○ NO ○
8c.	Has your physician indicated that you exhibit sudden bouts of high blood pressure (known as Autonomic Dysreflexia)?	YES ○ NO ○

9. Have you had a **Stroke?** *This includes Transient Ischemic Attack (TIA) or Cerebrovascular Event*

If the above condition(s) is/are present, answer questions 9a-9c   If **NO** ☐ go to question 10

9a.	Do you have difficulty controlling your condition with medications or other physician-prescribed therapies? (Answer **NO** if you are not currently taking medications or other treatments)	YES ○ NO ○
9b.	Do you have any impairment in walking or mobility?	YES ○ NO ○
9c.	Have you experienced a stroke or impairment in nerves or muscles in the past 6 months?	YES ○ NO ○

10. Do you have any **other medical condition not listed above** or do you have **two or more medical conditions?**

If you have other medical conditions, answer questions 10a-10c   If **NO** ☐ read the Page 4 recommendations

10a.	Have you experienced a blackout, fainted, or lost consciousness as a result of a head injury within the last 12 months **OR** have you had a diagnosed concussion within the last 12 months?	YES ○ NO ○
10b.	Do you have a medical condition that is not listed (such as epilepsy, neurological conditions, kidney problems)?	YES ○ NO ○
10c.	Do you currently live with two or more medical conditions?	YES ○ NO ○

PLEASE LIST YOUR MEDICAL CONDITION(S)
AND ANY RELATED MEDICATIONS HERE: _____

_____

GO to Page 4 for recommendations about your current medical condition(s) and sign the PARTICIPANT DECLARATION.

2016 PAR-Q+

If you answered NO to all of the follow-up questions about your medical condition, you are ready to become more physically active - sign the PARTICIPANT DECLARATION below:

- It is advised that you consult a qualified exercise professional to help you develop a safe and effective physical activity plan to meet your health needs.

- You are encouraged to start slowly and build up gradually - 20 to 60 minutes of low to moderate intensity exercise, 3-5 days per week including aerobic and muscle strengthening exercises.

- As you progress, you should aim to accumulate 150 minutes or more of moderate intensity physical activity per week.

- If you are over the age of 45 yr and **NOT** accustomed to regular vigorous to maximal effort exercise, consult a qualified exercise professional before engaging in this intensity of exercise.

If you answered YES to one or more of the follow-up questions about your medical condition:

You should seek further information before becoming more physically active or engaging in a fitness appraisal. You should complete the specially designed online screening and exercise recommendations program - the ePARmed-X+ at www.eparmedx.com and/or visit a qualified exercise professional to work through the ePARmed-X+ and for further information.

⚠ **Delay becoming more active if:**

- You have a temporary illness such as a cold or fever; it is best to wait until you feel better.

- You are pregnant - talk to your health care practitioner, your physician, a qualified exercise professional, and/or complete the ePARmed-X+ **at www.eparmedx.com** before becoming more physically active.

- Your health changes - talk to your doctor or qualified exercise professional before continuing with any physical activity program.

- You are encouraged to photocopy the PAR-Q+. You must use the entire questionnaire and NO changes are permitted.
- The authors, the PAR-Q+ Collaboration, partner organizations, and their agents assume no liability for persons who undertake physical activity and/or make use of the PAR-Q+ or ePARmed-X+. If in doubt after completing the questionnaire, consult your doctor prior to physical activity.

PARTICIPANT DECLARATION

- All persons who have completed the PAR-Q+ please read and sign the declaration below.

- If you are less than the legal age required for consent or require the assent of a care provider, your parent, guardian or care provider must also sign this form.

I, the undersigned, have read, understood to my full satisfaction and completed this questionnaire. I acknowledge that this physical activity clearance is valid for a maximum of 12 months from the date it is completed and becomes invalid if my condition changes. I also acknowledge that a Trustee (such as my employer, community/fitness centre, health care provider, or other designate) may retain a copy of this form for their records. In these instances, the Trustee will be required to adhere to local, national, and international guidelines regarding the storage of personal health information ensuring that the Trustee maintains the privacy of the information and does not misuse or wrongfully disclose such information.

NAME _____   DATE _____

SIGNATURE _____   WITNESS _____

SIGNATURE OF PARENT/GUARDIAN/CARE PROVIDER _____

The PAR-Q+ was created using the evidence-based AGREE process (1) by the PAR-Q+ Collaboration chaired by Dr. Darren E. R. Warburton with Dr. Norman Gledhill, Dr. Veronica Jamnik, and Dr. Donald C. McKenzie (2). Production of this document has been made possible through financial contributions from the Public Health Agency of Canada and the BC Ministry of Health Services. The views expressed herein do not necessarily represent the views of the Public Health Agency of Canada or the BC Ministry of Health Services.

Key References
1. Jamnik VK, Warburton DER, Makarski J, McKenzie DC, Shephard RJ, Stone J, and Gledhill N. Enhancing the effectiveness of clearance for physical activity participation; background and overall process. APNM 36(S1):S3-S13, 2011.
2. Warburton DER, Gledhill N, Jamnik VK, Bredin SSD, McKenzie DC, Stone J, Charlesworth S, and Shephard RJ. Evidence-based risk assessment and recommendations for physical activity clearance; Consensus Document. APNM 36(S1):S266-s298, 2011.
3. Chisholm DM, Collis ML, Kulak LL, Davenport W, and Gruber N. Physical activity readiness. British Columbia Medical Journal. 1975;17:375-378.
4. Thomas S, Reading J, and Shephard RJ. Revision of the Physical Activity Readiness Questionnaire (PAR-Q). Canadian Journal of Sport Science 1992;17:4 338-345.

Copyright @ 2016 PAR-Q+ Collaboration   4 / 4
01-01-2016

MAGNETIC RESONANCE SAFETY FORM

MR Safety Screening Questionnaire

Participant's Name _____ Today's date: _____

Study Name: _____ Investigator: _____

Year of birth: _____ Gender: _____ Height: _____ Weight: _____

Please read the following questions carefully. It is very important for us to know if you have any **metal devices or metal parts** anywhere in your body. If you do not understand a question, please ask us to explain!

1. Yes ☐ No ☐ Do you get upset or anxious in small spaces (claustrophobia)?
2. Yes ☐ No ☐ Did you ever have an aneurysm clip implanted during brain surgery?
3. Yes ☐ No ☐ Do you have embolization coils (Gianturco) in your brain?
4. Yes ☐ No ☐ Do you have a Carotid Artery Vascular clamp?
5. Yes ☐ No ☐ Do you have a "shunt" (a tube to drain fluid) in your brain, spine or heart?
6. Yes ☐ No ☐ Do you have a Vagus nerve stimulator to help you with convulsions or with epilepsy?
7. Yes ☐ No ☐ Have you ever had metal removed from your eyes by a doctor?
8. Yes ☐ No ☐ Have you ever worked with metal? (For example in a machine shop)?
9. Yes ☐ No ☐ Do you have implants in your eyes? Have you ever had cataract surgery?
10. Yes ☐ No ☐ Do you wear colored contact lenses or permanent eye liner?
11. Yes ☐ No ☐ Do you have shrapnel or metal in your head, eyes or skin?
12. Yes ☐ No ☐ Do you have implants in your ear (like cochlear implants) or a hearing aid?
13. Yes ☐ No ☐ Do you wear braces on your teeth or have a permanent retainer?
14. Yes ☐ No ☐ Do you have a heart pacemaker or a heart defibrillator?
15. Yes ☐ No ☐ Do you have a filter for blood clots (Umbrella, Greenfield, bird's nest)?
16. Yes ☐ No ☐ Do you have any stents (small metal tubes used to keep blood vessels open)?
17. Yes ☐ No ☐ Did you ever have a device implanted in your body such as a nerve stimulators?
18. Yes ☐ No ☐ Do you have an implanted pump to deliver medication?
19. Yes ☐ No ☐ Do you have metal joints, rods, plates, pins, screws, nails, or clips in any part of your body?
20. Yes ☐ No ☐ Have you ever had a gunshot wound? Or a B-B gun injury?
21. Yes ☐ No ☐ Do you wear a patch to deliver medicines through the skin?
22. Yes ☐ No ☐ Do you have any devices to make bones grow (like bone growth or bone fusion stimulators)?
23. Yes ☐ No ☐ Do you have unremoved body-piercing or a tattoo?
24. Yes ☐ No ☐ Have you ever had any surgery? Please list all:

FOR WOMEN

25. Yes ☐ No ☐ Do you use a diaphragm, IUD, or cervical pessary?
26. Yes ☐ No ☐ Do you think there is any possibility that you might be pregnant?

IMPORTANT INSTRUCTIONS: Before entering the Magnet Room, you must remove all metallic objects including hearing aids, dentures, partial plates, keys, beeper, cell phone, eyeglasses, hair pins, barrettes, jewelry including body piercing jewelry, watch, safety pins, paperclips, money clip, credit cards, bank cards, magnetic strip cards, coins, pens, pocket knife, nail clipper, tools, clothing with metal fasteners, and clothing with metallic threads in the material.

I attest that the above information is correct to the best of my knowledge. I have read and understand the entire contents of this form and have had the opportunity to ask questions regarding the information on this form and regarding the MR procedure that I am about to undergo.

Participant Signature: _____ Date: _____

MR Operator Signature: _____ Date: _____

7/1/2018

APPENDIX G

PHYSICAL ACTIVITY LOG

Participant #: _____

INFORMATION ABOUT THE ACTIVITY MONITOR

The Activity Monitor is a small, plastic box containing electronic circuitry. When you wear the Activity Monitor, it measures how much you are moving.

Please remember a few important things about the monitor:

- Snap the belt around your waist.
- The monitor should be worn around your waist and positioned at the top of the right hipbone.
- **DO NOT GET THE MONITOR WET** (sweat is okay).
- You should wear the monitor while you are awake for 7 days, removing the device only for sleep and water-based activities (e.g. bathing, showering, or swimming).
- The monitor will flash intermittently when it is **NOT** recording. If the monitor stops flashing, it indicates that the monitor **IS** recording.
- Please return the monitor and this log to the UMass Muscle Physiology Laboratory, Totman Bldg., Room 22.

INSTRUCTIONS FOR COMPLETING THIS ACTIVITY LOG

We want to know:

- When you woke up and when you went to bed
- When the monitor was put on and taken off
- Any activities you completed that day (e.g., long walks, yard work, etc.).
- If there was anything out of the ordinary about your activity pattern

If you went on a long walk from 11:00 am to 11:30 am, write walking in the activity column, 11:00 am to 11:30 am in the time column, and 30 minutes in the duration column.

If you have any questions please contact:

UMass Muscle Physiology Lab

Phone: (413) 545 – 5305

Email: umassmplab@umass.edu

Day 1

Date: _____ Day of the week _____

Wake up Time: _____   Bed Time: _____
Monitor on Time: _____   Monitor off Time: _____

List any physical activities (e.g., long walks, fitness club, etc), or naps during the day:

Activity: Time of day: Duration:

_____

_____

_____

Did you wear the monitor during all waking hours (except for showering)?

☐ Yes   ☐ No, Times not worn:_____

Was there anything out of the ordinary about your activity pattern this day?

☐ Yes, Explain Below   ☐ No

_____

_____

....

Day 2

Date: _____ Day of the week _____

Wake up Time: _____   Bed Time: _____
Monitor on Time: _____   Monitor off Time: _____

List any physical activities (e.g., long walks, fitness club, etc), or naps during the day:

Activity: Time of day: Duration:

_____

_____

_____

Did you wear the monitor during all waking hours (except for showering)?

☐ Yes   ☐ No, Times not worn:_____

Was there anything out of the ordinary about your activity pattern this day?

☐ Yes, Explain Below   ☐ No

_____

_____

Day 3   Date: _____ Day of the week _____

Wake up Time: _____   Bed Time: _____
Monitor on Time: _____   Monitor off Time: _____

List any physical activities (e.g., long walks, fitness club, etc), or naps during the day:

Activity: Time of day: Duration:
_____

_____

_____

Did you wear the monitor during all waking hours (except for showering)?

☐ Yes   ☐ No, Times not worn: _____

Was there anything out of the ordinary about your activity pattern this day?

☐ Yes, Explain Below   ☐ No

_____

_____

....

Day 4   Date: _____ Day of the week _____

Wake up Time: _____   Bed Time: _____
Monitor on Time: _____   Monitor off Time: _____

List any physical activities (e.g., long walks, fitness club, etc), or naps during the day:

Activity: Time of day: Duration:
_____

_____

_____

Did you wear the monitor during all waking hours (except for showering)?

☐ Yes   ☐ No, Times not worn: _____

Was there anything out of the ordinary about your activity pattern this day?

☐ Yes, Explain Below   ☐ No

_____

_____

Day 5   Date: _____ Day of the week _____

Wake up Time: _____   Bed Time: _____
Monitor on Time: _____   Monitor off Time: _____

List any physical activities (e.g., long walks, fitness club, etc), or naps during the day:

Activity: Time of day: Duration:
_____
_____
_____

Did you wear the monitor during all waking hours (except for showering)?

☐ Yes   ☐ No, Times not worn:_____

Was there anything out of the ordinary about your activity pattern this day?

☐ Yes, Explain Below   ☐ No

_____
_____

....

Day 6   Date: _____ Day of the week _____

Wake up Time: _____   Bed Time: _____
Monitor on Time: _____   Monitor off Time: _____

List any physical activities (e.g., long walks, fitness club, etc), or naps during the day:

Activity: Time of day: Duration:
_____
_____
_____

Did you wear the monitor during all waking hours (except for showering)?

☐ Yes   ☐ No, Times not worn:_____

Was there anything out of the ordinary about your activity pattern this day?

☐ Yes, Explain Below   ☐ No

_____
_____

Day 7 Date: _____ Day of the week _____

Wake up Time: _____ Bed Time: _____
Monitor on Time: _____ Monitor off Time: _____

List any physical activities (e.g., long walks, fitness club, etc), or naps during the day:

Activity: Time of day: Duration:

_____

_____

_____

Did you wear the monitor during all waking hours (except for showering)?

☐ Yes ☐ No, Times not worn:_____

Was there anything out of the ordinary about your activity pattern this day?

☐ Yes, Explain Below ☐ No

_____

_____

···

Day 8 Date: _____ Day of the week _____

Wake up Time: _____ Bed Time: _____
Monitor on Time: _____ Monitor off Time: _____

List any physical activities (e.g., long walks, fitness club, etc), or naps during the day:

Activity: Time of day: Duration:

_____

_____

_____

Did you wear the monitor during all waking hours (except for showering)?

☐ Yes ☐ No, Times not worn:_____

Was there anything out of the ordinary about your activity pattern this day?

☐ Yes, Explain Below ☐ No

_____

_____

APPENDIX H

INFORMED CONSENT (STUDY 2)

INFORMED CONSENT DOCUMENT
University of Massachusetts
Amherst, MA 01002

Project Title: *Does Mitochondrial Uncoupling Alter the Efficiency of Aerobic Metabolism in Contracting Skeletal Muscles?*
Principal Investigator: Miles F. Bartlett
Co-Investigators: Jane A. Kent, PhD, Rajakumar Nagarajan, PhD, Liam F. Fitzgerald, Joseph A. Gordon, Julia D. Miehm

Your written informed consent is required before you can participate in this project. Please read this document carefully and then sign your name on the last page if you agree to participate. This document is in accordance with regulations for the Protection of Human Research Subjects (45 CFR 46). You are encouraged to ask questions at any time before, during or after participating.

Purpose: During low- and moderate-intensity exercise, skeletal muscle metabolism rises in a predictable manner. However, during high-intensity exercise, muscle metabolism increases much more than would be predicted by the pattern seen at lower exercise intensities. The cause of this difference is not known, but we think that it has to do with changes in the efficiency of aerobic metabolism. We recently developed an experimental technique that allows us to measure the efficiency of aerobic metabolism in exercising skeletal muscle. Thus, the purpose of this study is to test the hypothesis that the efficiency of aerobic metabolism declines during high-intensity exercise.

Eligibility: To participate in this study you must be healthy and between 21-40 years of age. You may not have any: neurological or neuromuscular disease; a history of stroke, peripheral vascular disease, cardiovascular disease, blood vessel disorders such as deep vein thrombosis, pulmonary embolisms, or varicose veins cardiac or pulmonary disease; be a smoker; or have a history of any metabolic diseases/disorders. You may not be pregnant. You may not have any metal implants or anything that would prevent you from undergoing a magnetic resonance imaging (MRI) exam.

Procedures: Prior to your first visit, you will be screened by telephone interview for general health, medical history, current medications, usual physical activity habits, and eligibility for the study. If you are qualified and agree to participate, you will be invited to the Muscle Physiology Laboratory for your first visit.

Visit 1 – Paperwork and Familiarization (Muscle Physiology Laboratory, ~1 hour):
Upon arriving to the MPL, you will read this informed consent document and have any questions answered by the investigator. After agreeing to participate and signing this consent form, you will fill out the following documents (attached):

- Physical Activity Readiness Questionnaire
- Medical History Form
- Magnetic Resonance (MR) Safety Form

Next, measures of your blood pressure, height, and weight will be obtained. You will then be familiarized with the contraction protocols and procedures that will be performed during your second visit (described in detail below). First, you will be strapped into a knee extension dynamometer, which is very similar to a leg extension machine that you might find at a gym. We will start by measuring your maximal knee extension strength and power and then have you perform an incremental contraction test. The starting workload will be light but will get progressively heavier as the test continues. You will also experience the blood pressure cuff on your leg, as described in detail for visit 2.

Before leaving, we will schedule your second visit and give you a small activity monitor that you will wear at your waist. This monitor will record the amount and intensity of physical activity you perform over the next 7 days. You will be instructed on how and when to use it and how to keep a simple physical activity log. The activity monitor and log book will be returned at visit 2, or at the end of the week-long wear period. If the materials are not returned at visit 2, a member of the Muscle Physiology Laboratory will collect the monitor and log book at a time and location that is most convenient for you.

Visit 2 – Study Procedures (Human Magnetic Resonance Center, ~2 hours)

Upon arriving to the Human Magnetic Resonance Center at the Institute for Applied Life Sciences, you will meet with the MR Operator to review the MR Safety Form. Before entering the magnet room, you will remove any jewelry, empty your pockets, and walk through a metal detector. You will then be escorted to the MR scanner and positioned on your back with your dominant leg on top of our custom-built leg exercise apparatus, which is similar to a knee extension machine you would use at a gym. The lower leg (shin) will be strapped to the apparatus just above your ankle and at your knee using Velcro straps. Inelastic straps will also be secured over your hips to prevent unwanted movement during the muscle contractions, and a specially designed copper coil encased in a plastic box will be secured over your thigh muscles using Velcro straps. This coil will be used to measure changes in muscle metabolism during your contractions.

Two large inflatable blood pressure cuffs will then be wrapped around your leg, one each around the upper thigh and calf. To ensure that the inflatable cuffs are comfortable and positioned correctly, we will inflate the cuffs to a relatively low pressure (~150 mmHg) and then slowly increase the pressure to 240mmHg, which will be the target pressure during the study protocol. Once you are comfortable with the cuff placements, we will perform 1-2 rapid inflations (~ 1 second each), which will be used during the study procedures to temporarily block blood flow. If necessary, the cuffs will be repositioned to make you more comfortable.

Lastly, you will be given headphones to use, to limit the amount of noise from the MR scanner and allow you clear and constant communication with the investigators. We will talk with you and explain each set of measures as we go along. These measures are described next.

After you have been strapped to the exercise apparatus, we will position you in the center of the scanner and collect measures of your muscle metabolism at rest. During this time, you will lay quietly for about 10-15 minutes. Next, we will remeasure your knee extension strength to establish the workloads that you will perform during the incremental contraction test. About 1 minute of rest will be given between each of these contractions. You will then be refamiliarized with the dynamic contractions (1 contraction every 2 seconds) by performing a few sets of 2-3 maximal contractions at a fixed speed. Once you are comfortable with the dynamic contraction procedures, you will perform 24 seconds of maximal dynamic contractions, after which you will rest quietly without moving for up to 10 minutes. This procedure will be used to measure your muscle's maximal "aerobic" capacity.

Next, you will perform an incremental exercise test consisting of 6 stages of dynamic knee extension contractions, again 1 contraction every 2 seconds. These contractions will start with a very light load, and every 3 minutes, the load will be increased a little (by 8% of your maximum). Your muscle metabolism will be measured continuously throughout this protocol. At the end of each stage, we will measure the efficiency of your aerobic energy production, as follows:
5- Up to 12 seconds of rest will be given
6- The blood pressure cuffs will be inflated rapidly, to 240mmHg
7- The cuffs will remain inflated for up to 40 seconds while we measure your muscle biochemistry
8- The cuff will be rapidly deflated to allow your muscles to rest and recover
Following step 4, the next 3-minute stage of contractions will begin. This process of inflating and deflating the blood pressure cuffs may be uncomfortable, but will not cause any damage to your muscle, and any discomfort will subside quickly once the cuff is deflated. Additionally, after the cuff procedures have been completed for stage 6 (the final stage), you will complete one more minute of contractions followed by up to 10 minutes of rest, so that we can measure your muscle's maximal 'aerobic' capacity once again. Finally, after the 10-minute recovery period, you will undergo a final 10-minute cuff-inflation period while resting quietly. The cuffs will then be deflated and we will remove you from the scanner.

Subject Enrollment/Length of Study: We expect to enroll 10-20 participants in this study. Your participation will include 2 visits; the first lasting about 1 hour and the second lasting approximately 2 hours.

Possible Risks and Discomforts: There are minimal risks associated with the contraction procedures used in this research study. However, cardiovascular events and rises in blood pressure are possible due to the contractions, as well as muscle soreness in the days following the testing, but these are normal physiological responses and should be temporary. Injury is possible if you have any metal in or on you during the magnetic resonance testing, but we will check you beforehand to detect any such metal.

Magnetic Resonance Spectroscopy (MRS) and Imaging (MRI) – The United States Food and Drug Administration (FDA) has established guidelines for magnet strength and exposure to radio waves, and we carefully observe those guidelines. No ill effects have

been reported for the radio wave exposure associated with this protocol. Some people may feel uncomfortable or anxious while in the MR scanner, which is a large magnet. If this happens to you, you may ask to stop the study at any time and we will take you out of the MR scanner. On rare occasions, some people might feel dizzy, get an upset stomach, have a metallic taste, feel tingling sensations, or experience muscle twitches. These sensations usually go away quickly but please tell the research staff if you have them.

MRI and MRS pose some risks for certain people. If you have a pacemaker or certain types of metal objects inside your body, you may not be in this study because the strong magnet used for these MR studies might harm you. Another risk is a metallic object flying through the air toward the magnet and hitting you. To reduce this risk we require that all people involved with the study remove all metal from their person and all metal objects from their pockets. Nothing metal can be brought into the magnet room at any time. Also, once you are in the magnet, the door to the room will be closed so that no one accidentally bring a metal object near the magnet while you are in it.

Please read the Magnetic Resonance Safety Form and complete it very carefully. Those questions are for your safety. Take a moment now to be sure that you have read this Form and be sure to ask any questions and tell us any information you think might be important. **Even if you think that it is probably okay, we would rather have you ask us to make sure.**

If you experience significant claustrophobia during the MR testing, you will be removed immediately. You will be positioned feet-first in the magnet and your head will remain near the opening in order to minimize claustrophobia.

Blood Pressure Cuffs and Ischemia – All of our blood pressure cuff-inflation procedures are intended to temporarily block off blood flow and carry a risk of blood vessel injury. However, the inflation times we are using are short compared to those used in lower-limb surgeries, which can last over an hour, and the inflation pressure is also well below the recommended threshold of 300mmHg. You may experience discomfort and numbness in the leg during inflation, as well as warmth and a prickly, needle-like, feeling once the cuffs are deflated, but these feelings will go away shortly and will not cause long-term damage. You may experience some bruising from the cuffs, but this too will not cause any long-term damage and should clear up over the course of a few days. Overall, the risk to healthy young adults is low. If at any point in time you wish to stop the inflation procedures, just tell one of the data collectors and we will release the pressure cuff immediately. **However, if you have a history of cardiovascular or blood vessel disease, such as deep vein thrombosis or varicose veins, it is imperative that you inform us because the cuff-inflation procedures utilized in this study may pose a serious risk to your health.**

What if there is an unexpected finding on my MR scan? The investigators for this research project are not licensed or trained diagnosticians or clinicians. The testing performed in this project is not intended to find abnormalities, and the images or data

collected do not comprise a diagnostic or clinical study. However, occasionally in the process of research, investigators may perceive an abnormality, the health implications of which may not be clear. When this occurs, UMass Amherst researchers will consult with a radiologist. If the radiologist determines that an additional inquiry is warranted, the researcher will then contact you regarding the radiologist's opinion of the unexpected finding(s).

In such a case, you would be advised to consult with a licensed physician to determine whether further examination or treatment would be prudent. Although the images collected for this research project do not comprise a diagnostic or clinical study, the images can be made available to you for clinical follow-up. The costs for any care that will be needed to diagnose or treat an unexpected finding(s) would not be paid for by University of Massachusetts, Amherst. These costs would be your responsibility. If you have further tests done by your licensed physician, those results will then become part of your medical record, which may affect your current and future health or life insurance.

Regardless of the health implications, the discovery of an unexpected finding(s) may cause you to feel anxious or worried. You may wish to talk to your physician or a qualified mental health clinician. You can contact the Center for Counseling and Psychological Health (CCPH) at (413) 545-2337 (Mon-Fri from 8-5pm) - on weekends or after 5pm, call (413) 577-5000 and ask for the CCPH clinician on call. You can also contact the Psychological Services Center at 413-545-0041 (Monday-Friday 8am-5pm) or psc@psych.umass.edu. In a serious emergency, remember that you can also call 911 for immediate assistance.

Confidentiality: Steps are taken to protect the identities of you and the data collected in this study. The Informed Consent, Physical Activity Readiness Questionnaire, and MR Safety Form (all of which will have your name on them) will be stored and locked in a filing cabinet within a locked office. All other data collection sheets will be coded with your participant number and the study name instead of your name, so that no potential identifiers can be linked back to you. Data collection sheets and lists of participant codes and names are kept separate from all other study materials. Paper documents with names or codes will be stored in separate locked filing cabinets located in a locked office. All electronic data will be kept on a password-protected computer in a locked office. Any data that are published or used in a presentation will not include any names or identifiers that could link back to you.

In Case of Injury: In the unlikely event of an injury resulting directly from participation in this study, we will do everything we can to assist you in seeking medical treatment. The University of Massachusetts does not have a program for compensating subjects for injury or complications related to human subject research.

Benefits: You will receive no direct benefit from participating in this study.

Costs and Reimbursement: There is no cost to participate in this study. To compensate you for your participation, we will give you $20 cash for completing all of the contraction

and cuff inflation protocols for each visit ($40 total for completing both visits 1 and 2), and another $10 for completing all of the physical activity measures.

Withdrawal from Participation: Participation in this research is voluntary. You have the right to refuse to continue or withdraw from the study at any point, without prejudice.

Alternative Procedures: The procedures described above are non-invasive techniques that are commonly used in muscle research. There are no other non-invasive techniques that can be used to obtain the information necessary in this study.

Request for Additional Information: You are encouraged to ask questions about the study. The investigators will attempt to answer all of your questions to the best of their knowledge. The investigators fully intend to conduct the study with your best interest, safety, and comfort in mind. Please address any questions regarding the study to Miles Bartlett in the Muscle Physiology Laboratory. His phone number is (413) 545-5305. We can also be reached by email at umassmplab@umass.edu. You may also address questions to Prof. Kent by calling her at (413) 545-9477 or by emailing her at jkent@kin.umass.edu. If you would like to speak with someone not directly involved in the research study, you may contact the Human Research Protection Office at the University of Massachusetts via email at humansubjects@ora.umass.edu; telephone (413) 545-3428; or mail at the Human Research Protection Office (HRPO), Mass Venture Center, 100 Venture Way, Suite 116, Hadley 01035.

Subject Statement of Voluntary Consent: By signing this form, I am agreeing to voluntarily enter this study. I understand that, by signing this document, I do not waive any of my legal rights. I have had a chance to read this consent form, and it was explained to me in a language that I use and understand. I have had the opportunity to ask questions and have received satisfactory answers. A copy of this signed Informed Consent Form will be given to me.

_____

Participant's name   Address

_____

Signature   Phone Number   Date

STUDY REPRESENTATIVE STATEMENT:

The investigator has read and understands the federal regulations for the Protection of Human Research Subjects (45 CFR 46) and agrees to comply with all of its clauses to the best of her ability. The investigator also pledges to consider the best interests of the subject beyond the explicit statement contained in the aforementioned federal regulations and to exercise professional expertise to protect the rights and welfare of the subject.

_____

Signature of Person Obtaining Consent   Date

TELEPHONE ELIGIBILITY SCREENING SCRIPT (STUDY 2)

Muscle Physiology Lab

Does Mitochondrial Uncoupling Alter the Efficiency of Aerobic Metabolism in Contracting Skeletal Muscles?

<u>Telephone Screening Script</u>

"Hello, my name is _____ and I'm calling from the Muscle Physiology Lab at the University of Massachusetts Amherst. I am contacting you today because you have expressed interest in participating in our study about muscle metabolism. If now is a good time, I can explain the study to you, answer any questions you may have, then ask you a few questions about yourself to see if you would qualify. Passing this initial screening process means that you are likely qualified to participate but it not a guarantee. We will collect a more comprehensive medical history when you come in for your visit, and if those data reveal a contraindication, we will have to exclude you for your own safety.

Before we begin, what is your age?"

- *If the participant is not 21-40 years of age we will inform them that they do not qualify for the study and ask if they would like to be contacted for future studies. If their age falls within these ranges, we will move onto the script below.

  "As I describe the study to you, feel free to ask any questions that you may have."

  "In this study, we are investigating how high-intensity exercise affects aerobic metabolism in skeletal muscle. In short, during high-intensity exercise, muscle metabolism increases much more than would be predicted by the pattern seen at lower exercise intensities. The cause of this difference is not known, but we think that it has to do with changes in the efficiency of aerobic metabolism, which is similar to a car's gas mileage being reduced. Thus, the purpose of this study is to test the hypothesis that the efficiency of aerobic metabolism declines during high-intensity exercise."

  "The study involves two visits and will take about 3 hours in total. Visit 1 will take place at the Muscle Physiology Lab in Totman Gymnasium on the UMass Amherst Campus and require about 1 hour of time. Upon arriving, you will read an Informed Consent document and have any questions you might have answered by the investigators. Following completion of this consenting procedure, you will be asked to fill out a Medical History Form, Physical Activity Readiness Questionnaire, and Magnetic Resonance Safety Form. We will then measure your blood pressure while you are seated and obtain your height and weight. You will then be familiarized with the contraction protocols and pressurized cuff inflation procedures that will be performed during visit 2, which I will describe in detail next."

"Before leaving at the end of visit 1, we will schedule your second visit and give you a small activity monitor that will record the amount and intensity of physical activity you perform over the next 7 days. You will be instructed on how and when to use it and how to keep a simple physical activity log. The activity monitor and log book will be returned at visit 2, or at the end of the week-long wear period."

"Visit 2 will take place at the Human Magnetic Resonance Center in the new Life Sciences Lab building and require about 2 hours of time. Upon arriving you will remove any jewelry, empty your pockets, and walk through a metal detector. You will then be escorted to the MR scanner and positioned on your back with your dominant leg on top of our custom-built leg exercise apparatus, which is similar to a knee extension machine you would use at a gym. The lower leg (shin) will be strapped to the apparatus just above the ankle, knee, and hips. A specially designed copper coil encased in plastic will also be secured over the thigh muscles using Velcro straps. This coil will be used to measure changes in muscle metabolism and biochemistry during the contractions.

Two large inflatable cuffs will then be wrapped around your leg, one each around the upper thigh and calf. To ensure these inflatable cuffs are comfortable and positioned correctly, we will perform a familiarization procedure. First, we will inflate the cuffs to a relatively low pressure (~150 mmHg) and then slowly increase the pressure to 240mmHg, which will be the target pressure during the study protocol. Once you are comfortable with the cuff placements, we will perform 1-2 rapid inflations (~ 1 second), which will be used during the study procedures to temporarily block blood flow. If necessary, the cuffs will be repositioned to make you more comfortable.

Lastly, headphones will be provided to limit the amount of noise from the MR scanner, and to enable clear and constant communication between you and the investigators. We will talk with you and explain each set of measures as we go along. These measures are described next."

"To begin, you will lay quietly for about 15-20 minutes while we will measure your muscle biochemistry at rest. Next, we will measure your knee extension strength and power using 2-3 sets of maximal static and dynamic contractions. You will then perform a 24 second contraction protocol, after which you will rest quietly without moving for up to 10 minutes. This procedure will be used to measure your maximal "aerobic" capacity. <u>Do you have any questions thus far?"</u>

"Next, you will perform the study protocol, which is an incremental exercise test. The test will have 6 stages. Each stage will last 3 minutes, with 1 knee extension contraction being performed every 2 seconds. The workload for stage 1 will be light but will get progressively heavier with each stage as the test continues. Muscle metabolism will be measured continuously throughout the contraction period.

At the end of each stage, we will measure the efficiency of aerobic energy production using our intermittent-ischemia protocol, which will be performed in the following sequence:

9- Up to 12 seconds of rest will be given to allow muscle recovery

10- The blood pressure cuffs will be rapidly inflated
11- The cuffs will remain inflated for up to 40 seconds while we measure rates of muscle energy production and oxygen consumption
12- The cuff will be rapidly deflated to allow muscles to fully recover

<u>Do you have any questions about the blood pressure cuffs or intermittent ischemia protocol? I can go more into detail on those procedures if you'd like.</u>"

If the participant indicates they'd like more detail, the screener will go into more depth with examples of what will be done and what can be expected

"Following step 4 of the intermittent-ischemia protocol, the next 3-minute stage of contractions will begin. Additionally, after the cuff inflation procedures have been completed for the final stage, you will complete one more minute of knee extensions, which will allow us to remeasure your maximal 'aerobic' capacity. Lastly, after the recovery measures have been collected at the end of the incremental protocol, you will undergo 10 minutes of cuff inflation, which will allow us to calibrate the signal we use to calculate muscle oxygen consumption. <u>Do you have any questions?</u>"

"To compensate you for your participation, we will give you $20 cash for completing all of the contraction and cuff inflation protocols for each visit ($40 total for completing both visits 1 and 2), and another $10 for completing all of the physical activity measures. None of these tests will cause permanent damage and any discomfort that you may feel will go away shortly. You may have some muscle soreness in the 2-3 days following the study, but that will also go away. <u>Do you have any questions</u>?"

"If you don't mind, I am now going to ask you a few questions about your medical history to determine if you are eligible for the study. Any information I receive today and all information collected during the study will be kept private and locked in a filing cabinet within a locked room. If you do not qualify for the study and are not interested in participating in further studies, your information will be destroyed. We follow careful procedures to make sure your privacy is protected at all times. Do you have any questions?"

- *Complete 'Telephone Eligibility Screening Form' and 'MR Safety Form.'*

"Do you have any other questions? Thank you very much for your time. We will get back to you once we determine if you are eligible. If you are eligible, we schedule your first visit."

APPENDIX J

TELEPHONE ELIGIBILITY SCREENING FORM (STUDY 2)

Screened by:_____ Date:_____ Status:_____

TELEPHONE SCREENING FORM: MR STUDIES

23) Name_____

24) Phone # (Circle preferred contact):   Best time/day to contact: ____

    a. Home _____   Message?   Yes   No ____

    b. Work _____   Message?   Yes   No ____

    c. Cell _____   Message?   Yes   No ____

25) Email: _____

26) Age_____   Sex_____   Height _____   Weight _____   BMI _____

  (calculate)

27) How did you find out about this study?_____

28) Have you ever participated in a research study before?_____

    a. Are you currently participating in any other research studies right now?_____

        i. If yes, describe:_____

        ii. End date: _____

29) Current health status (general)_____

30) Do you have any physical limitations?_____

31) Are you pregnant?_____

32) Do you, or have you ever had, any of the following:

    a. Stroke?_____

b. Peripheral vascular disease?_____

c. Cardiac disease?_____

d. Pulmonary disease?_____

e. Neurological disease?_____

f. Arthritis in the lower leg?_____

g. Blood vessel disorders such as blood clotting, deep vein thrombosis, or

varicose veins?_____

Have you used ambulatory devices during the last month (i.e., ankle-foot

orthotic, cane, wheelchair, etc.)?_____

33) Do you smoke or have you ever smoked before?_____ For how long?____

Quit?_____

34) Do you have any allergic reactions?_____

35) Do you have any significant past medical history? (e.g. hypertension, CAD, etc.)

_____

36) Current medications:

Drug Name	Classification	Dosage	Frequency	Duration	Prescribed for?

a. Do you take any Statins?_____ If yes, please describe:_____

_____

b. Do you take any beta-blockers, sedatives, tranquilizers, or other medication

that may impair physical function?_____ If yes, please

describe:_____

37) Current physical activity level (regular exercise, none, athlete, etc.) _____

_____

38) Has your Doctor ever told you not to exercise?_____If yes, please

describe:_____

39) What was the date of your last doctor's

visit?_____

40) Is fatigue a problem for you*?*_____ Leg fatigue?_____

41) What type of transportation will you be using?____Will you need a parking pass? ___

42) Would you like to be contacted again for future studies?   Yes   No

43) Comments:_____

_____

44) Go through Magnetic Resonance Safety Questionnaire:

REFERENCES

1.   **Amara CE**, **Shankland EG**, **Jubrias SA**, **Marcinek DJ**, **Kushmerick MJ**, **Conley KE**. Mild mitochondrial uncoupling impacts cellular aging in human muscles in vivo. *Proc Natl Acad Sci U S A* 104: 1057–1062, 2007.

2.   **Andersen P**, **Adams RP**, **Sjogaard G**, **Thorboe A**, **Saltin B**. Dynamic knee extension as model for study of isolated exercising muscle in humans. *J Appl Physiol* 59: 1647–1653, 1985.

3.   **Anderson EJ**, **Neufer PD**. Type II skeletal myofibers possess unique properties that potentiate mitochondrial H2O2 generation. *Am J Physiol - Cell Physiol* 290: C844–C851, 2006.

4.   **Astrand PO**, **Saltin B**. Oxygen uptake during the first minutes of heavy muscular exercise. *J Appl Physiol* 16: 971–976, 1961.

5.   **Bangalore-Yogananda C-G**, **Rosenberry R**, **Soni S**, **Liu H**, **Nelson MD**, **Tian F**. Concurrent measurement of skeletal muscle blood flow during exercise with diffuse correlation spectroscopy and Doppler ultrasound. *Biomed Opt Express* 9: 131–141, 2018.

6.   **Bangsbo J**, **Gollnick PD**, **Graham TE**, **Saltin B**. Substrates for muscle glycogen synthesis in recovery from intense exercise in man. *J Physiol* 434: 423–440, 1991.

7.   **Bangsbo J**, **Hellsten Y**. Muscle blood flow and oxygen uptake in recovery from exercise. *Acta Physiol Scand* 162: 305–312, 1998.

8.   **Bangsbo J**, **Madsen K**, **Kiens B**, **Richter EA**. Muscle glycogen synthesis in recovery from intense exercise in humans. *Am J Physiol* 273: E416-424, 1997.

9.   **Barclay CJ**, **Woledge RC**, **Curtin NA**. Energy turnover for Ca2+ cycling in skeletal muscle. *J Muscle Res Cell Motil* 28: 259–274, 2007.

10. **Barstow TJ**, **Buchthal SD**, **Zanconato S**, **Cooper DM**. Changes in potential controllers of human skeletal muscle respiration during incremental calf exercise. *J Appl Physiol* 77: 2169–2176, 1994.

11. **Bartlett M**, **Hackney AC**, **Battaglini CL**, **Blackburn BT**. Effect of severe-heavy exercise transitions on measures of oxygen uptake and blood lactate accumulation in moderate-well trained males [master's thesis]. [Chapel Hill (NC)]: The University of North Carolina at Chapel Hill; 2012. 63 p. [date unknown].

12. **Bartlett MF**, **Kent JA**. Intramuscular hyperoxia: a potential mechanism for the slow component of oxygen uptake kinetics? Advances in Skeletal Muscle Biology in Health and Disease. 2017 Jan 20-23: Gainesville (USA). University of Florida; 2016. [date unknown].

13. **van Beekvelt MCP**, **van Engelen BGM**, **Wevers RA**, **Colier WNJM**. In vivo quantitative near-infrared spectroscopy in skeletal muscle during incremental isometric handgrip exercise. *Clin Physiol Funct Imaging* 22: 210–217, 2002.

14. **Bendahan D**, **Confort-Gouny S**, **Kozak-Reiss G**, **Cozzone PJ**. Pi trapping in glycogenolytic pathway can explain transient Pi disappearance during recovery from muscular exercise. A 31P NMR study in the human. *FEBS Lett* 269: 402–405, 1990.

15. **Bessman SP**, **Geiger PJ**. Transport of energy in muscle: the phosphorylcreatine shuttle. *Science* 211: 448–452, 1981.

16. **Binzoni T**, **Hiltbrand E**, **Yano T**, **Cerretelli P**. Step vs. progressive exercise: the kinetics of phosphocreatine hydrolysis in human muscle. *Acta Physiol Scand* 159: 209–215, 1997.

17. **van den Boogaart A**, **van Ormondt D**, **Pijnappel WWF**, **de Beer R**, **Ala-Korpela M**. *Mathematics in Signal Processing*. Oxford: Clarendon Press, 1994.

18. **Borrani F**, **Malatesta D**, **Candau R**. Is a progressive recruitment of muscle fibers required for the development of the slow component of VO2 kinetics? *J Appl Physiol* 106: 746; author reply 747, 2009.

19. **Boska M**. Estimating the ATP cost of force production in the human gastrocnemius/soleus muscle group using 31P MRS and 1H MRI. *NMR Biomed* 4: 173–181, 1991.

20. **Boska M**. ATP production rates as a function of force level in the human gastrocnemius/soleus using 31P MRS. *Magn Reson Med* 32: 1–10, 1994.

21. **Bottomley PA**, **Atalar E**, **Weiss RG**. Human cardiac high-energy phosphate metabolite concentrations by 1D-resolved NMR spectroscopy. *Magn Reson Med* 35: 664–670, 1996.

22. **Bottomley PA**, **Lee Y**, **Weiss RG**. Total creatine in muscle: imaging and quantification with proton MR spectroscopy. *Radiology* 204: 403–410, 1997.

23. **Bouckaert J**, **Jones AM**, **Koppo K**. Effect of glycogen depletion on the oxygen uptake slow component in humans. *Int J Sports Med* 25: 351–356, 2004.

24. **Boushel R**, **Gnaiger E**, **Calbet JAL**, **Gonzalez-Alonso J**, **Wright-Paradis C**, **Sondergaard H**, **Ara I**, **Helge JW**, **Saltin B**. Muscle mitochondrial capacity exceeds maximal oxygen delivery in humans. *Mitochondrion* 11: 303–307, 2011.

25. **Boushel R**, **Gnaiger E**, **Larsen FJ**, **Helge JW**, **González-Alonso J**, **Ara I**, **Munch-Andersen T**, **van Hall G**, **Søndergaard H**, **Saltin B**, **Calbet J a. L**. Maintained peak leg and pulmonary VO2 despite substantial reduction in muscle mitochondrial capacity. *Scand J Med Sci Sports* 25 Suppl 4: 135–143, 2015.

26. **Brand MD**. Mitochondrial generation of superoxide and hydrogen peroxide as the source of mitochondrial redox signaling. *Free Radic Biol Med* 100: 14–31, 2016.

27. **Brault JJ**, **Towse TF**, **Slade JM**, **Meyer RA**. Parallel increases in phosphocreatine and total creatine in human vastus lateralis muscle during creatine supplementation. *Int J Sport Nutr Exerc Metab* 17: 624–634, 2007.

28. **van den Broek N**, **De Feyter H**, **de Graaf L**, **Nicolay K**, **Prompers J**. Intersubject differences in the effect of acidosis on phosphocreatine recovery kinetics in muscle after exercise are due to differences in proton efflux rates. *Am J Physiol Cell Physiol* 293: C228-237, 2007.

29. **Broxterman RM**, **Layec G**, **Hureau TJ**, **Amann M**, **Richardson RS**. Skeletal muscle bioenergetics during all-out exercise: mechanistic insight into the oxygen uptake slow component and neuromuscular fatigue. *J Appl Physiol* 122: 1208–1217, 2017.

30. **Burnley M**, **Doust JH**, **Vanhatalo A**. A 3-min all-out test to determine peak oxygen uptake and the maximal steady state. *Med Sci Sports Exerc* 38: 1995–2003, 2006.

31. **Burnley M**, **Vanhatalo A**, **Fulford J**, **Jones AM**. Similar metabolic perturbations during all-out and constant force exhaustive exercise in humans: a (31)P magnetic resonance spectroscopy study. *Exp Physiol* 95: 798–807, 2010.

32. **Cady EB**. Absolute quantitation of phosphorus metabolites in the cerebral cortex of the newborn human infant and in the forearm muscles of young adults using a double-tuned surface coil. *J Magn Reson 1969* 87: 433–446, 1990.

33. **Callahan DM**, **Kent-Braun JA**. Effect of old age on human skeletal muscle force-velocity and fatigue properties. *J Appl Physiol* 111: 1345–1352, 2011.

34. **Campbell MD**, **Marcinek DJ**. Evaluation of in vivo mitochondrial bioenergetics in skeletal muscle using NMR and optical methods. *Biochim Biophys Acta* 1862: 716–724, 2016.

35. **Cannon DT**, **Bimson WE**, **Hampson SA**, **Bowen TS**, **Murgatroyd SR**, **Marwood S**, **Kemp GJ**, **Rossiter HB**. Skeletal muscle ATP turnover by 31P magnetic resonance spectroscopy during moderate and heavy bilateral knee extension. *J Physiol* 592: 5287–5300, 2014.

36. **Cannon DT**, **Howe FA**, **Whipp BJ**, **Ward SA**, **McIntyre DJ**, **Ladroue C**, **Griffiths JR**, **Kemp GJ**, **Rossiter HB**. Muscle metabolism and activation heterogeneity by combined 31P chemical shift and T2 imaging, and pulmonary O2 uptake during incremental knee-extensor exercise. *J Appl Physiol* 115: 839–849, 2013.

37. **Cannon DT**, **Kolkhorst FW**, **Cipriani DJ**. Electromyographic data do not support a progressive recruitment of muscle fibers during exercise exhibiting a VO2 slow component. *J Physiol Anthropol* 26: 541–546, 2007.

38. **Cettolo V**, **Cautero M**, **Tam E**, **Francescato MP**. Mitochondrial coupling in humans: assessment of the P/O2 ratio at the onset of calf exercise. *Eur J Appl Physiol* 99: 593–604, 2007.

39. **Chance B**. Reaction of oxygen with the respiratory chain in cells and tissues. *J Gen Physiol* 49: Suppl:163-195, 1965.

40. **Chance B**, **Leigh JS**, **Clark BJ**, **Maris J**, **Kent J**, **Nioka S**, **Smith D**. Control of oxidative metabolism and oxygen delivery in human skeletal muscle: a steady-state analysis of the work/energy cost transfer function. *Proc Natl Acad Sci U S A* 82: 8384–8388, 1985.

41. **Chance B**, **Leigh JS**, **Kent J**, **McCully K**, **Nioka S**, **Clark BJ**, **Maris JM**, **Graham T**. Multiple controls of oxidative metabolism in living tissues as studied by phosphorus magnetic resonance. *Proc Natl Acad Sci U S A* 83: 9458–9462, 1986.

42. **Chance B**, **Nioka S**, **Warren W**, **Yurtsever G**. Mitochondrial NADH as the bellwether of tissue O2 delivery. *Adv Exp Med Biol* 566: 231–242, 2005.

43. **Chance B**, **Williams GR**. Respiratory enzymes in oxidative phosphorylation. III. The steady state. *J Biol Chem* 217: 409–427, 1955.

44. **Chilibeck PD**, **McCreary CR**, **Marsh GD**, **Paterson DH**, **Noble EG**, **Taylor AW**, **Thompson RT**. Evaluation of muscle oxidative potential by 31P-MRS during incremental exercise in old and young humans. *Eur J Appl Physiol* 78: 460–465, 1998.

45. **Christie AD**, **Tonson A**, **Larsen RG**, **DeBlois JP**, **Kent JA**. Human skeletal muscle metabolic economy in vivo: effects of contraction intensity, age, and mobility impairment. *Am J Physiol Regul Integr Comp Physiol* 307: R1124-1135, 2014.

46. **Chung S**, **Rosenberry R**, **Ryan TE**, **Munson M**, **Dombrowsky T**, **Park S**, **Nasirian A**, **Haykowsky MJ**, **Nelson MD**. Near-infrared spectroscopy detects age-related differences in skeletal muscle oxidative function: promising implications for geroscience. *Physiol Rep* 6, 2018.

47. **Clausen T**. Quantification of Na+,K+ pumps and their transport rate in skeletal muscle: functional significance. *J Gen Physiol* 142: 327–345, 2013.

48. **Combs CA**, **Aletras AH**, **Balaban RS**. Effect of muscle action and metabolic strain on oxidative metabolic responses in human skeletal muscle. *J Appl Physiol* 87: 1768–1775, 1999.

49. **Conley KE**, **Amara CE**, **Bajpeyi S**, **Costford SR**, **Murray K**, **Jubrias SA**, **Arakaki L**, **Marcinek DJ**, **Smith SR**. Higher mitochondrial respiration and uncoupling with reduced electron transport chain content in vivo in muscle of sedentary versus active subjects. *J Clin Endocrinol Metab* 98: 129–136, 2013.

50. **Crow MT**, **Kushmerick MJ**. Chemical energetics of slow- and fast-twitch muscles of the mouse. *J Gen Physiol* 79: 147–166, 1982.

51. **Danovaro R**, **Dell'Anno A**, **Pusceddu A**, **Gambi C**, **Heiner I**, **Møbjerg Kristensen R**. The first metazoa living in permanently anoxic conditions. *BMC Biol* 8: 30, 2010.

52. **Debold EP**, **Longyear TJ**, **Turner MA**. The effects of phosphate and acidosis on regulated thin-filament velocity in an in vitro motility assay. *J Appl Physiol* 113: 1413–1422, 2012.

53. **Debold EP**, **Walcott S**, **Woodward M**, **Turner MA**. Direct observation of phosphate inhibiting the force-generating capacity of a miniensemble of Myosin molecules. *Biophys J* 105: 2374–2384, 2013.

54. **Dohlmann TL**, **Hindsø M**, **Dela F**, **Helge JW**, **Larsen S**. High-intensity interval training changes mitochondrial respiratory capacity differently in adipose tissue and skeletal muscle. *Physiol Rep* 6: e13857, 2018.

55. **Faraut B**, **Giannesini B**, **Matarazzo V**, **Marqueste T**, **Dalmasso C**, **Rougon G**, **Cozzone PJ**, **Bendahan D**. Downregulation of uncoupling protein-3 in vivo is linked to changes in muscle mitochondrial energy metabolism as a result of capsiate administration. *Am J Physiol Endocrinol Metab* 292: E1474-1482, 2007.

56. **Fraser SF**, **Li JL**, **Carey MF**, **Wang XN**, **Sangkabutra T**, **Sostaric S**, **Selig SE**, **Kjeldsen K**, **McKenna MJ**. Fatigue depresses maximal in vitro skeletal muscle Na(+)-K(+)-ATPase activity in untrained and trained individuals. *J Appl Physiol* 93: 1650–1659, 2002.

57. **Freedson PS**, **Melanson E**, **Sirard J**. Calibration of the Computer Science and Applications, Inc. accelerometer. *Med Sci Sports Exerc* 30: 777–781, 1998.

58. **Gaesser GA**, **Poole DC**. The slow component of oxygen uptake kinetics in humans. *Exerc Sport Sci Rev* 24: 35–71, 1996.

59. **Gao F**, **Bottomley PA**, **Arnold C**, **Weiss RG**. The effect of orientation on quantification of muscle creatine by 1H MR spectroscopy. *Magn Reson Imaging* 21: 561–566, 2003.

60. **Gardiner P**. Advanced Neuromuscular Exercise Physiology [Online]. Human Kinetics. http://www.humankinetics.com/products/all-products/advanced-neuromuscular-exercise-physiology [2 Aug. 2018].

61. **Garland SW**, **Wang W**, **Ward SA**. Indices of electromyographic activity and the "slow" component of oxygen uptake kinetics during high-intensity knee-extension exercise in humans. *Eur J Appl Physiol* 97: 413–423, 2006.

62. **Gifford JR**, **Garten RS**, **Nelson AD**, **Trinity JD**, **Layec G**, **Witman MAH**, **Weavil JC**, **Mangum T**, **Hart C**, **Etheredge C**, **Jessop J**, **Bledsoe A**, **Morgan DE**, **Wray DW**, **Rossman MJ**, **Richardson RS**. Symmorphosis and skeletal muscle V̇O2 max : in vivo and in vitro measures reveal differing constraints in the exercise-trained and untrained human. *J Physiol* 594: 1741–1751, 2016.

63. **Glancy B**, **Balaban RS**. Protein composition and function of red and white skeletal muscle mitochondria. *Am J Physiol Cell Physiol* 300: C1280-1290, 2011.

64. **Gnaiger E**, **Méndez G**, **Hand SC**. High phosphorylation efficiency and depression of uncoupled respiration in mitochondria under hypoxia. *Proc Natl Acad Sci U S A* 97: 11080–11085, 2000.

65.   **Golding EM**, **Teague WE**, **Dobson GP**. Adjustment of K' to varying pH and pMg for the creatine kinase, adenylate kinase and ATP hydrolysis equilibria permitting quantitative bioenergetic assessment. *J Exp Biol* 198: 1775–1782, 1995.

66.   **Goncalves RLS**, **Quinlan CL**, **Perevoshchikova IV**, **Hey-Mogensen M**, **Brand MD**. Sites of superoxide and hydrogen peroxide production by muscle mitochondria assessed ex vivo under conditions mimicking rest and exercise. *J Biol Chem* 290: 209–227, 2015.

67.   **Gueguen N**, **Lefaucheur L**, **Ecolan P**, **Fillaut M**, **Herpin P**. Ca2+-activated myosin-ATPases, creatine and adenylate kinases regulate mitochondrial function according to myofibre type in rabbit. *J Physiol* 564: 723–735, 2005.

68.   **Gurley K**, **Shang Y**, **Yu G**. Noninvasive optical quantification of absolute blood flow, blood oxygenation, and oxygen consumption rate in exercising skeletal muscle. *J Biomed Opt* 17: 075010, 2012.

69.   **Harkema SJ**, **Adams GR**, **Meyer RA**. Acidosis has no effect on the ATP cost of contraction in cat fast- and slow-twitch skeletal muscles. *Am J Physiol* 272: C485-490, 1997.

70.   **Harkema SJ**, **Meyer RA**. Effect of acidosis on control of respiration in skeletal muscle. *Am J Physiol* 272: C491-500, 1997.

71.   **Harris RC**, **Edwards RH**, **Hultman E**, **Nordesjö LO**, **Nylind B**, **Sahlin K**. The time course of phosphorylcreatine resynthesis during recovery of the quadriceps muscle in man. *Pflugers Arch* 367: 137–142, 1976.

72.   **Harris RC**, **Hultman E**, **Nordesjö LO**. Glycogen, glycolytic intermediates and high-energy phosphates determined in biopsy samples of musculus quadriceps femoris of man at rest. Methods and variance of values. *Scand J Clin Lab Invest* 33: 109–120, 1974.

73.   **Haseler LJ**, **Hogan MC**, **Richardson RS**. Skeletal muscle phosphocreatine recovery in exercise-trained humans is dependent on O2 availability. *J Appl Physiol* 86: 2013–2018, 1999.

74.   **Haseler LJ**, **Lin AP**, **Richardson RS**. Skeletal muscle oxidative metabolism in sedentary humans: 31P-MRS assessment of O2 supply and demand limitations. *J Appl Physiol* 97: 1077–1081, 2004.

75.   **He ZH**, **Bottinelli R**, **Pellegrino MA**, **Ferenczi MA**, **Reggiani C**. ATP consumption and efficiency of human single muscle fibers with different myosin isoform composition. *Biophys J* 79: 945–961, 2000.

76.   **Henson LC**, **Poole DC**, **Whipp BJ**. Fitness as a determinant of oxygen uptake response to constant-load exercise. *Eur J Appl Physiol* 59: 21–28, 1989.

77.   **Hesselink MK**, **Keizer HA**, **Borghouts LB**, **Schaart G**, **Kornips CF**, **Slieker LJ**, **Sloop KW**, **Saris WH**, **Schrauwen P**. Protein expression of UCP3 differs between human type 1, type 2a, and type 2b fibers. *FASEB J Off Publ Fed Am Soc Exp Biol* 15: 1071–1073, 2001.

78. **Hey-Mogensen M**, **Gram M**, **Jensen MB**, **Lund MT**, **Hansen CN**, **Scheibye-Knudsen M**, **Bohr VA**, **Dela F**. A novel method for determining human ex vivo submaximal skeletal muscle mitochondrial function. *J Physiol* 593: 3991–4010, 2015.

79. **Hill AV**, **Lupton H**. Muscular Exercise, Lactic Acid, and the Supply and Utilization of Oxygen. *QJM Int J Med* os-16: 135–171, 1923.

80. **Hill DW**, **Halcomb JN**, **Stevens EC**. Oxygen uptake kinetics during severe intensity running and cycling. *Eur J Appl Physiol* 89: 612–618, 2003.

81. **Hirai DM**, **Roseguini BT**, **Diefenthaeler F**, **Carpes FP**, **Vaz MA**, **Ferlin EL**, **Ribeiro JP**, **Nakamura FY**. Effects of altering pedal frequency on the slow component of pulmonary VO2 kinetics and EMG activity. *Int J Sports Med* 31: 529–536, 2010.

82. **Hochachka PW**, **Mommsen TP**. Protons and anaerobiosis. *Science* 219: 1391–1397, 1983.

83. **Hogan MC**, **Richardson RS**, **Haseler LJ**. Human muscle performance and PCr hydrolysis with varied inspired oxygen fractions: a 31P-MRS study. *J Appl Physiol* 86: 1367–1373, 1999.

84. **Holian A**, **Owen CS**, **Wilson DF**. Control of respiration in isolated mitochondria: quantitative evaluation of the dependence of respiratory rates on [ATP], [ADP], and [Pi]. *Arch Biochem Biophys* 181: 164–171, 1977.

85. **Homma T**, **Hamaoka T**, **Sako T**, **Murakami M**, **Esaki K**, **Kime R**, **Katsumura T**. Muscle oxidative metabolism accelerates with mild acidosis during incremental intermittent isometric plantar flexion exercise. *Dyn Med* 4: 2, 2005.

86. **Jackman MR**, **Willis WT**. Characteristics of mitochondria isolated from type I and type IIb skeletal muscle. *Am J Physiol* 270: C673-678, 1996.

87. **Jacobs RA**, **Lundby C**. Mitochondria express enhanced quality as well as quantity in association with aerobic fitness across recreationally active individuals up to elite athletes. *J Appl Physiol* 114: 344–350, 2013.

88. **Jacobus WE**, **Moreadith RW**, **Vandegaer KM**. Mitochondrial respiratory control. Evidence against the regulation of respiration by extramitochondrial phosphorylation potentials or by [ATP]/[ADP] ratios. *J Biol Chem* 257: 2397–2402, 1982.

89. **Jeneson JA**, **Wiseman RW**, **Westerhoff HV**, **Kushmerick MJ**. The signal transduction function for oxidative phosphorylation is at least second order in ADP. *J Biol Chem* 271: 27995–27998, 1996.

90. **Jeneson JAL**, **Schmitz JPJ**, **van den Broek NMA**, **van Riel NAW**, **Hilbers PAJ**, **Nicolay K**, **Prompers JJ**. Magnitude and control of mitochondrial sensitivity to ADP. *Am J Physiol Endocrinol Metab* 297: E774-784, 2009.

91. **Jeneson JAL**, **Schmitz JPJ**, **Hilbers PAJ**, **Nicolay K**. An MR-compatible bicycle ergometer for in-magnet whole-body human exercise testing. *Magn Reson Med* 63: 257–261, 2010.

92. **Jöbsis FF**, **Stainsby WN**. Oxidation of NADH during contractions of circulated mammalian skeletal muscle. *Respir Physiol* 4: 292–300, 1968.

93. **Jubrias SA**, **Crowther GJ**, **Shankland EG**, **Gronka RK**, **Conley KE**. Acidosis inhibits oxidative phosphorylation in contracting human skeletal muscle in vivo. *J Physiol* 553: 589–599, 2003.

94. **Kayser B**. Lactate during exercise at high altitude. *Eur J Appl Physiol* 74: 195–205, 1996.

95. **Kemp GJ**, **Ahmad RE**, **Nicolay K**, **Prompers JJ**. Quantification of skeletal muscle mitochondrial function by 31P magnetic resonance spectroscopy techniques: a quantitative review. *Acta Physiol Oxf Engl* 213: 107–144, 2015.

96. **Kemp GJ**, **Radda GK**. Quantitative interpretation of bioenergetic data from 31P and 1H magnetic resonance spectroscopic studies of skeletal muscle: an analytical review. *Magn Reson Q* 10: 43–63, 1994.

97. **Kemp GJ**, **Taylor DJ**, **Styles P**, **Radda GK**. The production, buffering and efflux of protons in human skeletal muscle during exercise and recovery. *NMR Biomed* 6: 73–83, 1993.

98. **Kemp GJ**, **Thompson CH**, **Barnes PR**, **Radda GK**. Comparisons of ATP turnover in human muscle during ischemic and aerobic exercise using 31P magnetic resonance spectroscopy. *Magn Reson Med* 31: 248–258, 1994.

99. **Kemp GJ**, **Thompson CH**, **Taylor DJ**, **Radda GK**. ATP production and mechanical work in exercising skeletal muscle: a theoretical analysis applied to 31P magnetic resonance spectroscopic studies of dialyzed uremic patients. *Magn Reson Med* 33: 601–609, 1995.

100. **Kent-Braun JA**. Central and peripheral contributions to muscle fatigue in humans during sustained maximal effort. *Eur J Appl Physiol* 80: 57–63, 1999.

101. **Kent-Braun JA**, **McCully KK**, **Chance B**. Metabolic effects of training in humans: a 31P-MRS study. *J Appl Physiol Bethesda Md 1985* 69: 1165–1170, 1990.

102. **Kent-Braun JA**, **Miller RG**, **Weiner MW**. Phases of metabolism during progressive exercise to fatigue in human skeletal muscle. *J Appl Physiol* 75: 573–580, 1993.

103. **Kent-Braun JA**, **Ng AV**. Skeletal muscle oxidative capacity in young and older women and men. *J Appl Physiol* 89: 1072–1078, 2000.

104. **Kent-Braun JA**, **Ng AV**, **Doyle JW**, **Towse TF**. Human skeletal muscle responses vary with age and gender during fatigue due to incremental isometric exercise. *J Appl Physiol* 93: 1813–1823, 2002.

105. **Klingenberg M**. The ADP and ATP transport in mitochondria and its carrier. *Biochim Biophys Acta* 1778: 1978–2021, 2008.

106. **Koga S**, **Okushima D**, **Barstow TJ**, **Rossiter HB**, **Kondo N**, **Poole DC**. Near-infrared spectroscopy of superficial and deep rectus femoris reveals markedly different exercise response to superficial vastus lateralis. *Physiol Rep* 5, 2017.

107. **Koga S**, **Poole DC**, **Shiojiri T**, **Kondo N**, **Fukuba Y**, **Miura A**, **Barstow TJ**. Comparison of oxygen uptake kinetics during knee extension and cycle exercise. *Am J Physiol-Regul Integr Comp Physiol* 288: R212–R220, 2005.

108. **Koo TK**, **Li MY**. A Guideline of Selecting and Reporting Intraclass Correlation Coefficients for Reliability Research. *J Chiropr Med* 15: 155–163, 2016.

109. **Korzeniewski B**, **Zoladz JA**. Possible mechanisms underlying slow component of V̇O2 on-kinetics in skeletal muscle. *J Appl Physiol* 118: 1240–1249, 2015.

110. **Kreis R**, **Bruegger K**, **Skjelsvik C**, **Zwicky S**, **Ith M**, **Jung B**, **Baumgartner I**, **Boesch C**. Quantitative (1)H magnetic resonance spectroscopy of myoglobin de- and reoxygenation in skeletal muscle: reproducibility and effects of location and disease. *Magn Reson Med* 46: 240–248, 2001.

111. **Krustrup P**, **Jones AM**, **Wilkerson DP**, **Calbet J a. L**, **Bangsbo J**. Muscular and pulmonary O2 uptake kinetics during moderate- and high-intensity sub-maximal knee-extensor exercise in humans. *J Physiol* 587: 1843–1856, 2009.

112. **Krustrup P**, **Secher NH**, **Relu MU**, **Hellsten Y**, **Söderlund K**, **Bangsbo J**. Neuromuscular blockade of slow twitch muscle fibres elevates muscle oxygen uptake and energy turnover during submaximal exercise in humans. *J Physiol* 586: 6037–6048, 2008.

113. **Krustrup P**, **Söderlund K**, **Mohr M**, **Bangsbo J**. The slow component of oxygen uptake during intense, sub-maximal exercise in man is associated with additional fibre recruitment. *Pflugers Arch* 447: 855–866, 2004.

114. **Krustrup P**, **Söderlund K**, **Mohr M**, **Bangsbo J**. Slow-twitch fiber glycogen depletion elevates moderate-exercise fast-twitch fiber activity and O2 uptake. *Med Sci Sports Exerc* 36: 973–982, 2004.

115. **Kushmerick MJ**, **Meyer RA**, **Brown TR**. Regulation of oxygen consumption in fast- and slow-twitch muscle. *Am J Physiol* 263: C598-606, 1992.

116. **Kuznetsov AV**, **Tiivel T**, **Sikk P**, **Kaambre T**, **Kay L**, **Daneshrad Z**, **Rossi A**, **Kadaja L**, **Peet N**, **Seppet E**, **Saks VA**. Striking differences between the kinetics of regulation of respiration by ADP in slow-twitch and fast-twitch muscles in vivo. *Eur J Biochem* 241: 909–915, 1996.

117. **LaNoue KF**, **Schoolwerth AC**. Metabolite transport in mitochondria. *Annu Rev Biochem* 48: 871–922, 1979.

118. **LaNoue KF**, **Tischler ME**. Electrogenic characteristics of the mitochondrial glutamate-aspartate antiporter. *J Biol Chem* 249: 7522–7528, 1974.

119. **Lanza IR**, **Befroy DE**, **Kent-Braun JA**. Age-related changes in ATP-producing pathways in human skeletal muscle in vivo. *J Appl Physiol* 99: 1736–1744, 2005.

120. **Lanza IR**, **Larsen RG**, **Kent-Braun JA**. Effects of old age on human skeletal muscle energetics during fatiguing contractions with and without blood flow. *J Physiol* 583: 1093–1105, 2007.

121. **Lanza IR**, **Tevald MA**, **Befroy DE**, **Kent-Braun JA**. Intracellular energetics and critical PO2 in resting ischemic human skeletal muscle in vivo. *Am J Physiol Regul Integr Comp Physiol* 299: R1415-1422, 2010.

122. **Lanza IR**, **Wigmore DM**, **Befroy DE**, **Kent-Braun JA**. In vivo ATP production during free-flow and ischaemic muscle contractions in humans. *J Physiol* 577: 353–367, 2006.

123. **Larsen RG**, **Befroy DE**, **Kent-Braun JA**. High-intensity interval training increases in vivo oxidative capacity with no effect on P(i)→ATP rate in resting human muscle. *Am J Physiol Regul Integr Comp Physiol* 304: R333-342, 2013.

124. **Larsen RG**, **Callahan DM**, **Foulis SA**, **Kent-Braun JA**. In vivo oxidative capacity varies with muscle and training status in young adults. *J Appl Physiol* 107: 873–879, 2009.

125. **Larsen RG**, **Maynard L**, **Kent JA**. High-intensity interval training alters ATP pathway flux during maximal muscle contractions in humans. *Acta Physiol Oxf Engl* 211: 147–160, 2014.

126. **Larsen S**, **Nielsen J**, **Hansen CN**, **Nielsen LB**, **Wibrand F**, **Stride N**, **Schroder HD**, **Boushel R**, **Helge JW**, **Dela F**, **Hey-Mogensen M**. Biomarkers of mitochondrial content in skeletal muscle of healthy young human subjects. *J Physiol* 590: 3349–3360, 2012.

127. **Layec G**, **Blain GM**, **Rossman MJ**, **Park SY**, **Hart CR**, **Trinity JD**, **Gifford JR**, **Sidhu SK**, **Weavil JC**, **Hureau TJ**, **Amann M**, **Richardson RS**. Acute High-Intensity Exercise Impairs Skeletal Muscle Respiratory Capacity. *Med. Sci. Sports Exerc.* (August 10, 2018). doi: 10.1249/MSS.0000000000001735.

128. **Layec G**, **Bringard A**, **Le Fur Y**, **Micallef J-P**, **Vilmen C**, **Perrey S**, **Cozzone PJ**, **Bendahan D**. Mitochondrial Coupling and Contractile Efficiency in Humans with High and Low V˙O2peaks. *Med Sci Sports Exerc* 48: 811–821, 2016.

129. **Layec G**, **Bringard A**, **Le Fur Y**, **Vilmen C**, **Micallef J-P**, **Perrey S**, **Cozzone PJ**, **Bendahan D**. Comparative determination of energy production rates and mitochondrial function using different 31P MRS quantitative methods in sedentary and trained subjects. *NMR Biomed* 24: 425–438, 2011.

130. **Layec G**, **Bringard A**, **Vilmen C**, **Micallef J-P**, **Le Fur Y**, **Perrey S**, **Cozzone PJ**, **Bendahan D**. Does oxidative capacity affect energy cost? An in vivo MR investigation of skeletal muscle energetics. *Eur J Appl Physiol* 106: 229–242, 2009.

131. **Layec G**, **Gifford JR**, **Trinity JD**, **Hart CR**, **Garten RS**, **Park SY**, **Le Fur Y**, **Jeong E-K**, **Richardson RS**. Accuracy and precision of quantitative 31P-MRS measurements of human skeletal muscle mitochondrial function. *Am J Physiol-Endocrinol Metab* 311: E358–E366, 2016.

132. **Layec G**, **Hart CR**, **Trinity JD**, **Le Fur Y**, **Jeong E-K**, **Richardson RS**. Skeletal muscle work efficiency with age: the role of non-contractile processes. *Clin Sci* 128: 213–223, 2015.

133. **Layec G**, **Haseler LJ**, **Hoff J**, **Hart CR**, **Liu X**, **Le Fur Y**, **Jeong E-K**, **Richardson RS**. Short-term training alters the control of mitochondrial respiration rate before maximal oxidative ATP synthesis. *Acta Physiol Oxf Engl* 208: 376–386, 2013.

134. **Layec G**, **Haseler LJ**, **Trinity JD**, **Hart CR**, **Liu X**, **Le Fur Y**, **Jeong E-K**, **Richardson RS**. Mitochondrial function and increased convective O2 transport: implications for the assessment of mitochondrial respiration in vivo. *J Appl Physiol Bethesda Md 1985* 115: 803–811, 2013.

135. **Layec G**, **Malucelli E**, **Le Fur Y**, **Manners D**, **Yashiro K**, **Testa C**, **Cozzone PJ**, **Iotti S**, **Bendahan D**. Effects of exercise-induced intracellular acidosis on the phosphocreatine recovery kinetics: a 31P MRS study in three muscle groups in humans. *NMR Biomed* 26: 1403–1411, 2013.

136. **Leone V**, **Faraldo-Gómez JD**. Structure and mechanism of the ATP synthase membrane motor inferred from quantitative integrative modeling. *J Gen Physiol* 148: 441–457, 2016.

137. **Leppik JA**, **Aughey RJ**, **Medved I**, **Fairweather I**, **Carey MF**, **McKenna MJ**. Prolonged exercise to fatigue in humans impairs skeletal muscle Na+-K+-ATPase activity, sarcoplasmic reticulum Ca2+ release, and Ca2+ uptake. *J Appl Physiol* 97: 1414–1423, 2004.

138. **Li JL**, **Wang XN**, **Fraser SF**, **Carey MF**, **Wrigley TV**, **McKenna MJ**. Effects of fatigue and training on sarcoplasmic reticulum Ca(2+) regulation in human skeletal muscle. *J Appl Physiol* 92: 912–922, 2002.

139. **Lucía A**, **Rivero J-LL**, **Pérez M**, **Serrano AL**, **Calbet JAL**, **Santalla A**, **Chicharro JL**. Determinants of VO(2) kinetics at high power outputs during a ramp exercise protocol. *Med Sci Sports Exerc* 34: 326–331, 2002.

140. **Mahler M**. First-order kinetics of muscle oxygen consumption, and an equivalent proportionality between QO2 and phosphorylcreatine level. Implications for the control of respiration. *J Gen Physiol* 86: 135–165, 1985.

141. **Majerczak J**, **Nieckarz Z**, **Karasinski J**, **Zoladz JA**. Myosin heavy chain composition in the vastus lateralis muscle in relation to oxygen uptake and heart rate during cycling in humans. *J Physiol Pharmacol* 65: 217–227, 2014.

142. **Majerczak J**, **Szkutnik Z**, **Duda K**, **Komorowska M**, **Kolodziejski L**, **Karasinski J**, **Zoladz JA**. Effect of pedaling rates and myosin heavy chain

composition in the vastus lateralis muscle on the power generating capability during incremental cycling in humans. *Physiol Res* 57: 873–884, 2008.

143. **Majerczak J**, **Szkutnik Z**, **Karasinski J**, **Duda K**, **Kolodziejski L**, **Zoladz JA**. High content of MYHC II in vastus lateralis is accompanied by higher VO2/power output ratio during moderate intensity cycling performed both at low and at high pedalling rates. *J Physiol Pharmacol* 57: 199–215, 2006.

144. **Marcinek DJ**, **Kushmerick MJ**, **Conley KE**. Lactic acidosis in vivo: testing the link between lactate generation and H+ accumulation in ischemic mouse muscle. *J Appl Physiol* 108: 1479–1486, 2010.

145. **Marcinek DJ**, **Schenkman KA**, **Ciesielski WA**, **Conley KE**. Mitochondrial coupling in vivo in mouse skeletal muscle. *Am J Physiol Cell Physiol* 286: C457-463, 2004.

146. **Marcinek DJ**, **Schenkman KA**, **Ciesielski WA**, **Lee D**, **Conley KE**. Reduced mitochondrial coupling in vivo alters cellular energetics in aged mouse skeletal muscle. *J Physiol* 569: 467–473, 2005.

147. **Matsunaga S**, **Mishima T**, **Yamada T**, **Inashima S**, **Wada M**. Alterations in in vitro function and protein oxidation of rat sarcoplasmic reticulum Ca2+-ATPase during recovery from high-intensity exercise. *Exp Physiol* 93: 426–433, 2008.

148. **Medbø JI**, **Sejersted OM**. Plasma potassium changes with high intensity exercise. *J Physiol* 421: 105–122, 1990.

149. **Meyer RA**. A linear model of muscle respiration explains monoexponential phosphocreatine changes. *Am J Physiol* 254: C548-553, 1988.

150. **Meyer RA**. Linear dependence of muscle phosphocreatine kinetics on total creatine content. *Am J Physiol* 257: C1149-1157, 1989.

151. **Mitchell P**. Coupling of phosphorylation to electron and hydrogen transfer by a chemi-osmotic type of mechanism. *Nature* 191: 144–148, 1961.

152. **Mogensen M**, **Bagger M**, **Pedersen PK**, **Fernström M**, **Sahlin K**. Cycling efficiency in humans is related to low UCP3 content and to type I fibres but not to mitochondrial efficiency. *J Physiol* 571: 669–681, 2006.

153. **Mogensen M**, **Sahlin K**. Mitochondrial efficiency in rat skeletal muscle: influence of respiration rate, substrate and muscle type. *Acta Physiol Scand* 185: 229–236, 2005.

154. **Moon RB**, **Richards JH**. Determination of intracellular pH by 31P magnetic resonance. *J Biol Chem* 248: 7276–7278, 1973.

155. **Nagesser AS**, **Van der Laarse WJ**, **Elzinga G**. ATP formation and ATP hydrolysis during fatiguing, intermittent stimulation of different types of single muscle fibres from Xenopus laevis. *J Muscle Res Cell Motil* 14: 608–618, 1993.

156. **Naressi A**, **Couturier C**, **Castang I**, **de Beer R**, **Graveron-Demilly D**. Java-based graphical user interface for MRUI, a software package for quantitation of in vivo/medical magnetic resonance spectroscopy signals. *Comput Biol Med* 31: 269–286, 2001.

157. **Nelson CR**, **Debold EP**, **Fitts RH**. Phosphate and acidosis act synergistically to depress peak power in rat muscle fibers. *Am J Physiol Cell Physiol* 307: C939-950, 2014.

158. **Newcomer BR**, **Boska MD**. Adenosine triphosphate production rates, metabolic economy calculations, pH, phosphomonoesters, phosphodiesters, and force output during short-duration maximal isometric plantar flexion exercises and repeated maximal isometric plantar flexion exercises. *Muscle Nerve* 20: 336–346, 1997.

159. **Nicholls DG**, **Ferguson SJ**. *Bioenergetics, Fourth Edition*. 4 edition. Amsterdam: Academic Press, 2013.

160. **Nogueira L**, **Shiah AA**, **Gandra PG**, **Hogan MC**. Ca^{2+}-pumping impairment during repetitive fatiguing contractions in single myofibers: role of cross-bridge cycling. *Am J Physiol Regul Integr Comp Physiol* 305: R118-125, 2013.

161. **Osborne MA**, **Schneider DA**. Muscle glycogen reduction in man: relationship between surface EMG activity and oxygen uptake kinetics during heavy exercise. *Exp Physiol* 91: 179–189, 2006.

162. **Paganini AT**, **Foley JM**, **Meyer RA**. Linear dependence of muscle phosphocreatine kinetics on oxidative capacity. *Am J Physiol* 272: C501-510, 1997.

163. **Pesta D**, **Hoppel F**, **Macek C**, **Messner H**, **Faulhaber M**, **Kobel C**, **Parson W**, **Burtscher M**, **Schocke M**, **Gnaiger E**. Similar qualitative and quantitative changes of mitochondrial respiration following strength and endurance training in normoxia and hypoxia in sedentary humans. *Am J Physiol Regul Integr Comp Physiol* 301: R1078-1087, 2011.

164. **Petersen AC**, **Murphy KT**, **Snow RJ**, **Leppik JA**, **Aughey RJ**, **Garnham AP**, **Cameron-Smith D**, **McKenna MJ**. Depressed Na+-K+-ATPase activity in skeletal muscle at fatigue is correlated with increased Na+-K+-ATPase mRNA expression following intense exercise. *Am J Physiol Regul Integr Comp Physiol* 289: R266-274, 2005.

165. **Picard M**, **Ritchie D**, **Thomas MM**, **Wright KJ**, **Hepple RT**. Alterations in intrinsic mitochondrial function with aging are fiber type-specific and do not explain differential atrophy between muscles. *Aging Cell* 10: 1047–1055, 2011.

166. **Poole DC**, **Burnley M**, **Vanhatalo A**, **Rossiter HB**, **Jones AM**. Critical Power: An Important Fatigue Threshold in Exercise Physiology. *Med Sci Sports Exerc* 48: 2320–2334, 2016.

167. **Poole DC**, **Schaffartzik W**, **Knight DR**, **Derion T**, **Kennedy B**, **Guy HJ**, **Prediletto R**, **Wagner PD**. Contribution of exercising legs to the slow component of oxygen uptake kinetics in humans. *J Appl Physiol* 71: 1245–1260, 1991.

168. **Quistorff B**, **Johansen L**, **Sahlin K**. Absence of phosphocreatine resynthesis in human calf muscle during ischaemic recovery. *Biochem J* 291 (Pt 3): 681–686, 1993.

169. **Rasmussen UF**, **Rasmussen HN**, **Krustrup P**, **Quistorff B**, **Saltin B**, **Bangsbo J**. Aerobic metabolism of human quadriceps muscle: in vivo data parallel measurements on isolated mitochondria. *Am J Physiol Endocrinol Metab* 280: E301-307, 2001.

170. **Raymer GH**, **Forbes SC**, **Kowalchuk JM**, **Thompson RT**, **Marsh GD**. Prior exercise delays the onset of acidosis during incremental exercise. *J Appl Physiol* 102: 1799–1805, 2007.

171. **Rosenberry R**, **Chung S**, **Nelson MD**. Skeletal Muscle Neurovascular Coupling, Oxidative Capacity, and Microvascular Function with "One Stop Shop" Near-infrared Spectroscopy. *J Vis Exp JoVE* , 2018.

172. **Rosenberry R**, **Munson M**, **Chung S**, **Samuel TJ**, **Patik J**, **Tucker WJ**, **Haykowsky MJ**, **Nelson MD**. Age-related microvascular dysfunction: novel insight from near-infrared spectroscopy. *Exp Physiol* 103: 190–200, 2018.

173. **Rossiter HB**, **Ward SA**, **Howe FA**, **Kowalchuk JM**, **Griffiths JR**, **Whipp BJ**. Dynamics of intramuscular 31P-MRS P(i) peak splitting and the slow components of PCr and O2 uptake during exercise. *J Appl Physiol* 93: 2059–2069, 2002.

174. **Rossiter HB**, **Ward SA**, **Kowalchuk JM**, **Howe FA**, **Griffiths JR**, **Whipp BJ**. Dynamic asymmetry of phosphocreatine concentration and O(2) uptake between the on- and off-transients of moderate- and high-intensity exercise in humans. *J Physiol* 541: 991–1002, 2002.

175. **Roston WL**, **Whipp BJ**, **Davis JA**, **Cunningham DA**, **Effros RM**, **Wasserman K**. Oxygen uptake kinetics and lactate concentration during exercise in humans. *Am Rev Respir Dis* 135: 1080–1084, 1987.

176. **Russell AP**, **Somm E**, **Praz M**, **Crettenand A**, **Hartley O**, **Melotti A**, **Giacobino J-P**, **Muzzin P**, **Gobelet C**, **Dériaz O**. UCP3 protein regulation in human skeletal muscle fibre types I, IIa and IIx is dependent on exercise intensity. *J Physiol* 550: 855–861, 2003.

177. **Ryan TE**, **Southern WM**, **Reynolds MA**, **McCully KK**. A cross-validation of near-infrared spectroscopy measurements of skeletal muscle oxidative capacity with phosphorus magnetic resonance spectroscopy. *J Appl Physiol* 115: 1757–1766, 2013.

178. **Ryschon TW**, **Fowler MD**, **Wysong RE**, **Anthony A**, **Balaban RS**. Efficiency of human skeletal muscle in vivo: comparison of isometric, concentric, and eccentric muscle action. *J Appl Physiol* 83: 867–874, 1997.

179. **Sabapathy S**, **Schneider DA**, **Morris NR**. The VO2 slow component: relationship between plasma ammonia and EMG activity. *Med Sci Sports Exerc* 37: 1502–1509, 2005.

180. **Sahlin K**, **Harris RC**, **Hultman E**. Resynthesis of creatine phosphate in human muscle after exercise in relation to intramuscular pH and availability of oxygen. *Scand J Clin Lab Invest* 39: 551–558, 1979.

181. **Sahlin K**, **Sørensen JB**, **Gladden LB**, **Rossiter HB**, **Pedersen PK**. Prior heavy exercise eliminates VO2 slow component and reduces efficiency during submaximal exercise in humans. *J Physiol* 564: 765–773, 2005.

182. **Sahlin K**, **Tonkonogi M**, **Söderlund K**. Energy supply and muscle fatigue in humans. *Acta Physiol Scand* 162: 261–266, 1998.

183. **Saunders MJ**, **Evans EM**, **Arngrimsson SA**, **Allison JD**, **Warren GL**, **Cureton KJ**. Muscle activation and the slow component rise in oxygen uptake during cycling. *Med Sci Sports Exerc* 32: 2040–2045, 2000.

184. **Schantz PG**, **Henriksson J**. Enzyme levels of the NADH shuttle systems: measurements in isolated muscle fibres from humans of differing physical activity. *Acta Physiol Scand* 129: 505–515, 1987.

185. **Schantz PG**, **Sjöberg B**, **Svedenhag J**. Malate-aspartate and alpha-glycerophosphate shuttle enzyme levels in human skeletal muscle: methodological considerations and effect of endurance training. *Acta Physiol Scand* 128: 397–407, 1986.

186. **Scheuermann BW**, **Hoelting BD**, **Noble ML**, **Barstow TJ**. The slow component of O(2) uptake is not accompanied by changes in muscle EMG during repeated bouts of heavy exercise in humans. *J Physiol* 531: 245–256, 2001.

187. **Schlagowski AI**, **Singh F**, **Charles AL**, **Gali Ramamoorthy T**, **Favret F**, **Piquard F**, **Geny B**, **Zoll J**. Mitochondrial uncoupling reduces exercise capacity despite several skeletal muscle metabolic adaptations. *J Appl Physiol* 116: 364–375, 2014.

188. **Schoolwerth AC**, **LaNoue KF**. Transport of metabolic substrates in renal mitochondria. *Annu Rev Physiol* 47: 143–171, 1985.

189. **Segel I**. *Biochemical Calculations, Segel 2a*. 2nd ed. New York, New York: John Wiley and Sons, 1976.

190. **Stienen GJ**, **Papp Z**, **Zaremba R**. Influence of inorganic phosphate and pH on sarcoplasmic reticular ATPase in skinned muscle fibres of Xenopus laevis. *J Physiol* 518 (Pt 3): 735–744, 1999.

191. **Systrom DM**, **Kanarek DJ**, **Kohler SJ**, **Kazemi H**. 31P nuclear magnetic resonance spectroscopy study of the anaerobic threshold in humans. *J Appl Physiol* 68: 2060–2066, 1990.

192. **Takahashi H**, **Inaki M**, **Fujimoto K**, **Katsuta S**, **Anno I**, **Niitsu M**, **Itai Y**. Control of the rate of phosphocreatine resynthesis after exercise in trained and untrained human quadriceps muscles. *Eur J Appl Physiol* 71: 396–404, 1995.

193. **Taylor DJ**, **Styles P**, **Matthews PM**, **Arnold DA**, **Gadian DG**, **Bore P**, **Radda GK**. Energetics of human muscle: exercise-induced ATP depletion. *Magn Reson Med* 3: 44–54, 1986.

194. **Tevald MA**, **Lanza IR**, **Befroy DE**, **Kent-Braun JA**. Intramyocellular oxygenation during ischemic muscle contractions in vivo. *Eur J Appl Physiol* 106: 333–343, 2009.

195. **Tischler ME**, **Pachence J**, **Williamson JR**, **La Noue KF**. Mechanism of glutamate-aspartate translocation across the mitochondrial inner membrane. *Arch Biochem Biophys* 173: 448–461, 1976.

196. **Toime LJ**, **Brand MD**. Uncoupling protein-3 lowers reactive oxygen species production in isolated mitochondria. *Free Radic Biol Med* 49: 606–611, 2010.

197. **Trenell MI**, **Sue CM**, **Kemp GJ**, **Sachinwalla T**, **Thompson CH**. Aerobic exercise and muscle metabolism in patients with mitochondrial myopathy. *Muscle Nerve* 33: 524–531, 2006.

198. **Tucker WJ**, **Rosenberry R**, **Trojacek D**, **Chamseddine HH**, **Arena-Marshall CA**, **Zhu Y**, **Wang J**, **Kellawan JM**, **Haykowsky MJ**, **Tian F**, **Nelson MD**. Studies into the determinants of skeletal muscle oxygen consumption: novel insight from near-infrared diffuse correlation spectroscopy. *J. Physiol.* (April 14, 2019). doi: 10.1113/JP277580.

199. **Vanhamme L**, **van den Boogaart A**, **Van Huffel S**. Improved method for accurate and efficient quantification of MRS data with use of prior knowledge. *J Magn Reson San Diego Calif 1997* 129: 35–43, 1997.

200. **Vanhatalo A**, **Black MI**, **DiMenna FJ**, **Blackwell JR**, **Schmidt JF**, **Thompson C**, **Wylie LJ**, **Mohr M**, **Bangsbo J**, **Krustrup P**, **Jones AM**. The mechanistic bases of the power-time relationship: muscle metabolic responses and relationships to muscle fibre type. *J Physiol* 594: 4407–4423, 2016.

201. **Vanhatalo A**, **Fulford J**, **DiMenna FJ**, **Jones AM**. Influence of hyperoxia on muscle metabolic responses and the power-duration relationship during severe-intensity exercise in humans: a 31P magnetic resonance spectroscopy study. *Exp Physiol* 95: 528–540, 2010.

202. **Venkatasubramanian PN**, **Mafee MF**, **Bárány M**. Quantitation of phosphate metabolites in human leg in vivo. *Magn Reson Med* 6: 359–363, 1988.

203. **Vinnakota KC**, **Kushmerick MJ**. Point: Muscle lactate and H^+ production do have a 1:1 association in skeletal muscle. *J Appl Physiol* 110: 1487–1489; discussion 1497, 2011.

204. **Wagner PD**, **Lundby C**. The lactate paradox: does acclimatization to high altitude affect blood lactate during exercise? *Med Sci Sports Exerc* 39: 749–755, 2007.

205. **Walsh B**, **Tiivel T**, **Tonkonogi M**, **Sahlin K**. Increased concentrations of P(i) and lactic acid reduce creatine-stimulated respiration in muscle fibers. *J Appl Physiol* 92: 2273–2276, 2002.

206. **Walter G**, **Vandenborne K**, **Elliott M**, **Leigh JS**. In vivo ATP synthesis rates in single human muscles during high intensity exercise. *J Physiol* 519 Pt 3: 901–910, 1999.

207. **Walter G**, **Vandenborne K**, **McCully KK**, **Leigh JS**. Noninvasive measurement of phosphocreatine recovery kinetics in single human muscles. *Am J Physiol* 272: C525-534, 1997.

208. **Wasserman K**, **Beaver WL**, **Davis JA**, **Pu JZ**, **Heber D**, **Whipp BJ**. Lactate, pyruvate, and lactate-to-pyruvate ratio during exercise and recovery. *J Appl Physiol* 59: 935–940, 1985.

209. **Wasserman K**, **Whipp BJ**, **Koyl SN**, **Beaver WL**. Anaerobic threshold and respiratory gas exchange during exercise. *J Appl Physiol* 35: 236–243, 1973.

210. **Westerblad H**, **Allen DG**. The contribution of [Ca2+]i to the slowing of relaxation in fatigued single fibres from mouse skeletal muscle. *J Physiol* 468: 729–740, 1993.

211. **Whipp BJ**, **Rossiter HB**, **Ward SA**. Exertional oxygen uptake kinetics: a stamen of stamina? *Biochem Soc Trans* 30: 237–247, 2002.

212. **Whipp BJ**, **Wasserman K**. Oxygen uptake kinetics for various intensities of constant-load work. *J Appl Physiol* 33: 351–356, 1972.

213. **Whipp BJ**, **Wasserman K**. Effect of anaerobiosis on the kinetics of O2 uptake during exercise. *Fed Proc* 45: 2942–2947, 1986.

214. **Willis WT**, **Jackman MR**. Mitochondrial function during heavy exercise. *Med Sci Sports Exerc* 26: 1347–1353, 1994.

215. **Willis WT**, **Jackman MR**, **Messer JI**, **Kuzmiak-Glancy S**, **Glancy B**. A Simple Hydraulic Analog Model of Oxidative Phosphorylation. *Med Sci Sports Exerc* 48: 990–1000, 2016.

216. **Willis WT**, **Miranda-Grandjean D**, **Hudgens J**, **Willis EA**, **Finlayson J**, **De Filippis EA**, **Zapata Bustos R**, **Langlais PR**, **Mielke C**, **Mandarino LJ**. Dominant and sensitive control of oxidative flux by the ATP-ADP Carrier in human skeletal muscle mitochondria: Effect of lysine acetylation. *Arch. Biochem. Biophys.* (April 10, 2018). doi: 10.1016/j.abb.2018.04.006.

217. **Wood MA**, **Bailey SJ**, **Jones AM**. Influence of all-out start duration on pulmonary oxygen uptake kinetics and high-intensity exercise performance. *J Strength Cond Res* 28: 2187–2194, 2014.

218. **Wüst RCI**, **Grassi B**, **Hogan MC**, **Howlett RA**, **Gladden LB**, **Rossiter HB**. Kinetic control of oxygen consumption during contractions in self-perfused skeletal muscle. *J Physiol* 589: 3995–4009, 2011.

219. **Xu F**, **Rhodes EC**. Oxygen uptake kinetics during exercise. *Sports Med Auckl NZ* 27: 313–327, 1999.

220. **Zoladz JA**, **Duda K**, **Karasinski J**, **Majerczak J**, **Kolodziejski L**, **Korzeniewski B**. MyHC II content in the vastus lateralis m. quadricipitis femoris is positively correlated with the magnitude of the non-linear increase in the VO2 / power output relationship in humans. *J Physiol Pharmacol Off J Pol Physiol Soc* 53: 805–821, 2002.

221. **Zoladz JA**, **Gladden LB**, **Hogan MC**, **Nieckarz Z**, **Grassi B**. Progressive recruitment of muscle fibers is not necessary for the slow component of VO2 kinetics. *J Appl Physiol* 105: 575–580, 2008.